CLNS 93/1261
UH-511-778-93
OHSTPY-HEP-E-93-018
HEPSY 93-10
February 10, 1994

A Review of Hadronic and Rare B Decays[1]

Thomas E. Browder
University of Hawaii at Manoa, Honolulu, Hawaii 96822

Klaus Honscheid
Ohio State University, Columbus, Ohio 43210

Stephen Playfer
Syracuse University, Syracuse, New York 13244

(To appear in B Decays, 2nd edition, Ed. by S. Stone, World Scientific)

Abstract

We review recent experimental results on B meson decays. These include measurements of the inclusive production of charmed and non-charmed mesons and baryons, the reconstruction of a large number of exclusive hadronic final states with charmed mesons, the search for exclusive hadronic final states without charmed mesons, and the first observation of the decay $B \to K^*\gamma$ which is described by an electromagnetic penguin diagram. The theoretical implications of these results will be considered.

Contents

I. INTRODUCTION

In the past two years there have been major advances in our knowledge of the decays of B mesons. This is primarily a result of the large data sample of about 2 fb^{-1} that has been collected on the $\Upsilon(4S)$ by the CLEO II collaboration at the Cornell Electron Storage Ring (CESR). The CLEO II detector has excellent capabilities for measuring both charged tracks and neutral showers, and has reconstructed a large number of exclusive hadronic B decays. We will discuss the results that have been obtained on Cabibbo favored hadronic B decays [2], as well as the new results on rare B decays [3,4]. Older results from the ARGUS experiment, which operated at the DORIS storage ring and from the CLEO 1.5 experiment, which preceded the CLEO II detector are also discussed. We note that the LEP experiments and the CDF experiment at the Tevatron Collider have recently observed exclusive hadronic decays of both B and B_s mesons. This demonstration of the feasibility of reconstructing B decays in e^+e^- collisions at the Z^0, and in high energy $p\bar{p}$ collisions, is an indication of the possibilities for future studies of B mesons.

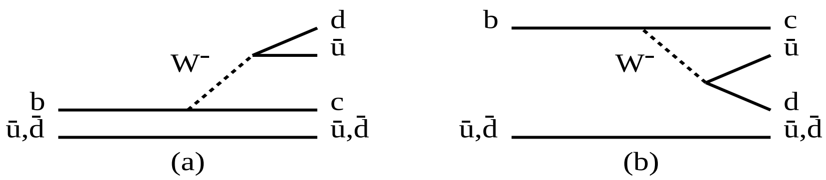

FIG. 1. B meson decay diagrams: (a) external spectator and (b) color suppressed spectator.

Since the top quark mass is large, B mesons are expected to be the only weakly decaying mesons containing quarks of the third generation. This means that their decays are a unique window on the Cabibbo-Kobayashi-Maskawa (CKM) matrix elements V_{cb}, V_{ub}, V_{ts} and V_{td}, describing the couplings of the third generation of quarks to the lighter quarks. Hadronic B meson decays occur primarily through the Cabibbo favored $b \to c$ transition. In such decays the dominant weak decay diagram is the spectator diagram, shown in Fig. 1(a), where the virtual W^- materializes into either a $\bar{u}d$ or a $\bar{c}s$ pair. This pair becomes one of the final state hadrons while the c quark pairs with the spectator anti-quark to form the other hadron.

The spectator diagram is modified by hard gluon exchanges between the initial and final quark lines. This leads to the "color suppressed" diagram shown in Fig. 1(b), which has a different set of quark pairings. Observation of $B \to \psi X_s$ decays, where X_s is a strange meson, gives experimental evidence for the presence of this diagram. Further information on the size of the color suppressed contribution can be obtained from $\bar{B}^0 \to D^0$ (or D^{*0})X^0 transitions, where X^0 is a neutral meson. In B^- decays, both types of diagrams are present and can interfere. By comparing the rates for B^- and $\bar{B}^0$ decays, the size and the sign of the color suppressed amplitude can be determined.

It has been suggested by Bjorken [5] that, in analogy to semileptonic decays, two body decays of B mesons can be expressed as the product of two independent hadronic currents, one describing the formation of a charm meson and the other the hadronization of the $\bar{u}d$ (or $\bar{c}s$) system from the virtual W^-. Qualitatively, he argues that for a B decay with a large energy release the $\bar{u}d$ pair, which is produced as a color singlet, travels fast enough to leave the interaction region without influencing the second hadron formed from the c quark and the spectator anti-quark. The assumption that the amplitude can be expressed as the product of two hadronic currents is called "factorization" in this paper. It is expected that the simple approximation of the strong interaction effects by the factorization hypothesis will be more reliable in B meson decays than in the equivalent D meson decays due to the larger characteristic energy transfers and the consequent suppression of final state interactions. We will discuss several tests of the factorization hypothesis based on the comparison of semileptonic and hadronic B meson decays.

All B meson decays that do not occur through the usual $b \to c$ transition are known as rare B decays. The simplest diagram for a rare B decay is obtained by replacing the $b \to c$ transition by a Cabibbo suppressed $b \to u$ transition. These decays probe the small CKM matrix element V_{ub}, the magnitude of which sets bounds on the combination $\rho^2 + \eta^2$ in the Wolfenstein parameterization of the CKM matrix. So far the only measurement of the magnitude of V_{ub} has been obtained from semileptonic B decays [6]. We discuss the status of the search for rare hadronic B decays, and in particular the possibility of measuring the decay $B^0 \to \pi^+\pi^-$ which is important for the study of CP violation in B decays.

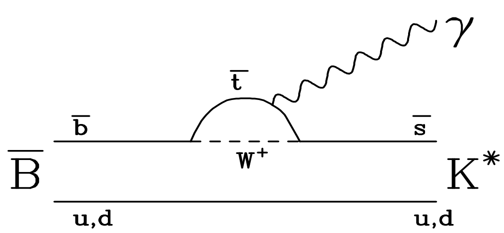

FIG. 2. Diagram for the electromagnetic penguin in B meson decay.

Since the contribution of the spectator diagram to rare B decays is suppressed it is expected that additional diagrams will make a large contribution to some decay modes. The most significant of these diagrams is the one-loop flavor-changing neutral current diagram known as the "penguin" diagram (Fig. 2). The Cabibbo allowed part of this diagram, corresponding to a $b \to s$ transition, is expected to dominate the amplitude of rare decays to final states with one or three s-quarks. There is also a Cabibbo suppressed $b \to d$ amplitude which may not be negligible in decays to final states with no c or s quarks. It should be noted that the loop diagram is much more significant in B decays than in D decays because the $b \to s$ loop contains the heavy top quark with large couplings V_{tb} and V_{ts}, whereas contributions to the equivalent $c \to u$ loop are suppressed either by the small couplings V_{cb} and V_{ub}, or by the small s and d quark masses.

The observation of the decay $B \to K^*(892)\gamma$, recently reported by the CLEO II experiment, is the first direct evidence for the penguin diagram.

This decay is described by the electromagnetic transition $b \to s\gamma$, which is a $b \to s$ penguin loop accompanied by the radiation of a photon from either the loop, or the initial or final state quarks. This important new result will be discussed in some detail. We will also comment on the recent discussion about the sensitivity of the $b \to s\gamma$ process to non-standard model contributions within the loop [7]. In many extensions of the standard model an additional contribution to $b \to s\gamma$ is expected to come from a charged Higgs. We will discuss the extent to which the data from the CLEO II experiment allow bounds to be set on such non-standard model contributions.

II. THE EXPERIMENTAL STUDY OF B DECAY

A. $\Upsilon(4S)$ Experiments

The first fully reconstructed B mesons were reported in 1983 by the CLEO I collaboration [8]. Since then the CLEO 1.5 experiment [9,10] has collected 212 pb^{-1} [11], the ARGUS experiment [12–14] has collected 246 pb^{-1}, and the CLEO II experiment has collected about 2 fb^{-1}, of which between 0.9 and 1.4 fb^{-1} have been used to obtain the results described in this review [2–4]. All these experiments take data on the $\Upsilon(4S)$ resonance at e^+e^- colliders. The techniques used by experiments which operate at the $\Upsilon(4S)$ resonance are discussed in detail in the review by M. Artuso in this volume. It is assumed here that the $\Upsilon(4S)$ resonance always decays to pairs of B mesons, and that f_+, the fraction of B^+B^- pairs produced in $\Upsilon(4S)$ decay, is equal to f_0, the fraction of $B^0\bar{B}^0$ pairs produced in these decays. Older results which assumed other values of f_+ and f_0 have been rescaled.

The $\Upsilon(4S)$ resonance sits on a continuum background consisting of $e^+e^- \to q\bar{q}$, where q can be any of u, d, s, c. This continuum background is studied by taking a significant amount of data at an energy just below the $\Upsilon(4S)$ resonance, e.g. CLEO II records a third of its data at an energy 55 MeV below the resonance. Using this data sample, and Monte Carlo simulations of $q\bar{q}$ jets, cuts have been devised to suppress the continuum background. In $\Upsilon(4S)$ production of $B\bar{B}$ pairs, the B mesons are produced almost at rest, and their decay axes are uncorrelated. These events are rather spherical in shape, and can be distinguished from jetlike continuum events using a variety of event shape variables. For the study of inclusive production in B decays a particularly useful variable is the normalized second Fox-Wolfram moment [15], R_2, which is 0 for a perfectly spherical event, and 1 for an event completely collimated around the jet axis. For the study of exclusive B decay modes it is more useful to compare the axis of the reconstructed B candidate with the axis of the rest of the event. Examples of variables used are the direction of the sphericity axis or the thrust axis of the rest of the event with respect to the B candidate, θ_S or θ_T, and the sum of the momenta transverse to the axis of the B candidate, known as $s_\perp$ [16]. There is also some information in the direction of flight of the B meson, which is expected to be distributed like $\sin^2\theta_B$, whereas the continuum background is flat. We will discuss the use of these cuts, and their effectiveness for particular analyses, but refer the reader to the article by M. Artuso for a more detailed discussion of the shape variables.

B. High Energy Collider Experiments

In the past, evidence for the production of b quarks in high energy experiments has been deduced from the presence of high p_T leptons. Recently, significant progress in the isolation of events containing b quarks has been made possible by the installation of silicon vertex detectors near the interaction point at several collider experiments. These b quarks hadronize as B_d, B_u, B_s mesons and baryons containing b quarks. Evidence for B_s and Λ_b production has been reported but the relative production fractions are not well known [17]. With the improvement in background suppression provided by these solid state detectors, signals for exclusive hadronic B_d, B_u and B_s meson decays have been isolated in the invariant mass spectra for low multiplicity final states (e.g. $B_s \to \psi\phi$). However, the resolution in invariant mass (O(20 MeV)) is poorer than the resolution in beam constrained mass in threshold experiments and is not sufficient to clearly separate modes with an additional photon or modes where one kaon is replaced with a pion. Although collider experiments cannot determine absolute branching fractions without making further assumptions or using information from experiments at the $\Upsilon(4S)$, they can measure relative branching fractions. Some high energy experiments have also obtained inclusive signals for D^0, D^{*+}, ψ mesons in B decay. However, it is difficult to distinguish the contribution of B_d, B_u and B_s mesons.

C. Determination of B Meson Branching Fractions

To extract B meson branching ratios, the detection efficiencies are determined from a Monte Carlo simulation and the yields are corrected for the charmed meson branching fractions. In order to determine new average branching ratios for B meson decays the results from individual experiments must be normalized with respect to a common set of charm meson and baryon absolute branching fractions. The branching fractions for the D^0 and D^+ modes used to calculate the B branching fractions are given in the Tables below. We have chosen the precise value of the $D^0 \to K^-\pi^+$ branching fraction recently reported by CLEO II to normalize the results [18]. The branching fractions of other D^0 decay modes relative to $D^0 \to K^-\pi^+$ are taken from the PDG compilation [19]. The D^+ branching ratio is taken from the Mark III experiment [20].

TABLE I. D^0 branching fractions [%] used in previous publications and this review.

Mode	ARGUS, CLEO 1.5 [10], [13]	ARGUS (DD_s) [21]	CLEO II [2]	This review
$K^-\pi^+$	4.2 ± 0.6	3.7 ± 0.3	3.91 ± 0.19	3.9 ± 0.2
$K^-\pi^+\pi^-\pi^+$	9.1 ± 1.1	7.5 ± 0.5	8.0 ± 0.5	8.0 ± 0.5
$K^-\pi^+\pi^0$	13.3 ± 1.8	11.3 ± 1.1	12.1 ± 1.1	12.1 ± 1.1
$K^0\pi^+\pi^-$	6.4 ± 1.1	5.4 ± 0.5		5.8 ± 0.5

Branching ratios for all D_s decay modes are normalized relative to $\mathcal{B}(D_s \to \phi\pi)$. There are no model-independent measurements of the absolute branching fraction for $D_s \to \phi\pi$. The currently favored method uses measurements of $\Gamma(D_s \to \phi l\nu)/\Gamma(D_s \to \phi\pi)$. The rate $\Gamma(D_s \to \phi l\nu)$ is determined from measurements of τ_{D_s}/τ_{D^+}, $\Gamma(D^+ \to K^* l\nu)$, and using

TABLE II. D^+ branching fractions [%] used in previous publications and this review.

Mode	ARGUS, CLEO 1.5 [10], [13]	ARGUS (DD_s) [21]	CLEO II [2]	This review
$K^-\pi^+\pi^+$	9.1 ± 1.4	7.7 ± 1.0	9.1 ± 1.4	9.1 ± 1.4
$K^0\pi^+$	3.2 ± 0.5	2.6 ± 0.4		
$K^0\pi^+\pi^+\pi^-$		6.9 ± 1.1		

$\Gamma(D^+ \to K^* l\nu)/\ \Gamma(D_s \to \phi l\nu)$ obtained from theory. We use the value of $\mathcal{B}(D_s \to \phi\pi)$ derived in reference [22] .

TABLE III. D_s branching fraction [%] used in previous publications and this review.

Mode	CLEO 1.5 [10]	ARGUS (DD_s) [21]	This review
$\phi\pi^+$	2.7 ± 0.7	3.0 ± 1.1	3.7 ± 0.9

Since the publication of the ARGUS and CLEO 1.5 papers on hadronic decays, the branching fractions for the $D^* \to D\pi(\gamma)$ modes have been significantly improved by more precise measurements from CLEO II [23]. For modes which contain D^* mesons we have recalculated the branching ratios using the CLEO II measurements.

TABLE IV. D^* branching fractions [%] used in previous publications and this review.

Mode	ARGUS, CLEO 1.5 [10], [13]	CLEO II [2]	This review
$D^{*0} \to D^0\pi^0$	55.0 ± 6	63.6 ± 4.0	63.6 ± 4.0
$D^{*0} \to D^0\gamma$	45.0 ± 6	36.4 ± 4.0	36.4 ± 4.0
$D^{*+} \to D^0\pi^+$	57.0 ± 6	68.1 ± 1.6	68.1 ± 1.6

TABLE V. Charmonium branching fractions [%] used in previous publications and this review.

Mode	ARGUS, CLEO 1.5 [10], [13]	CLEO II [2]	This review [24]
$\psi \to e^+e^-$	6.9 ± 0.9	6.3 ± 0.2	5.9 ± 0.25
$\psi \to \mu^+\mu^-$	6.9 ± 0.9	6.0 ± 0.25	5.9 ± 0.25
$\psi' \to e^+e^-$ and $\mu^+\mu^-$	1.7 ± 0.3	1.7 ± 0.3	1.7 ± 0.3
$\psi' \to \psi\pi + \pi-$	32.4 ± 2.6	32.4 ± 2.6	32.4 ± 2.6
$\chi_{c1} \to \psi\gamma$	27.3 ± 1.6	27.3 ± 1.6	27.3 ± 1.6

We also give the old and new values assumed for the decays $\psi \to e^+e^-$ and $\psi \to \mu^+\mu^-$. We have chosen to use the precise measurement of these decays recently performed by the MARK III collaboration [24]. The modes $\psi' \to \ell^+\ell^-$ and $\psi' \to \psi\pi^+\pi^-$ are used to form B meson candidates in modes involving ψ' mesons. B meson decays into final states containing χ_c mesons are reconstructed using the channel $\chi_{c1} \to \psi\gamma$. Product branching ratios for all modes containing ψ mesons have been rescaled to account for the improved ψ branching fractions.

In the cases where only one D^0 decay mode was used to reconstruct the B meson the published branching ratio is simply rescaled. The procedure for recalculating the branching ratios becomes more complicated when more than one D decay channel is used. All experiments used the following procedure to obtain their results

$$\mathcal{B}(B) = \frac{N_{observed}}{\epsilon \times N_B \times (\mathcal{B}(D^*)) \times \sum \mathcal{B}_i(D^0)}$$

where N_B is the number of B mesons. The efficiency ϵ is defined as

$$\epsilon = \frac{\sum \mathcal{B}_i(D^0)\epsilon_i}{\sum \mathcal{B}_i(D^0)}$$

The index i refers to the D meson decay channel. Therefore the rescaled branching ratio is given by

$$\mathcal{B} = \frac{N_{observed}}{N_B \times (\mathcal{B}(D^*)) \times \sum \mathcal{B}_i(D^0)\epsilon_i}$$

The CLEO collaboration published enough information, including the yields and the efficiencies for the individual D^0 decay channels, so that rescaling their B branching ratios is straightforward.

Although the D^0 reconstruction efficiencies depend slightly on the B meson decay channel under study, the only information available from the ARGUS collaboration are average D^0 reconstruction efficiencies $< \epsilon >_i$. Therefore we had to make the assumption that the correct way to renormalize the ARGUS results is to multiply their branching ratios by the scale factor F where

$$F = \frac{\sum < \epsilon >_i \times \mathcal{B}_i(D^0)_{old}}{\sum < \epsilon >_i \times \mathcal{B}_i(D^0)_{new}}$$

The validity of this assumption has been checked using CLEO 1.5 data.

Statistical errors are recalculated in the same way as the branching ratios. For the results from individual experiments on B decays to final states with D mesons two systematic errors are quoted. The second systematic error contains the contribution due to the uncertainties in the $D^0 \to K^-\pi^+$ or $D^+ \to K^-\pi^+\pi^+$ branching fractions. This will allow easier rescaling when these branching ratios are measured more precisely. The first systematic error includes the experimental uncertainties and when relevant the uncertainties in the ratios of charm branching ratios, e.g. $\Gamma(D^0 \to K^-\pi^+\pi^+\pi^-)/\Gamma(D^0 \to K^-\pi^+)$, the error in the D^* branching fractions and the error in $\mathcal{B}(D_s \to \phi\pi^+)$. For all other modes only one systematic error is given. For the world averages the statistical and the first systematic error are combined in quadrature while the errors due to the D^0 and D^+ scales are still listed separately. With the improvement in the precision of the D^0 and D^* branching fractions these are no longer the dominant source of systematic error in the study of hadronic B meson decay.

III. INCLUSIVE B DECAY

A. Motivation

Due to the large mass of the b quark B meson decays give rise to a large number of secondary decay products. For instance, CLEO finds that the charged and photon multiplicities at the $\Upsilon(4S)$ are: $n_{\text{charged}} = 10.99 \pm 0.06 \pm 0.29$, $n_\gamma = 10.00 \pm 0.53 \pm 0.50$, respectively [25]. Similarly, ARGUS [26] finds $n_{\text{charged}} = 10.74 \pm 0.02$. The high multiplicity of final state particles leads to a large number of possible exclusive final states. Even with a detector that has a large acceptance for both charged tracks and showers, it is difficult to reconstruct many exclusive final states because of the combinatorial backgrounds. Furthermore the detection efficiency drops for high multiplicity final states. Thus, to get a complete picture of B meson decay, it is important to study inclusive decay rates.

A number of theoretical calculations of inclusive B decay rates have been made using the parton model. It is believed that measurements of such inclusive rates can be more reliably compared to the theoretical calculations than can measurements of exclusive decays (e.g. see the contribution by Bigi in this volume). While this is sufficient motivation for studying the inclusive rates, there is also a need for accurate measurements in order to model the decays of B mesons both for high energy collider experiments, and for experiments at the $\Upsilon(4S)$. As a specific example, the inclusive rate for $B \to \psi$ has been used to determine the B meson production cross-section at the Tevatron [27].

The branching ratios for inclusive B decays to particular final state particles are determined by measuring the inclusive yields of these particles in data taken on the $\Upsilon(4S)$ resonance, and subtracting the non-resonant background using data taken at energies below the $\Upsilon(4S)$ resonance. The off-resonance data are scaled to correct for the energy dependence of the continuum cross-section. Results on inclusive production at the $\Upsilon(4S)$ are usually presented as a function of the variable x, which is the fraction of the maximum possible momentum carried by the particle, $p_{max} = \sqrt{E_{beam}^2 - M^2}$. The endpoint for production in B decays is at $x = 0.5$.

B. Inclusive B Decay to Mesons

CLEO 1.5 [28] has measured the branching fractions of inclusive B decays to light mesons, while ARGUS has determined the average multiplicities of light mesons in B decay. If more than one meson of the particle type under study is produced in a $B\bar{B}$ decay, then the branching fraction and the multiplicity will differ. Unless otherwise noted, the results reported in Table VI are averaged over B and $\bar{B}$ decay.

In the decay $b \to c \to s$ the charge of the kaon can be used to determine the flavor of the b quark. A first attempt to measure the tagging efficiency and misidentification probability for this method has been performed by ARGUS [29]. With the large sample of reconstructed B^0 and B^+ decays from CLEO II it should be possible to measure these quantities directly. The experiments also measure the momentum spectra for the particles listed in Table VI. These results provide important information needed to improve Monte Carlo generators for future B experiments.

TABLE VI. Multiplicities or branching fractions of light mesons per B meson decay.

Mode	CLEO 1.5 [28] (Branching Ratio)	ARGUS [29] (Multiplicity)
$B/\bar{B} \to \pi^{\pm}$ (not from K_s, Λ)		$3.59 \pm 0.03 \pm 0.07$
$B/\bar{B} \to \pi^{\pm}$ (incl. K_s, Λ)		$4.11 \pm 0.03 \pm 0.08$
$B/\bar{B} \to K^{\pm}$	$0.85 \pm 0.07 \pm 0.09$	$0.78 \pm 0.02 \pm 0.03$
$\bar{B} \to K^-$	$0.66 \pm 0.05 \pm 0.07$	
$\bar{B} \to K^+$	$0.19 \pm 0.05 \pm 0.02$	
$B/\bar{B} \to K^0/\bar{K}^0$	$0.63 \pm 0.06 \pm 0.06$	$0.64 \pm 0.01 \pm 0.04$
$B/\bar{B} \to K^{*0}$		$0.146 \pm 0.016 \pm 0.020$
$B/\bar{B} \to K^{*+}$		$0.182 \pm 0.054 \pm 0.024$
$B/\bar{B} \to \rho^0$		$0.209 \pm 0.042 \pm 0.033$
$B/\bar{B} \to \omega$		< 0.41 (90% C.L.)
$B/\bar{B} \to f_0(975)$		< 0.025 (90% C.L.)
$B/\bar{B} \to \eta'$		< 0.15 (90% C.L.)
$B/\bar{B} \to \phi$		$0.039 \pm 0.003 \pm 0.004$

The inclusive production of D^0, D^+, D_s^+ and D^{*+} mesons in B decay has been measured by ARGUS [30] and CLEO 1.5 [31]. To improve signal to background, only the $D^0 \to K^-\pi^+$, $D^+ \to K^-\pi^+\pi^+$ and $D_s^+ \to \phi\pi^+$ decay modes are used. The results, rescaled for the charm branching ratios, are given in Tables VIII–IX. The momentum spectrum for the inclusive decay of B mesons to D^0, D^+, and D^{*+} as measured by CLEO 1.5 are shown in Fig. 3. The D^{*+} spectrum is not measured for $x < 0.1$ due to poor reconstruction efficiency for slow tracks. The shape of the D_s momentum spectrum (Fig. 4) indicates that there is a substantial two body component. In model dependent fits the ARGUS and CLEO 1.5 experiments find two body fractions of $(58 \pm 7 \pm 9)\%$ [30] and $(56 \pm 10)\%$ [31], respectively.

The polarization as a function of x for $B \to D^{*+}$ has also been measured and found to agree with the predictions of Wirbel and Wu [32] and of Pietschmann and Rupertsberger [33].

Results on inclusive B decay to final states with ψ and ψ' mesons have been reported by CLEO 1.5 [10], ARGUS [34], and CLEO II [35]. In the most recent high statistics analysis from CLEO II, the effect of final state radiation has been taken into account [36]. This effect leads to a significant tail on the low side of the $\psi \to e^+e^-$ mass peak and a smaller effect in the $\mu^+\mu^-$ spectrum. Even with a large mass window that extends from 2.50 to 3.05 GeV/c^2, this effect can modify the calculated detection efficiency by more than 10%. Corrections are also made for non-resonant ψ production in the CLEO II analysis [37]. The resulting invariant dielectron and dimuon mass distributions are shown in Fig. 5.

The momentum spectrum for $B \to \psi, \psi'$ transitions has been measured (Fig. 6 shows the ψ momentum spectrum). The two body component due to $B \to \psi K$ and $B \to \psi K^*$ saturates the spectrum in the momentum range between 1.4 and 2.0 GeV. ARGUS has determined $\mathcal{B}(B \to \psi$, where ψ not from $\psi') = (0.95 \pm 0.27)\%$. The two body component constitutes about 1/3 of direct ψ production.

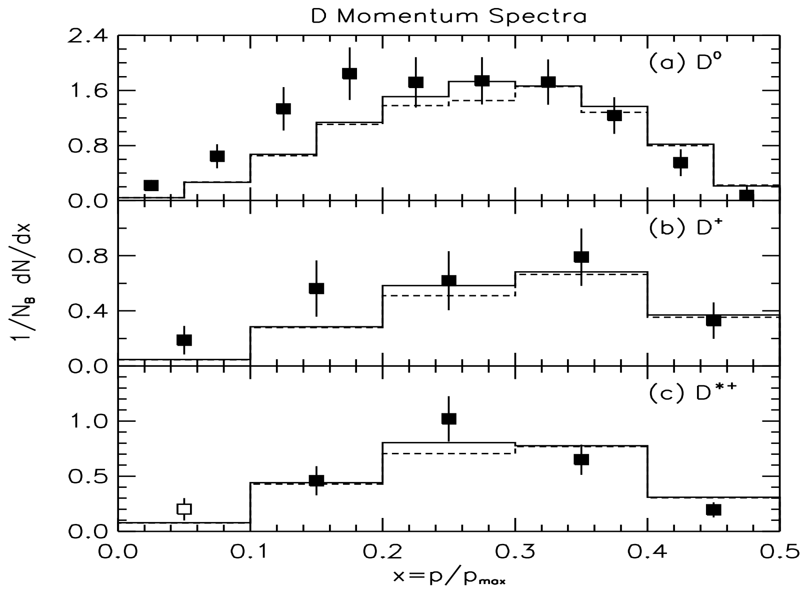

FIG. 3. $B \to D^0X$, D^+X, and $D^{*+}X$ momentum spectra in CLEO 1.5 data. The dashed curve is the prediction of the phenomenological model of Wirbel and Wu while the solid histogram is the prediction of their free quark model

TABLE VII. ψ polarization Γ_L/Γ in inclusive B meson decays.

ψ momentum	CLEO II [38]	ARGUS [39]
$p_\psi < 0.8$ GeV/c	0.55 ± 0.35	
0.8 GeV/c $< p_\psi <$ 1.4 GeV/c	0.49 ± 0.32	
1.4 GeV/c $< p_\psi <$ 2.0 GeV/c	0.78 ± 0.17	1.17 ± 0.17
all $p_\psi < 2.0$ GeV/c	0.59 ± 0.15	

The polarization Γ_L/Γ as a function of momentum for $B \to \psi$ transitions has also been determined (see Table VII). According to ARGUS, the ψ mesons in the highest momentum bin are completely longitudinally polarized. Since the highest momentum bin is dominated by two body B decay, the polarization measured in this bin can be used to estimate the polarization of $B \to \psi K^*$ after correcting for the contribution of $B \to \psi K$. Therefore the ARGUS result indicates that the $B \to \psi K^*$ mode is dominated by a single orbital angular momentum state and hence by a single CP eigenstate.

CLEO II [37] and ARGUS [40] have reported results on inclusive $B \to \chi_c X, \chi_c \to \gamma\psi$ decays. ARGUS assumes there is no χ_{c2} production. CLEO II has a 4.5 times better χ_c mass resolution than ARGUS and allows for both possibilities. The branching ratio for $\chi_{c0} \to \gamma\psi$ is $(6.6 \pm 1.8) \times 10^{-3}$ so the contribution of the χ_{c0} meson can be neglected.

In a parton level calculation, Palmer and Stech [41] find that $\mathcal{B}(B \to X_{c\bar{c}}) = 19 \pm 1\%$ where the theoretical error is the uncertainty due to the choice of quark masses. This can

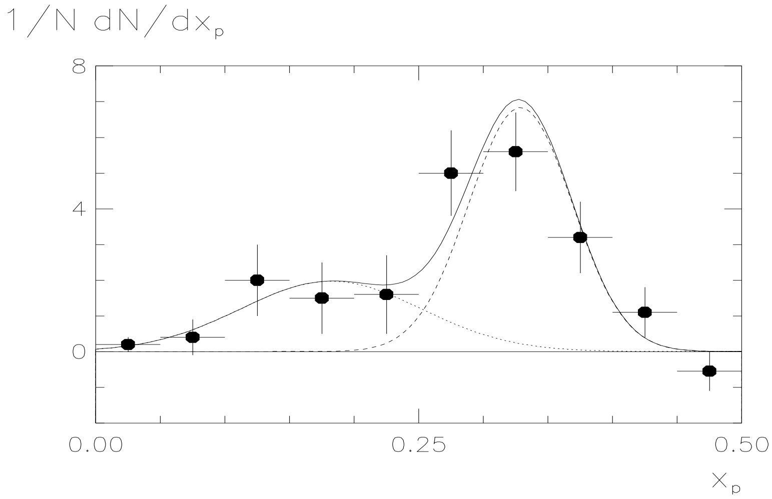

FIG. 4. $B \to D_s X$ momentum spectrum in ARGUS data. The solid line is the sum of the two components. The two dotted lines indicate the two body component and three body process.

be compared to the sum of the experimental measurements $\mathcal{B}(B \to D_s X) + 4 * \mathcal{B}(B \to \psi X) + \mathcal{B}(B \to \psi' X) = 12.9 \pm 1.0\%$ where the factor of 4 which multiplies $\mathcal{B}(B \to \psi X)$ includes a factor of 2 for the two charm quarks, and an additional factor of 2 which is a generous estimate of the unobserved contributions from B decays to η_c and χ states.

C. Inclusive B Decay to Baryons

ARGUS [42] and CLEO 1.5 [43] have observed inclusive yields of $\bar{p}$, Λ, Ξ and the charmed Λ_c baryon, and recently CLEO II has reported the observation of $B \to \Sigma_c X$ [44]. The measured branching ratios for these decays and the world averages can be found in Table

TABLE VIII. Branching fractions for inclusive B decays to charm mesons.

Particle	Signature	ARGUS	CLEO 1.5	CLEO II
D^0	$K^-\pi^+$	$49.5 \pm 3.8 \pm 6.4 \pm 2.0$	$59.7 \pm 3.2 \pm 3.6 \pm 2.4$	
D^+	$K^-\pi^+\pi^+$	$23.9 \pm 2.9 \pm 4.4 \pm 2.4$	$24.9 \pm 3.3 \pm 2.0 \pm 2.5$	
D^{*+}	$D^0\pi^+$	$27.6 \pm 2.3 \pm 4.7 \pm 1.1$	$22.7 \pm 1.3 \pm 2.3 \pm 0.9$	
D_s^+	$\phi\pi^+$	$7.9 \pm 1.1 \pm 0.8 \pm 2.6$	$8.3 \pm 1.2 \pm 0.8 \pm 2.7$	
ψ	$e^+e^-, \mu^+\mu^-$	$1.25 \pm 0.19 \pm 0.26$	$1.31 \pm 0.12 \pm 0.27$	$1.09 \pm 0.04 \pm 0.07$
ψ'	$\ell^+\ell^-, \psi\pi^+\pi^-$	$0.50 \pm 0.19 \pm 0.12$	$0.36 \pm 0.09 \pm 0.13$	$0.30 \pm 0.05 \pm 0.03$
χ_{c1}	$\psi\gamma$	$1.23 \pm 0.41 \pm 0.29$		$0.56 \pm 0.16 \pm 0.14$

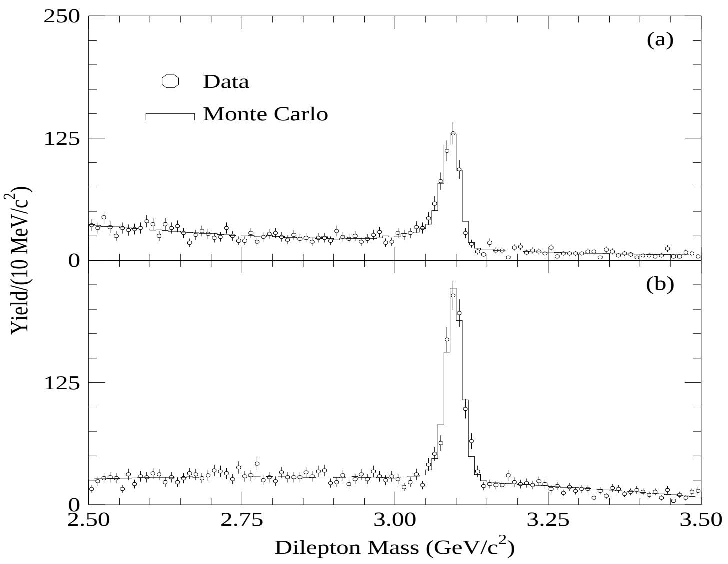

FIG. 5. $B \to \psi X$ mass spectra from CLEO II: (a) $\psi \to e^+e^-$ channel and (b) $\psi \to \mu^+\mu^-$ channel.

X. The determination of branching ratios for inclusive B decays to the charmed baryons Λ_c and Σ_c requires knowledge of $\mathcal{B}(\Lambda_c \to pK^-\pi^+)$. However, the uncertainty in this quantity is still large and it can only be determined by indirect methods. The results given in this review use $\mathcal{B}(\Lambda_c \to pK^-\pi^+) = (4.3 \pm 1.0 \pm 0.8)\%$ [43]. For modes involving Λ_c baryons the uncertainty due to the Λ_c branching ratio scale is listed as a separate error.

In a parton level calculation with diquark correlation taken into account, Palmer and Stech [41] have performed a calculation of the total rate for inclusive B decay to charmed baryons. They find $\mathcal{B}(B \to \text{charmed baryons}) \approx 6\%$. Neglecting small contributions from $B \to \Xi_c$ transitions, we assume all B to charmed baryon decays proceed through a Λ_c baryon so we can compare this prediction to the experimental result $\mathcal{B}(B \to \Lambda_c X) = (6.4 \pm 1.3 \pm 1.9)\%$.

TABLE IX. World averages for branching fractions of inclusive B decays to charm mesons.

Particle	Signature	Branching Ratio
D^0	$K^-\pi^+$	$56.7 \pm 4.0 \pm 2.3$
D^+	$K^-\pi^+\pi^+$	$24.6 \pm 3.1 \pm 2.5$
D^{*+}	$D^0\pi^+$	$23.7 \pm 2.3 \pm 0.9$
D_s^+	$\phi\pi^+$	$8.1 \pm 0.9 \pm 0.1$
ψ	e^+e^-, $\mu^+\mu^-$	1.11 ± 0.08
ψ'	$\ell^+\ell^-$, $\psi\pi^+\pi^-$	0.32 ± 0.05
χ_{c1}	$\psi\gamma$	0.66 ± 0.20

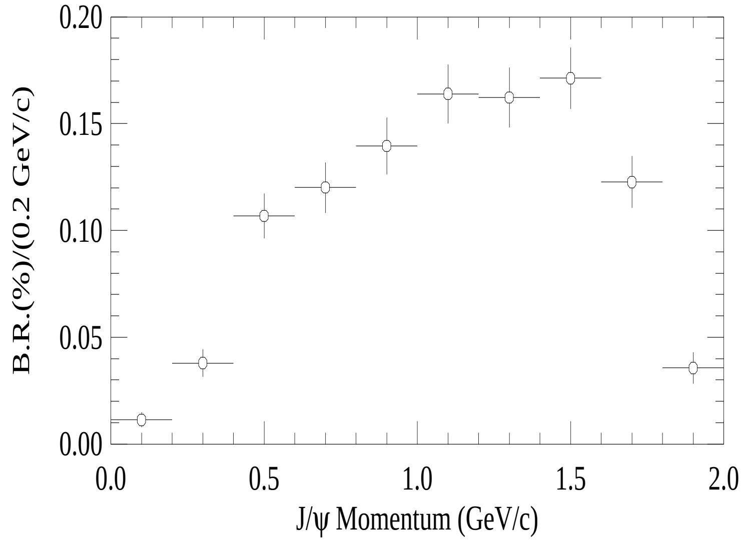

FIG. 6. $B \to \psi X$ momentum spectra in CLEO II data.

The momentum spectrum of $B \to \Lambda_c$ transitions has been measured by CLEO 1.5 [43] and ARGUS [42]. No significant two body component is found. Similarly, CLEO II has found that $B \to \Sigma_c^0 X$ and $B \to \Sigma_c^{++} X$ have no two body contribution. To date, no exclusive $B \to$ baryon decays have been reconstructed.

In addition to the inclusive branching ratios given above, CLEO 1.5 [43] and ARGUS [42] have investigated baryon correlations in B decay in order to elucidate the underlying decay process. We follow the notation of Reference [43] . Let N denote baryons with $S = C = 0$ (e.g. p, n, Δ, N^*). Let Y refer to baryons with $S = -1, C = 0$ (e.g. Λ, Σ^0, Σ^+). Let Y_c refer to baryons with $S = 0, C = 1$ [e.g. Λ_c^+, $\Sigma_c^{(+,0,++)}$] . Then the following final states can be used to distinguish possible mechanisms for baryon production in B decay (Fig. 7).

1. $\bar{B} \to Y_c \bar{N} X$, $\bar{B} \to \Xi_c \bar{Y} X$
   These final states are produced by the usual $b \to cW^-$ coupling in a spectator or exchange diagram in conjunction with the popping of two quark pairs from the vacuum (as shown in Figs. 7(a),(b)). It should be noted that the two mechanisms can be distinguished by examination of the Y_c momentum spectrum, since the exchange diagram will produce two body final states (e.g. $\Lambda_c \bar{p}$ or $\Sigma_c^{++} \bar{\Delta}^{--}$).

2. $\bar{B} \to D N \bar{N} X$, $\bar{B} \to D Y \bar{Y} X$
   The noncharmed baryon-antibaryon is produced from W fragmentation after hadronization with two quark-antiquark pairs popped from the vacuum (as shown in Figs. 7(c),(d)). The D meson is formed from the charm spectator quark system. If this mechanism is significant, inclusive production of charmless baryon-antibaryon pairs should be observed in B decay.

TABLE X. Branching fractions [%] of inclusive B decays to baryons.

Mode	CLEO 1.5	ARGUS	CLEO II	Average
$B \to \bar{p}\ X$ (incl. Λ)	$8.0 \pm 0.5 \pm 0.3$	$8.2 \pm 0.5^{+1.3}_{-1.0}$		8.0 ± 0.5
$B \to \bar{p}\ X$ (not from Λ)	$5.6 \pm 0.6 \pm 0.5$	5.5 ± 1.6		5.6 ± 0.7
$B \to \Lambda\ X$	$3.8 \pm 0.4 \pm 0.6$	$4.2 \pm 0.5 \pm 0.6$		4.0 ± 0.5
$B \to \Xi^-\ X$	$0.27 \pm 0.05 \pm 0.04$	0.28 ± 0.14		0.27 ± 0.06
$\bar{B} \to \Lambda_c\ X$	$6.3 \pm 1.2 \pm 0.9 \pm 1.9$	$7.0 \pm 2.8 \pm 1.4 \pm 2.1$		$6.4 \pm 1.3 \pm 1.9$
$\bar{B} \to \Sigma_c^0\ X$			$0.53 \pm 0.19 \pm 0.16 \pm 0.16$	
$\bar{B} \to \Sigma_c^{++}\ X$			$0.50 \pm 0.18 \pm 0.15 \pm 0.15$	
$\bar{B} \to \Sigma_c^0 \bar{N}$			< 0.17 (90% C.L.)	
$\bar{B} \to \Sigma_c^{++} \bar{\Delta}^{--}$			< 0.12 (90% C.L.)	

TABLE XI. Branching fractions [%] of inclusive B decays to baryon pairs.

Mode	CLEO 1.5	ARGUS
$B \to p\bar{p}\ X$	$2.4 \pm 0.1 \pm 0.4$	$2.5 \pm 0.2 \pm 0.2$
$B \to \Lambda\bar{\Lambda}\ X$	< 0.5 (90% C.L.)	< 0.88 (90% C.L.)
$B \to \Lambda\bar{p}\ X$	$2.9 \pm 0.5 \pm 0.5$	$2.3 \pm 0.4 \pm 0.3$
$B \to D^{*+}p\bar{p}\ X$	< 0.35 (90% C.L.)	
$B \to DN\bar{N}\ X$	< 5.2 (90% C.L.)	

3. $\bar{B} \to Y_c \bar{Y} X$, $\bar{B} \to \Xi_c \bar{Y}_c X$
   These states are produced by the internal spectator graph with $W^- \to \bar{c}s$ in conjunction with the popping of two quark antiquark pairs. Since $\mathcal{B}(W^- \to \bar{c}s)/\mathcal{B}(W^- \to all)$ is about 0.15, this mechanism may be suppressed.

4. $\bar{B} \to D_s^- Y_c \bar{N} X$, $\bar{B} \to D_s^- \Xi_c \bar{Y} X$
   This is the same as mechanism (1) with $W^- \to \bar{c}s$.

The low rates for $B \to \Lambda\bar{\Lambda}X$, $\Lambda\bar{p}X$ and $D^* p\bar{p}X$ suggest that mechanism (2) is small (Table XI). The absence of a two body component in the momenta spectra of $B \to \Lambda_c X$, $\Sigma_c X$ indicates that the W-exchange and internal spectator mechanisms are small. Thus it is reasonable to assume that $\bar{B} \to Y_c \bar{N} X$ with an external spectator $b \to cW^-$ coupling (Fig. 7(a)) is the principal mechanism in B to baryon transitions.

If B decays to baryons are dominated by $\bar{B} \to \Lambda_c \bar{p} X$ and $\bar{B} \to \Lambda_c \bar{n} X$ then measurements of the branching ratios for $B \to \bar{p}X$, $B \to p\bar{p}X$ can be used to extract the absolute $\Lambda_c \to pK^-\pi^+$ branching ratio. The CLEO 1.5 measurements give $B(\Lambda_c \to pK^-\pi^+) = 4.3 \pm 1.0 \pm 0.8\%$ which can be used to normalize all other measured Λ_c branching ratios. In a similar analysis ARGUS finds $(4.1 \pm 2.4)\%$ for this branching ratio.

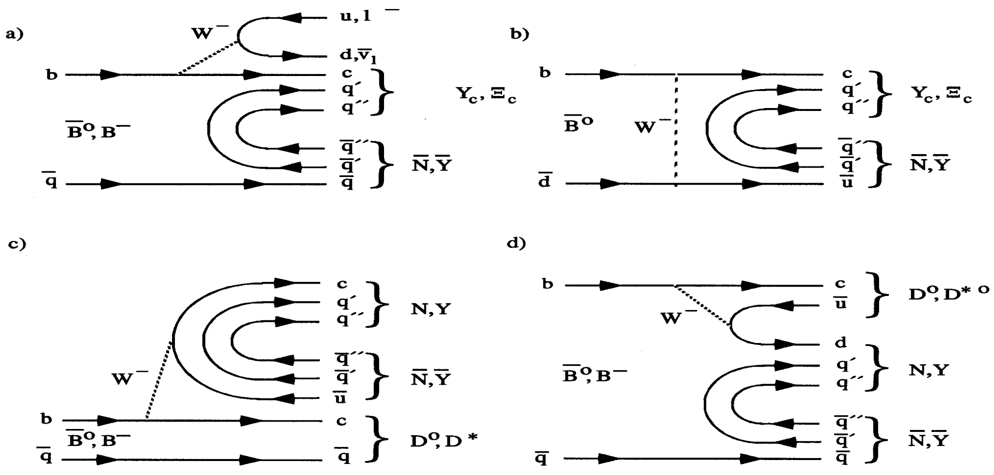

FIG. 7. Decay diagrams for B meson decays to baryons: (a) External Spectator Diagram (b) W Exchange Diagram (c) External Spectator Diagram producing $DN\bar{N}X$ and $DY\bar{Y}X$ (d) Internal Spectator Diagram producing $DN\bar{N}X$ and $DY\bar{Y}X$.

D. Charm Production in B Decay

The measurements of inclusive decay rates can be used to test the parton level expectation that almost all B decays proceed via a $b \to c$ transition. This means $\mathcal{B}(B \to D^0 X) + \mathcal{B}(B \to D^+ X) + \mathcal{B}(B \to D_s X) + \mathcal{B}(B \to \Lambda_c X) + 2f \times \mathcal{B}(B \to \psi X)$ should be about 115%, where the extra 15% is due to the fact that the virtual W should form a $s\bar{c}$ quark pair with a probability of 0.15 . The small contributions from $b \to u$, penguin transitions and contributions from $B \to \Xi_c X$ not proceeding through a Λ_c have been neglected. The factor of 2 which multiplies $\mathcal{B}(B \to \psi X)$ accounts for the two charm quarks, while the factor $f = 2$ is a generous estimate of the contribution from charmonium states that do not decay via ψ. The CLEO 1.5 result of $104.4 \pm 7.7\%$ and the ARGUS result of $93.3 \pm 10.5\%$ can be combined to give a world average of $100.2 \pm 6.6\%$ for the average number of charm quarks produced in a B decay. While the existing data are not yet sufficiently precise to make a convincing case for a charm deficit in B decay, there are several possible explanations for a deviation from the parton level expectation. There may be systematic biases in the method of determining inclusive production rates at the $\Upsilon(4S)$. The charm meson absolute branching fractions can also contribute a systematic uncertainty, although this error has been significantly reduced by the new determination of $\mathcal{B}(D^0 \to K^- \pi^+)$ [18]. There could be a breakdown of the parton level approximation in B decay, or there could be a large contribution to the inclusive rate that has not been included. It has been suggested by Palmer and Stech [41], that $b \to c\bar{c}s$ followed by $c\bar{c} \to$ gluons, which in turn hadronize into a final state with no charm, has a large branching ratio. Another suggestion is that the rate for the hadronic penguin diagram $b \to sg$ is larger than expected.

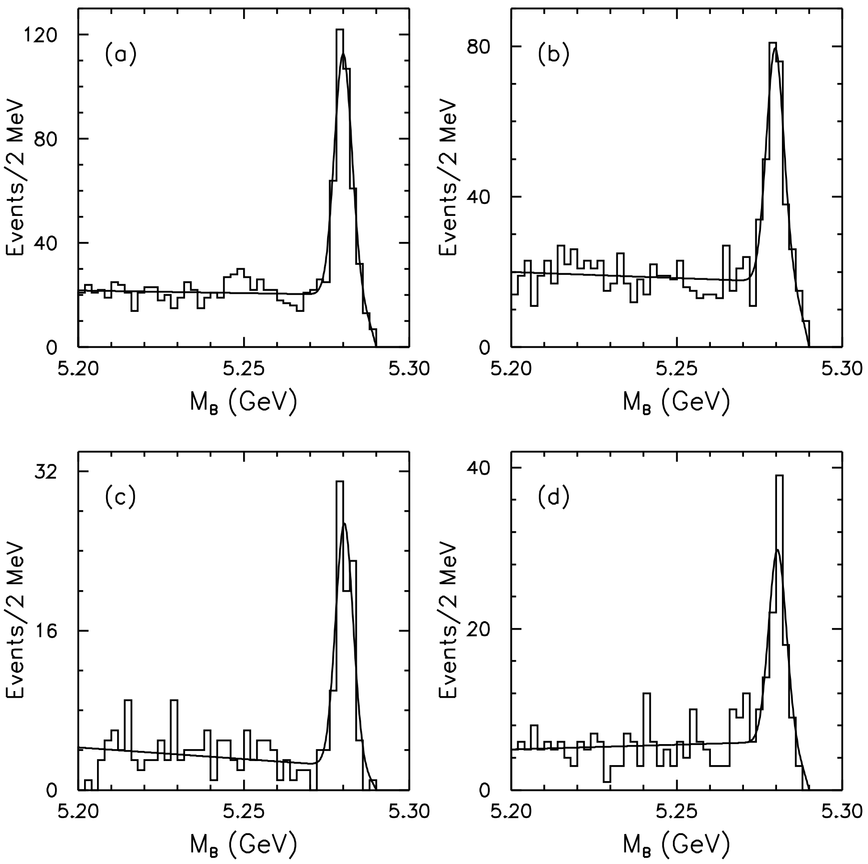

FIG. 8. The beam constrained mass distributions from CLEO II for: (a) $B^- \to D^0\pi^-$ decays. (b) $B^- \to D^0\rho^-$ decays for $|\cos\Theta_\rho| > 0.4$. (c) $\bar{B}^0 \to D^+\pi^-$ decays . (d) $\bar{B}^0 \to D^+\rho^-$ decays for $|\cos\Theta_\rho| > 0.4$.

IV. B MESON RECONSTRUCTION

A. Selection of B Candidates

As an example of the techniques of B reconstruction we will briefly describe the procedure used by the CLEO II experiment to reconstruct the decay modes $B \to D^{(*)}(n\pi)^-$. The CLEO II detector is described in detail elsewhere [45]. It has a momentum resolution for charged tracks given by $(\delta p/p)^2 = (0.0015p)^2 + (0.005)^2$, and an energy resolution for isolated photons from the CsI barrel calorimeter of $\delta E/E[\%] = 0.35/E^{0.75} + 1.9 - 0.1E$, where p and E are in GeV. Charged tracks are identified as pions or kaons if they have ionization loss information (dE/dx), and/or time-of-flight information (ToF), consistent with the correct particle hypothesis. Photon candidates are selected from showers in the calorimeter barrel with a minimum energy of 30 MeV, which are not matched to charged tracks, and which have a lateral energy distribution consistent with that expected for a photon. Neutral pions are selected from pairs of photons with an invariant mass within 2.5σ of the known π^0 mass.

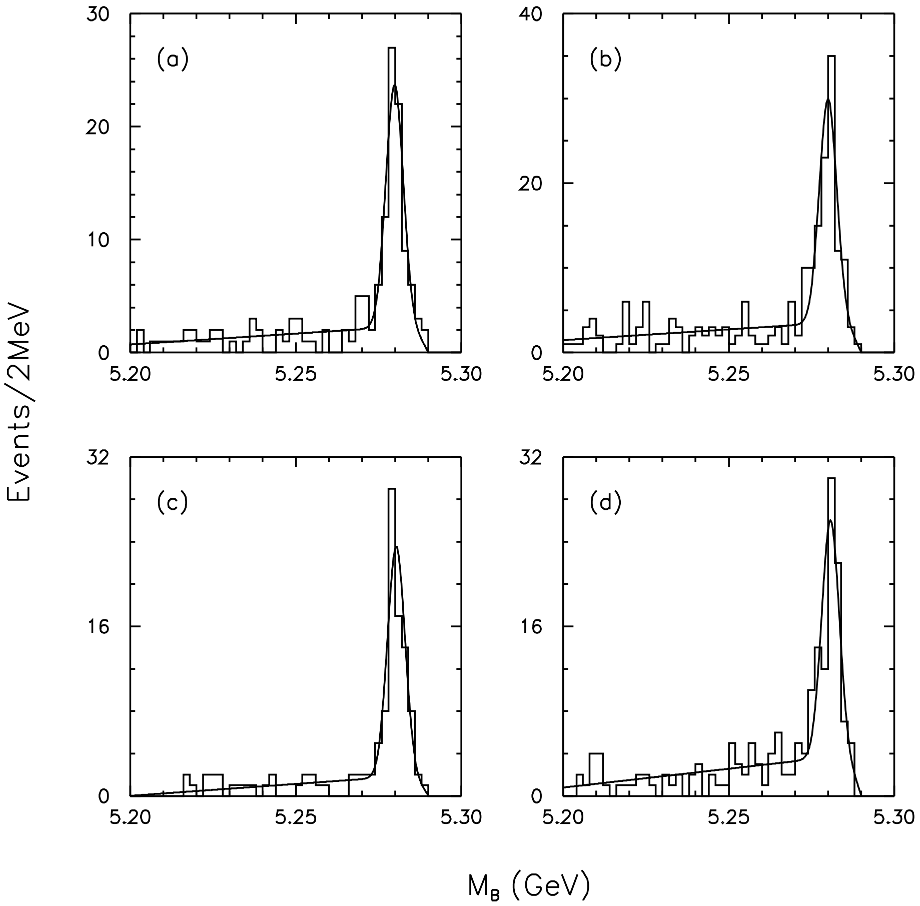

FIG. 9. Beam constrained mass distributions from CLEO II for: (a) $B^- \to D^{*0}\pi^-$ decays, (b) $B^- \to D^{*0}\rho^-$ decays, (c) $\bar{B}^0 \to D^{*+}\pi^-$ decays, and (d) $\bar{B}^0 \to D^{*+}\rho^-$ decays.

Candidate D^0 mesons are identified in the decay modes $D^0 \to K^-\pi^+$, $D^0 \to K^-\pi^+\pi^0$, and $D^0 \to K^-\pi^+\pi^+\pi^-$, while D^+ mesons are identified in the decay mode $D^+ \to K^-\pi^+\pi^+$. Charged D^* candidates are found using the decay $D^{*+} \to D^0\pi^+$, while neutral D^* candidates are found using the decay $D^{*0} \to D^0\pi^0$. Other D and D^* decay modes are not used because of poorer signal to background ratios, or because of lower yields [46]. The reconstructed D masses and $D^* - D^0$ mass differences are required to be within 2.5σ of the known values.

The D meson candidates are combined with one or more additional pions to form a B candidate. Cuts on the topology of the rest of the event are made in order to distinguish $B\bar{B}$ events from continuum background, as discussed in Section II A. The following requirements are imposed: $R_2 < 0.5$, and $|\cos(\theta_S)| < 0.9(0.8, 0.7)$ depending on whether there are one(two,three) pions added to the D meson. The cosine of the sphericity angle θ_S is uniformly distributed for signal, but peaks near ± 1 for continuum background. Requiring that $|\cos(\theta_S)|$ be less than 0.7 typically removes 80% of the continuum background, while retaining 70% of the B decays.

The measured sum of charged and neutral energies, E_{meas}, of correctly reconstructed B mesons produced at the $\Upsilon(4S)$, must equal the beam energy, E_{beam}, to within the exper-

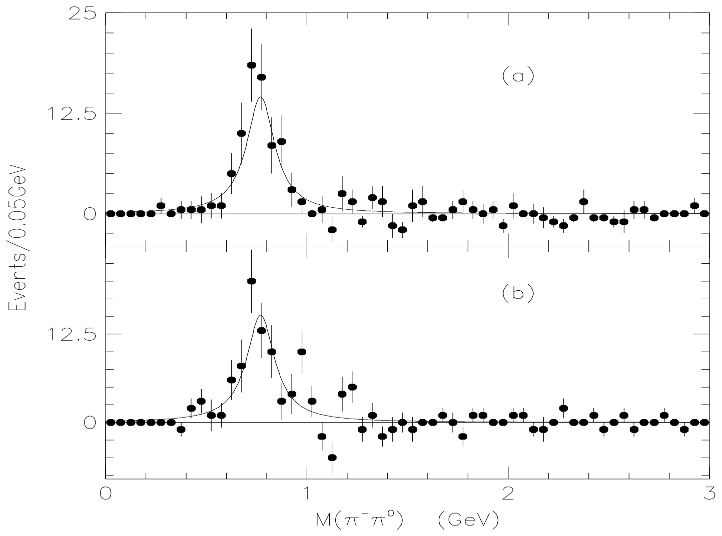

FIG. 10. Resonant substructure for $B \to D^*\rho^-$ from CLEO II for: (a) the $\pi^0\pi^-$ invariant mass spectrum for the $\bar{B}^0 \to D^{*+}\pi^0\pi^-$ decay mode in data. (b) the $\pi^0\pi^-$ invariant mass spectrum for the $\bar{B}^0 \to D^{*+}\pi^0\pi^-$ decay mode in data.

imental resolution. Depending on the B decay mode, $\sigma_{\Delta E}$, the resolution on the energy difference $\Delta E = E_{beam} - E_{meas}$ varies between 14 and 46 MeV. Note that this resolution is usually sufficient to distinguish the correct B decay mode from a mode that differs by one pion. For final states with a fast ρ^- the energy resolution depends on the momenta of the final state pions from the ρ meson. This dependence is conveniently parameterized as a function of the angle between the π^- direction in the ρ^- rest frame and the ρ^- direction in the lab frame, which we denote as the ρ helicity angle, Θ_ρ. When $\cos\Theta_\rho = +1$, the error in the energy measurement is dominated by the momentum resolution on the fast π^-, whereas at $\cos\Theta_\rho = -1$ the largest contribution to the error in the energy measurement comes from the calorimeter energy resolution on the fast π^0.

To determine the signal yield and display the data the beam constrained mass is formed

$$M_B^2 = E_{beam}^2 - \left(\sum_i \vec{p_i}\right)^2, \tag{1}$$

where $\vec{p_i}$ is the momentum of the i-th daughter of the B candidate. The resolution in this variable is determined by the beam energy spread, and is about 2.7 MeV for CLEO II, and about 4.0 MeV for ARGUS. [47] These resolutions are a factor of ten better than the resolution in invariant mass obtained without the beam energy constraint.

For a specific B decay chain, such as $B^- \to D^0\pi^-$, $D^0 \to K^-\pi^+\pi^0$ there may be multiple combinations in a given decay chain. In the CLEO II analysis, if there are multiple candidates only the entry with the smallest absolute value of ΔE is selected for events with $M_B > 5.2$ GeV. An alternative method is to select the candidate with the highest total probability as calculated from the sum of all χ^2 contributions from particle identification, kinematical fits and the beam energy constraint [14].

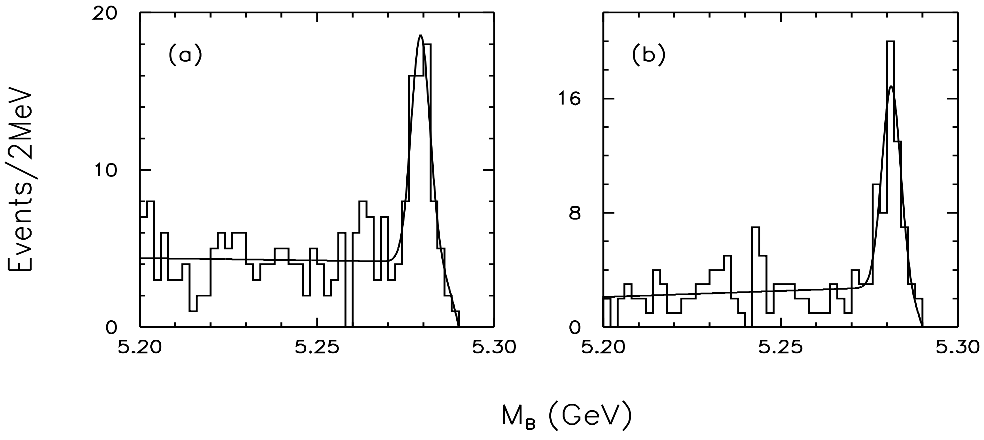

FIG. 11. Beam constrained mass distributions from CLEO II for: (a) $B^- \to D^{*0} a_1^-$ and (b) $\bar{B}^0 \to D^{*+} a_1^-$.

B. Background Studies

In order to extract the number of signal events it is crucial to understand the shape of the background in the M_B distribution. There are two contributions to this background, continuum and other $B\bar{B}$ decays. The fraction of continuum background varies between 58% and 91% depending on the B decay mode [48]. The shape of the continuum background is well understood since it depends primarily on the transverse momentum distributions of the final state particles relative to the jet axis. This has been studied using the off-resonance data sample, and using Monte Carlo techniques.

The shape of the $B\bar{B}$ background is more difficult to understand since it is mode dependent. It also has a tendency to peak in the signal region, since the combinatorial background comes mostly from combinations in which the true final state is altered by one low energy particle. A particularly troublesome background occurs when the decay $D^{*0} \to D^0\gamma$ is replaced by the decay $D^{*0} \to D^0\pi^0$. To determine the correct background shape for each B decay mode, CLEO II has studied the M_B distributions for ΔE sidebands, and for combinations in which the charged particles have the wrong charges for the expected spectator decay diagram, e.g. $D^+\pi^+$ and $\bar{D}^0\pi^+$.

It is found that all of the background distributions can be fitted with a linear background below M_B=5.282 GeV, and a smooth kinematical cutoff at the endpoint, which is chosen to be parabolic. For each B decay mode CLEO II uses this background function and a Gaussian signal with a fixed width of 2.64 MeV to determine the yield of signal events. In the ARGUS and CLEO 1.5 experiments slightly different background parameterizations were used [49].

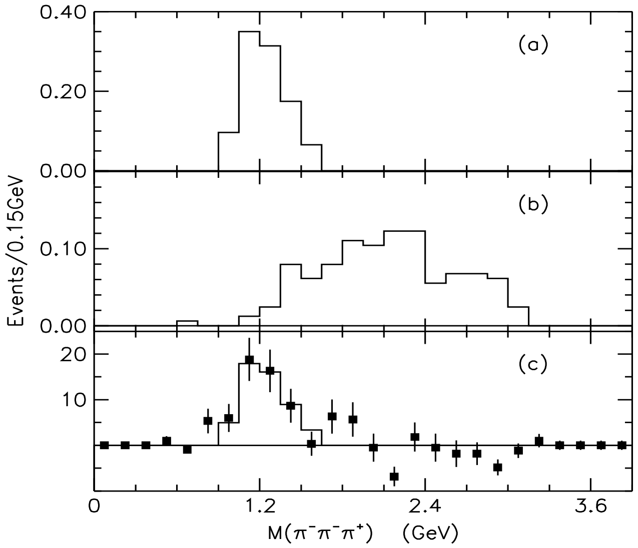

FIG. 12. Resonant substructure of $\bar{B}^0 \to D^{*+} a_1$ from CLEO II: (a) The $\pi^-\pi^-\pi^+$ invariant mass spectrum from a Monte Carlo simulation of $\bar{B}^0 \to D^{*+} a_1^-$ (b) The $\pi^-\pi^-\pi^+$ invariant mass spectrum from Monte Carlo simulation for $\bar{B}^0 \to D^{*+}(\pi^-\rho^0)_{NR}$ (c) The $\pi^-\pi^-\pi^+$ mass spectrum from data after B mass sideband subtraction. The fit to the sum of (a) and (b) is superimposed.

V. EXCLUSIVE B DECAY TO D MESONS

A. Measurements of $D(n\pi)^-$ Final States

The decay modes $\bar{B}^0 \to D^+\pi^-$, $\bar{B}^0 \to D^+\rho^-$, $B^- \to D^0\pi^-$, and $B^- \to D^0\rho^-$ are reconstructed following the procedures outlined in Section IV. The beam constrained mass distributions from CLEO II are shown in Fig. 8, while the experimental branching ratios are given in Tables XVI and XVII .

To select $\bar{B} \to D\rho^-$ candidates additional requirements are imposed on the $\pi^-\pi^0$ invariant mass and the ρ helicity angle. The CLEO II analysis requires $|m(\pi^-\pi^0) - 770| < 150$ MeV and $|\cos\Theta_\rho| > 0.4$. For the $B \to D\rho^-$ modes there are events which are consistent with both $B \to D\rho^-$ and with $B \to D^*\pi^-$, followed by $D^* \to D\pi^0$. These events are removed from the $B \to D\rho^-$ sample using a cut on the $D^* - D$ mass difference. By fitting the $\pi^-\pi^0$ mass spectrum and the helicity angle distribution, CLEO II finds that at least 97.5% of the $B \to D\pi^-\pi^0$ rate is described by the decay $B \to D\rho^-$ [50]. ARGUS [12] also finds that the $\pi^-\pi^0$ mass spectrum is consistent with the dominance of ρ production.

B. Measurements of $D^*(n\pi)^-$ Final States

We now consider final states containing a D^* meson and one, two or three pions. These include the $B \to D^*\pi^-$, $B \to D^*\rho^-$, and $B \to D^* a_1^-$ decay channels. The results for the

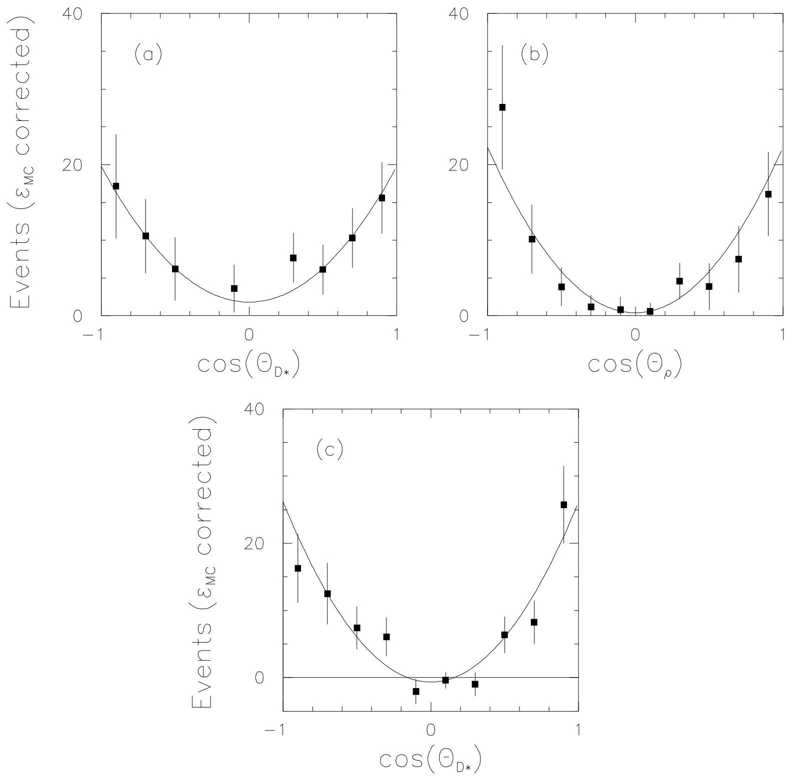

FIG. 13. Angular distributions (efficiency corrected) from CLEO II for (a) the helicity angle from $D^{*+} \to D^0\pi^+$ in $\bar{B}^0 \to D^{*+}\rho^-$ and (b)the helicity angle from $\rho^- \to \pi^-\pi^0$ in $\bar{B}^0 \to D^{*+}\rho^-$ (c) the helicity angle from $D^{*+} \to D^0\pi^+$ in $\bar{B}^0 \to D^{*+}\pi^-$

decays $\bar{B}^0 \to D^{*+}\pi^-$, $\bar{B}^0 \to D^{*+}\rho^-$ and $\bar{B}^0 \to D^{*+}\pi^-\pi^-\pi^+$ are listed in Table XVII, and the results for $B^- \to D^{*0}\pi^-$, $B^- \to D^{*0}\rho^-$ and $B^- \to D^{*0}\pi^-\pi^-\pi^+$ are given in Table XVI.

The CLEO II B^- and $\bar{B}^0$ signals in the $D^*\pi$ and $D^*\rho$ decay channels are shown in Fig. 9. They find that $B \to D^*\pi^-\pi^0$ is saturated by the decay $B \to D^*\rho^-$ (Fig. 10) and set a tight upper limit of $< 9\%$ at 90% C.L. on a possible non-resonant contribution [51]. This disagrees with an ARGUS analysis that finds about 50% of $\bar{B}^0 \to D^{*+}\pi^-\pi^0$ decays do not contain a ρ^- meson [14].

The CLEO II data suggest that the signal in $B \to D^*\pi^-\pi^-\pi^+$ arises dominantly from $B \to D^*a_1^-$. Taking into account the $a_1 \to \pi^-\pi^-\pi^+$ branching fractions it follows that $\mathcal{B}(B \to D^*a_1^-) = 2 \times \mathcal{B}(B \to D^*\pi^-\pi^-\pi^+)$. In Fig. 11 we show the M_B distributions when the $\pi^-\pi^-\pi^+$ invariant mass is required to be in the interval $1.0 < \pi^-\pi^-\pi^+ < 1.6$ GeV. Fig. 12 shows a fit to the $\pi^-\pi^-\pi^+$ mass distributions with contributions from $B \to D^{*+}a_1^-$ and a $B \to D^{*+}\pi^-\rho^0$ non-resonant background. The a_1 meson has been parameterized as a Breit-Wigner resonance shape with $m_{a_1} = 1182$ MeV and $\Gamma_{a1} = 466$ MeV. This fit gives an upper limit of 13% on the non-resonant component in this decay. This conclusion differs from CLEO 1.5 which attributed $(35 \pm 15 \pm 8)\%$ of their $\bar{B}^0 \to D^{*+}\pi^-\pi^-\pi^+$ signal to non-resonant $\bar{B}^0 \to D^{*+}\pi^-\rho^0$ decays [9]. ARGUS also finds a significant non-a_1 component in

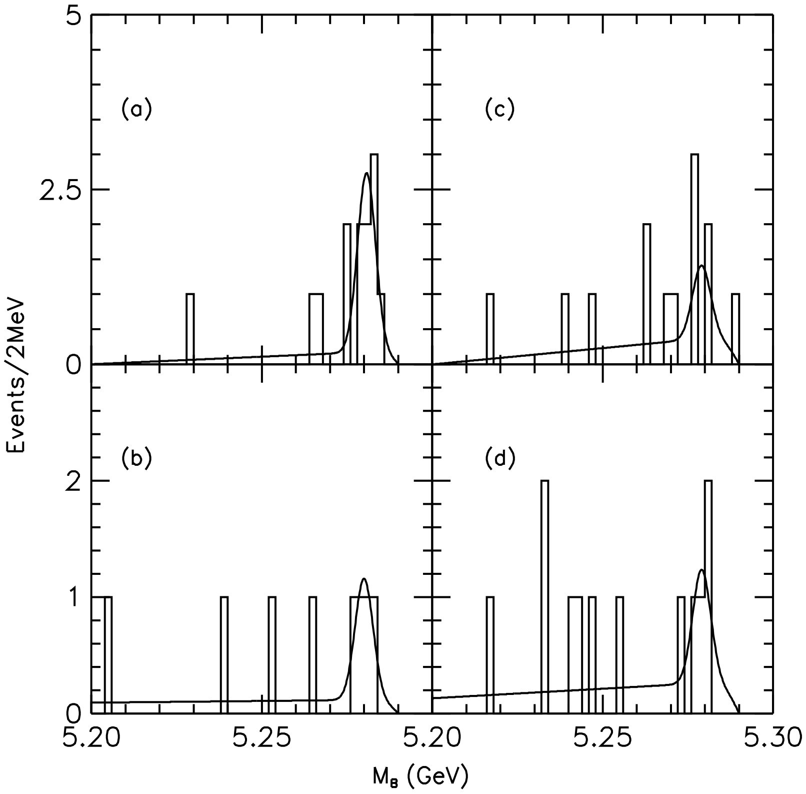

FIG. 14. Beam constrained mass distributions from CLEO II for: (a) $B^- \to D^{**0}(2420)\pi^-$ where $D^{**0}(2420) \to D^{*+}\pi^-$, (b) $B^- \to D^{**0}(2460)\pi^-$ where $D^{**0}(2460) \to D^{*+}\pi^-$, (c) $B^- \to D^{**0}(2420)\pi^-\pi^0$ where $D^{**0}(2420) \to D^{*+}\pi^-$, (d) $B^- \to D^{**0}(2460)\pi^-\pi^0$ where $D^{**0}(2460) \to D^{*+}\pi^-$

this decay but does not quote a quantitative result [14].

C. Polarization in $B \to D^{*+}\rho^-$ Decays

The sample of fully reconstructed $\bar{B}^0 \to D^{*+}\rho^-$ decays from CLEO II has been used to measure the D^{*+} and ρ^- polarizations. By comparing the measured polarizations in $\bar{B}^0 \to D^{*+}\rho^-$ with the expectation from the corresponding semileptonic B decay a test of the factorization hypothesis can be performed (see Sec. IX B). The polarization is obtained from the distributions of the helicity angles Θ_ρ and Θ_{D^*}. The D^{*+} helicity angle, Θ_{D^*}, is the angle between the D^0 direction in the D^{*+} rest frame and the D^{*+} direction in the rest frame of the B meson. After integration over χ, the angle between the normals to the D^{*+} and the ρ^- decay planes, the helicity angle distribution can be expressed as:

$$\frac{d^2\Gamma}{d\cos\Theta_{D^*}\, d\cos\Theta_\rho} \propto \frac{1}{4}\sin^2\Theta_{D^*}\sin^2\Theta_\rho(|H_{+1}|^2 + |H_{-1}|^2) + \cos^2\Theta_{D^*}\cos^2\Theta_\rho|H_0|^2 \qquad (2)$$

The fraction of longitudinal polarization is defined by

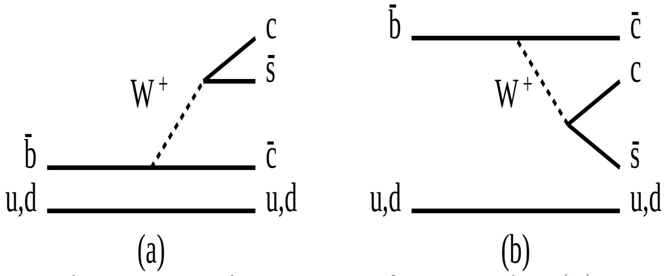

FIG. 15. B meson decay diagrams with emission of $c\,\bar{s}$ quarks: (a) external spectator and (b) color suppressed.

$$\frac{\Gamma_L}{\Gamma} = \frac{|H_0|^2}{|H_{+1}|^2 + |H_{-1}|^2 + |H_0|^2} \tag{3}$$

If Γ_L is large both the D^{*+} and the ρ^- helicity angles will follow a $\cos^2\Theta$ distribution, whereas a large transverse polarization, Γ_T, gives a $\sin^2\Theta$ distribution for both helicity angles.

To measure the polarization the helicity angle distributions in the B signal region are corrected by subtracting the distributions from a properly scaled mass sideband. The resulting helicity angle distributions, corrected for efficiency, are fitted to the functional form:

$$\frac{d\Gamma}{d\cos\Theta} = N\ \left[\cos^2\Theta\ +\ \frac{1}{2}\frac{\Gamma_T}{\Gamma}(1 - 3\cos^2\Theta)\right]. \tag{4}$$

This form is derived from the angular distribution given above. It is well behaved for large longitudinal polarization. From the fit to the D^{*+} helicity angle distribution, they find $\Gamma_L/\Gamma = (88 \pm 10)\%$, while a fit to the ρ helicity angle distribution gives $\Gamma_L/\Gamma = (91 \pm 10)\%$. The results of the fit are shown in Fig. 13(a) and (b). As a consistency check they have verified that the D^{*+} mesons in $\bar{B}^0 \to D^{*+}\pi^-$ are completely longitudinally polarized, as expected from angular momentum conservation (Fig. 13(c)).

The statistical errors can be reduced by taking advantage of the correlation between the two helicity angles. An unbinned two dimensional likelihood fit to the joint $(\cos\Theta_{D^*}, \cos\Theta_\rho)$ distribution gives

$$(\Gamma_L/\Gamma)_{\bar{B^0}\to D^{*+}\rho^-}\ =\ 90 \pm 7 \pm 5\% \tag{5}$$

D. Measurements of D^{**} Final States

In addition to the production of D and D^* mesons, the charm quark and spectator antiquark can hadronize as a D^{**} meson. The $D^{**0}(2460)$ has been observed experimentally and identified as the $J^P = 2^+$ state, while the $D^{**0}(2420)$ has been identified as the 1^+ state. These states have full widths of approximately 20 MeV. Two other states, a 0^+ and another 1^+ are predicted but have not yet been observed, presumably because of their large intrinsic

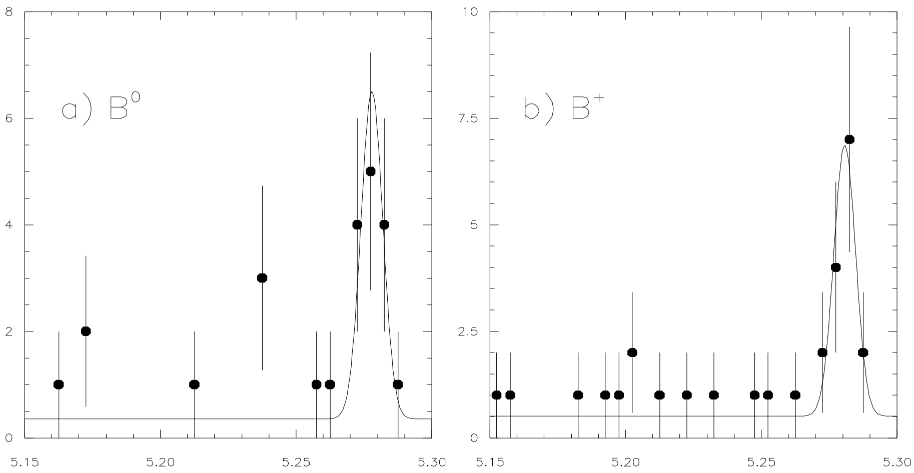

FIG. 16. The beam constrained mass distributions from ARGUS for: (a) the sum of $\bar{B}^0 \to D_s^- D^+$, $\bar{B}^0 \to D_s^- D^{*+}$, $\bar{B}^0 \to D_s^{*-} D^+$, and $\bar{B}^0 \to D_s^{*-} D^{*+}$ and (b) the sum of $B^+ \to D_s^+ \bar{D}^0$, $B^+ \to D_s^+ \bar{D}^{*0}$, $B^+ \to D_s^{*+} \bar{D}^0$, and $B^+ \to D_s^{*+} \bar{D}^{*0}$.

widths. There is evidence for D^{**} production in semileptonic B decays [53], and D^{**} mesons have also been seen in hadronic decays. However, early experiments did not have sufficient data to separate the two narrow D^{**} states and hence reported branching ratios only for the combination of the two (see results listed under $B \to D_J^{(*)0}$ in Tables XVI – XIX).

In order to search for D^{**} mesons from B decays the final states $B^- \to D^{*+}\pi^-\pi^-$ and $B^- \to D^{*+}\pi^-\pi^-\pi^0$ are studied. These decay modes are not expected to occur via a spectator diagram in which the c quark and the spectator antiquark form a D^* rather than a D^{**} meson. The D^{*+} is combined with a π^- to form a D^{**} candidate. If the D^{**} candidate is within one full width of the nominal mass of either a $D^{**0}(2420)$ or a $D^{**0}(2460)$, it is combined with a π^- or ρ^- to form a B^- candidate. CLEO II has also looked for D^{**} production in the channels $B^- \to D^+\pi^-\pi^-$ and $\bar{B}^0 \to D^0\pi^-\pi^+$. Since $D^{**0}(2420) \to D\pi$ is forbidden, only the $D^{**0}(2460)$ is searched for in the $D\pi\pi$ final state.

Fig. 14 shows candidate B mass distributions obtained by CLEO II for the four combinations of $D^{**0}(2460)$ or $D^{**0}(2420)$, and π^- or ρ^-. In the $D^{**0}(2420)\pi^-$ mode, there is a significant signal of 8.5 events on a background of 1.5 events. In this channel CLEO II quotes the branching ratio given in Table XVI, while for the other three channels, they give upper limits. ARGUS has also found evidence for $B \to D^{**}(2420)\pi^-$ using a partial reconstruction technique in which they observe a fast and slow pion from the D^{**} decay but do not reconstruct the D^0 meson [52].

E. Exclusive Decays to D and D_s Mesons

Another important class of modes are decays to two charmed mesons. As shown in Fig. 15 (a) the production of an isolated pair of charmed mesons ($D_s^{(*)}$ and $D^{(*)}$) proceeds through

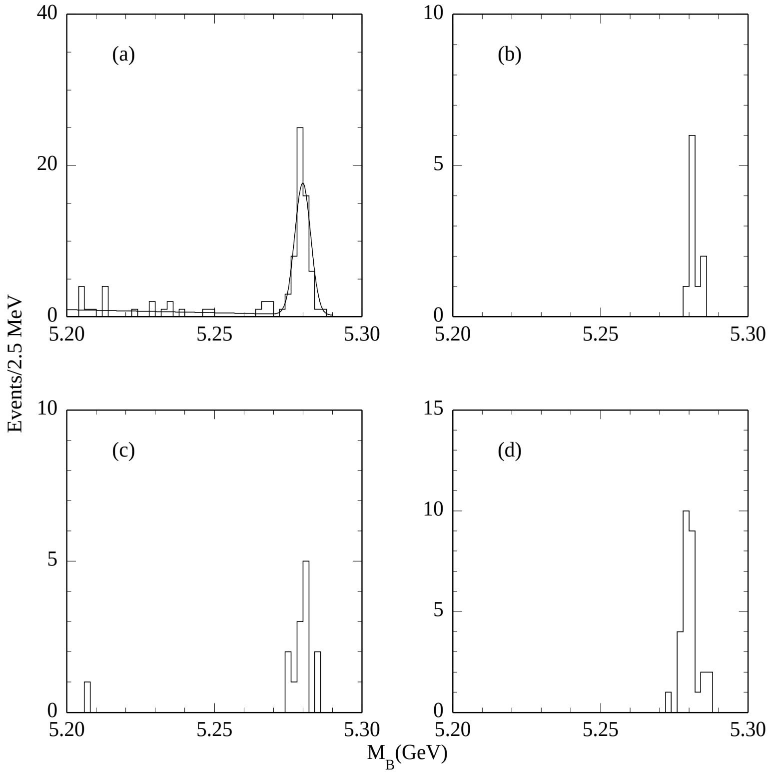

FIG. 17. Beam-constrained mass from CLEO II for: (a) $B^- \to \psi K^-$, (b) $\bar{B}^0 \to \psi \bar{K}^0$, (c) $B^- \to \psi \bar{K}^{*-}$, and (d) $\bar{B}^0 \to \psi K^{*0}$.

a Cabibbo favored spectator diagram in which the $s\bar{c}$ pair from the virtual W^- hadronizes into a D_s^- or a D_s^{*-} meson and the remaining spectator quark and the c quark form a $D^{(*)}$ meson. These modes have been observed by the CLEO 1.5 [54] and ARGUS [21] experiments. The decay channels listed in Table XII are used to form D_s meson candidates. B mesons are then reconstructed in eight decay modes: $D_s^- D^+$, $D_s^- D^0$, $D_s^{*-} D^+$, $D_s^{*-} D^0$, $D_s^- D^{*+}$, $D_s^- D^{*0}$, $D_s^{*-} D^{*+}$, and $D_s^{*-} D^{*0}$. The results of the ARGUS experiment are shown in Fig. 16.

Improvements in the size of the signals for these modes are expected from CLEO II which has measured additional D_s modes with neutrals (e.g. $D_s \to \eta\pi, \eta\rho$) [55]. Partial reconstruction techniques are also being investigated for $B \to D^* D_s^*$.

VI. COLOR SUPPRESSED B DECAY

A. Exclusive B Decays to Charmonium

In B decays to charmonium the c quark from the b combines with a $\bar{c}$ quark from the virtual W^- to form a charmonium state. This process is described by the color suppressed diagram shown in Fig. 15(b). By comparing B meson decays to different final states with charmonium mesons the dynamics of this decay mechanism can be investigated.

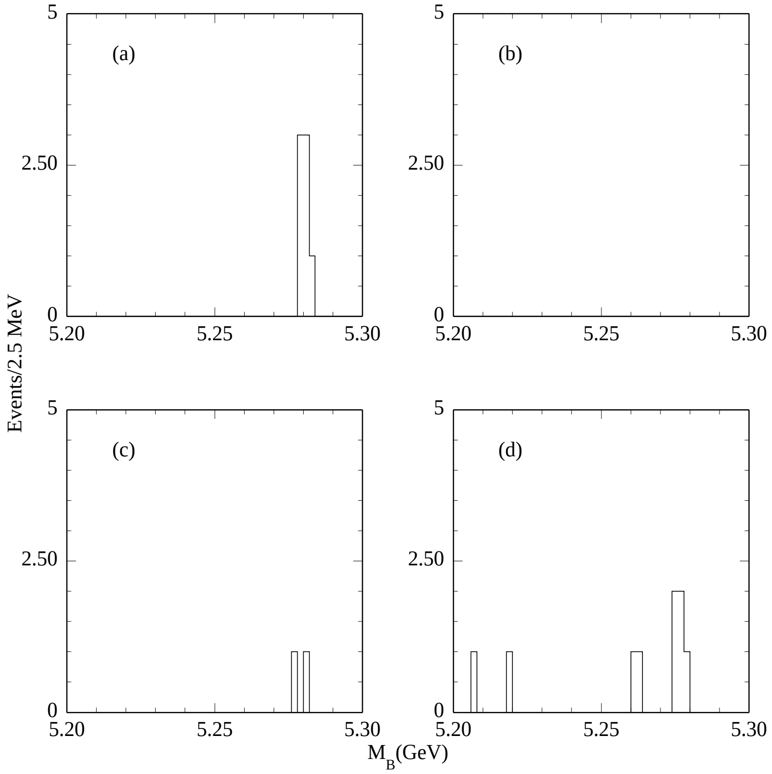

FIG. 18. Beam-constrained mass from CLEO II for: (a) $B^- \to \psi' K^-$, (b) $\bar{B}^0 \to \psi' \bar{K}^0$, (c) $B^- \to \psi' \bar{K}^{*-}$, and (d) $\bar{B}^0 \to \psi' K^{*0}$.

The decay modes $\bar{B}^0 \to \psi K^0$ and $\bar{B}^0 \to \psi' K^0$ are of special interest since the final states are CP eigenstates. These decays are of great importance for the investigation of one of the three CP violating angles accessible to study in B decays. It is also possible to use the decay $\bar{B}^0 \to \psi K^{*0}$, $K^{*0} \to K^0 \pi^0$ which has a somewhat higher branching ratio, but this final state consists of a mixture of CP eigenstates. It has even CP if the orbital angular momentum L is 0 or 2 and odd CP for L=1. If both CP states are present the CP asymmetry will be diluted. A measurement of CP violation in this channel is only possible if one of the CP states dominates, or if a detailed moments analysis of the various decay components is performed [56]. Recent measurements of the polarization in the decay $\bar{B}^0 \to \psi \bar{K}^{*0}$ allow us to determine the fractions of the two CP states.

B meson candidates are formed by combining a charmonium and a strange meson candidate. CLEO 1.5 and ARGUS have observed signals for some of these modes. Using the procedures outlined in Sec. IV the beam constrained mass distributions shown in Fig. 17 and Fig. 18 are obtained by CLEO II. The branching ratios are listed in Tables XVI and XVII . Recently, CDF has reported signals for $B \to \psi K^{*0}$ and $B \to \psi K^-$ (see Fig. 21).

The ratio of vector to pseudoscalar meson production

$$\frac{\mathcal{B}(B \to \psi K^*)}{\mathcal{B}(B \to \psi K)} = 1.64 \pm 0.34. \tag{6}$$

can be calculated using factorization and the ratio of the $B \to K^*$ and $B \to K$ form factors.

TABLE XII. D_s decay channels used to reconstruct $B \to DD_s$ decays.

ARGUS [21]	CLEO 1.5 [54]
$D_s^+ \to \phi\pi^+$	$D_s^+ \to \phi\pi^+$
$D_s^+ \to \phi\pi^+\pi^0$	
$D_s^+ \to \phi\pi^+\pi^+\pi^-$	
$D_s^+ \to K_sK^+$	$D_s^+ \to K_sK^+$
$D_s^+ \to K_sK^{*+}$	
$D_s^+ \to \bar{K}^{*0}K^+$	$D_s^+ \to \bar{K}^{*0}K^+$
$D_s^+ \to K^{*0}\bar{K}^*+$	$D_s^+ \to \bar{K}^{*0}K^{*+}$
$D_s^+ \to \eta'\pi^+$	

TABLE XIII. Upper limits (90% C.L) on color suppressed B decays.

Decay Mode	Events	U. L. (%)
$\bar{B}^0 \to D^0\pi^0$	< 14.7	< 0.035
$\bar{B}^0 \to D^0\rho^0$	< 10.4	< 0.042
$\bar{B}^0 \to D^0\eta$	< 9.2	< 0.075
$\bar{B}^0 \to D^0\eta'$	< 2.3	< 0.074
$\bar{B}^0 \to D^0\omega$	< 9.1	< 0.048
$\bar{B}^0 \to D^{*0}\pi^0$	< 7.0	< 0.072
$\bar{B}^0 \to D^{*0}\rho^0$	< 6.8	< 0.092
$\bar{B}^0 \to D^{*0}\eta$	< 2.3	< 0.086
$\bar{B}^0 \to D^{*0}\eta'$	< 2.3	< 0.33
$\bar{B}^0 \to D^{*0}\omega$	< 5.6	< 0.13

However, it is not certain that factorization is a good approximation for the color suppressed diagram. The revised BSW model [57] predicts a value of 1.61 for this ratio, which is close to the experimental value. Another test is the ratio

$$\frac{\mathcal{B}(B \to \psi' K^*)}{\mathcal{B}(B \to \psi' K)} = 1.9 \pm 1.1. \qquad (7)$$

This can be compared to the revised BSW model which predicts 1.85 for this ratio. Evidence for the decay mode $B \to \chi_c K$ has been reported by CLEO II and ARGUS. The average branching fraction is $\mathcal{B}(B^- \to \chi_c K^-) = (0.133 \pm 0.065)\%$.

B. Polarization in $B \to \psi K^*$

The polarization in $B \to \psi K^*$ is studied using the methods described for the $\bar{B}^0 \to D^{*+}\rho^-$ polarization measurement in Section V C. After integration over the azimuthal angle between the ψ and the K^* decay planes, the angular distribution in $B \to \psi K^*$ decays can be written as

$$\frac{d^2\Gamma}{d\cos\Theta_\psi \, d\cos\Theta_{K^*}} \propto \frac{1}{4}\sin^2\Theta_{K^*}(1+\cos^2\Theta_\psi)(|H_{+1}|^2 + |H_{-1}|^2) + \cos^2\Theta_{K^*}\sin^2\Theta_\psi |H_0|^2, \quad (8)$$

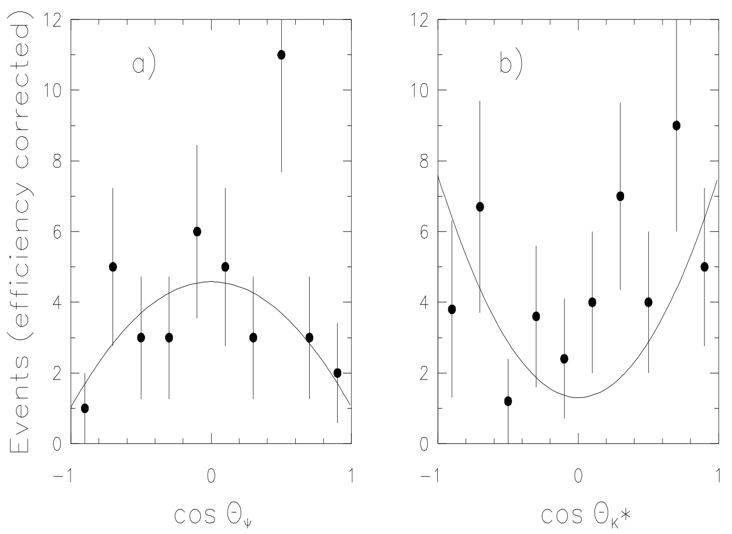

FIG. 19. Distributions of the efficiency corrected ψ and K^* helicity angles in $B \to \psi K^*$ decays from CLEO II. The overlaid smooth curves are projections of the unbinned maximum likelihood fit described in the text.

where the K^* helicity angle Θ_{K^*} is the angle between the kaon direction in the K^* rest frame and the K^* direction in the B rest frame and Θ_ψ is the corresponding ψ helicity angle, and $H_{\pm1,0}$ are the helicity amplitudes. The fraction of longitudinal polarization in $B \to \psi K^*$ is determined by an unbinned fit to the ψ and K^* helicity angle distributions. CLEO II finds

$$\left(\frac{\Gamma_L}{\Gamma}\right)_{B\to\psi K^*} = 0.84 \pm 0.06 \pm 0.08 \tag{9}$$

The efficiency corrected distributions in each of the helicity angles $\cos\Theta_\psi$ and $\cos\Theta_{K^*}$ are shown in Fig. 19.

ARGUS has also determined the polarization in $B \to \psi K^*$ decays and found that their data are consistent with 100% longitudinal polarization [39]. They find $\Gamma_L/\Gamma > 78\%$ (90% C.L.). These results can be compared to the theoretical predictions of Krämer and Palmer [58] which again depend on the assumption of factorization and on the unmeasured $B \to K^*$ form factor. Using the BSW model to estimate the form factor, they find $\Gamma_L/\Gamma = 0.57$. Using HQET to extrapolate from the E691 measurements of the $D \to K^*$ form factor, they obtain $\Gamma_L/\Gamma = 0.73$.

Although the decay mode $B \to \psi K^*$ may not be completely polarized, it is still dominated by a single CP eigenstate. This mode will therefore be useful for measurements of CP violation.

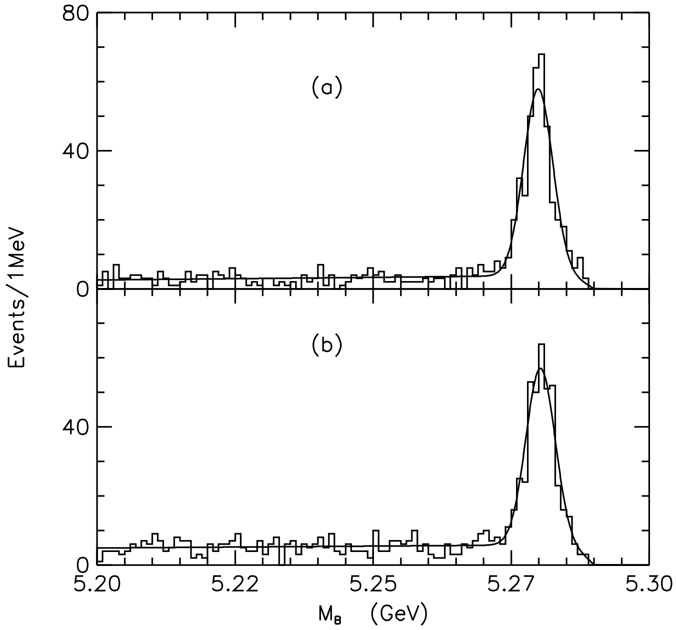

FIG. 20. Beam constrained mass distributions from CLEO II for (a) B^- events and (b) $\bar{B}^0$ events.

C. Exclusive Decays to a $D^{0(*)}$ and a Neutral Meson.

We now discuss searches for B decays which can occur via an internal W-emission graph but which do not yield charmonium mesons in the final state. Naively, one expects that these decays will be suppressed relative to decays which occur via the external W-emission graph. For the internal graph, in the absence of gluons, the colors of the quarks from the virtual W must match the colors of the c quark and the accompanying spectator antiquark. In this simple picture, one expects that the suppression factor should be 1/18 for decays involving π^0, ρ^0 and ω mesons [59]. In heavy quark decays the effects of gluons cannot be neglected, and QCD based calculations [57] predict suppression factors of order 1/50. If color suppressed B decay modes are not greatly suppressed then these modes could also be useful for CP violation studies [60].

CLEO II has searched for color suppressed decay modes of B mesons which contain a single D^0 or D^{*0} meson in the final state [61]. The relevant color suppressed modes are listed in Table XIII. The decay channels used are $\eta \to \gamma\gamma$, $\omega \to \pi^+\pi^-\pi^0$ and $\eta^{'} \to \eta\pi^+\pi^-$, followed by $\eta \to \gamma\gamma$ [62]. For decays of a pseudoscalar meson into a final state containing a pseudoscalar and a vector meson (V), a helicity angle cut of $|\cos\Theta_V| > 0.4$ is used [63]. No signals were observed. Upper limits [64] on the branching ratios for color suppressed modes are given in Table XIII. Upper limits on the ratios of color suppressed modes to normalization modes are given in Table XIV. These limits show that there is color suppression of these B decay modes.

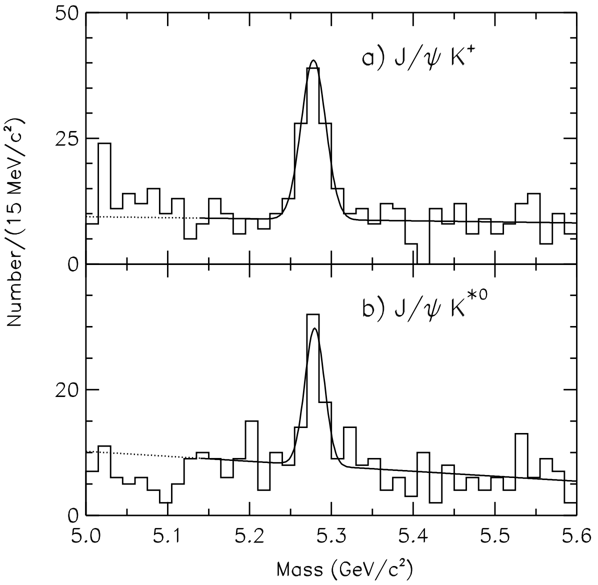

FIG. 21. (a) The ψK^+ mass distribution from the CDF experiment (b) The ψK^{*0} mass distribution from the CDF experiment. The solid line indicates the fitted region.

VII. B MESON MASSES

A. Masses of the $\bar{B}^0$ and B^- Mesons.

We now discuss measurements of the $\bar{B}^0$ and B^- masses and the mass difference between them. For these analyses only fully reconstructed B decays in modes with good signal to background are used. As an example, CLEO II uses the modes $B^- \to \psi K^-$, $\bar{B}^0 \to \psi K^{*0}$, $B^- \to D^0\pi^-$, $B^- \to D^0\rho^-$, $B^- \to D^{*0}\pi^-$, $B^- \to D^{*0}\rho^-$, $\bar{B}^0 \to D^+\pi^-$, $\bar{B}^0 \to D^+\rho^-$, $\bar{B}^0 \to D^{*+}\pi^-$, and $\bar{B}^0 \to D^{*+}\rho^-$. With tight cuts, there are 362 B^- and 340 B^0 candidates reconstructed. The M_B distributions for the sum of these modes are shown in Fig. 20.

The absolute values of the B^- and $\bar{B}^0$ masses are limited in accuracy by the knowledge of the beam energy. A correction of (-1.1$\pm$0.5) MeV is made for initial state radiation as described in Ref. [65]. The systematic error from the uncertainty in the absolute value of the CESR/DORIS energy scale is determined by calibrating to the known $\Upsilon(1S)$ mass. The mass difference is determined more accurately than the masses themselves, because the beam energy uncertainty cancels, as do many systematic errors associated with the measurement errors on the charged tracks and neutral pions. There are several models which predict the isospin mass difference [66], which give values between 1.2 and 2.3 MeV which are larger than the experimental results given in Table XV. However, papers by Goity and Hou and by Lebed [67] discuss models that can lead to small values of the mass difference. That the $\bar{B}^0 - B^-$ mass difference is much smaller than the corresponding mass differences in the K and D mesons is somewhat surprising.

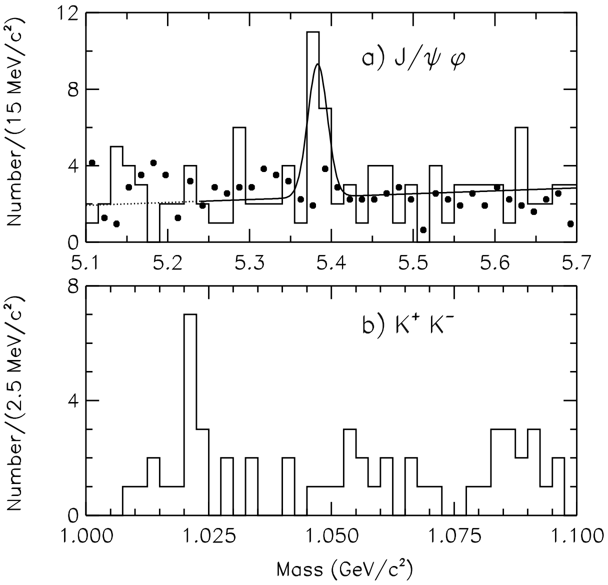

FIG. 22. (a) The ψK^+K^- mass distribution from the CDF experiment for K^+K^- mass within 10 MeV/c^2 of the ϕ mass (solid) and for the normalized ϕ sideband region (b) The K^+K^- mass distribution for ψK^+K^- combinations within 20 MeV/c^2 of 5380 MeV/c^2.

B. Measurement of the B_s Mass

First evidence for exclusive B_s decays has recently been reported by the CDF [68], OPAL [69] and ALEPH collaborations [70] . CDF observes a signal of 14.0 ± 4.7 events in the $B_s \to \psi\phi$ mode (see Fig. 22) and determines the B_s mass to be $5383.3 \pm 4.5 \pm 5.0$ MeV. ALEPH finds two unambiguous B_s events in the $B_s \to D_s^- \pi^+$ and $B_s \to \psi'\phi$ modes and obtains a mass of $5368.6 \pm 5.6 \pm 1.5$ MeV. OPAL finds one B_s candidate in the $\psi\phi$ mode with a mass of 5360 ± 70 MeV. By reconstructing exclusive B^- and $\bar{B}^0$ decays (see Fig. 21), the high energy experiments calibrate their B_s measurements relative to the known B^- and $\bar{B}^0$ masses. The three B_s mass measurements are consistent with each other and with a non-relativistic quark model prediction of a mass in the range $5345 - 5388$ MeV [71]. In the near future, the B_s mass will be measured more precisely, and it is expected that exclusive Λ_b decays will also be reconstructed.

VIII. THEORETICAL INTERPRETATION OF HADRONIC B DECAY

A. Introduction

The simple spectator diagram for two-body hadronic B meson decays that occur through the Cabibbo favored $b \to c$ transition is described by the Hamiltonian [72]:

$$H = \frac{G_F}{\sqrt{2}} V_{cb} \left\{ \left[(\bar{d}u) + (\bar{s}c) \right] (\bar{c}b) \right\} \tag{10}$$

TABLE XIV. Upper limits on ratios of branching fractions for color suppressed to normalization modes.

Ratio of Branching Ratios	CLEO II (90% C.L.)
$\mathcal{B}(\bar{B}^0 \to D^0\pi^0)/\mathcal{B}(B^- \to D^0\pi^-)$	< 0.08
$\mathcal{B}(\bar{B}^0 \to D^0\rho^0)/\mathcal{B}(B^- \to D^0\rho^-)$	< 0.04
$\mathcal{B}(\bar{B}^0 \to D^0\eta)/\mathcal{B}(B^- \to D^0\pi^-)$	< 0.16
$\mathcal{B}(\bar{B}^0 \to D^0\eta')/\mathcal{B}(B^- \to D^0\pi^-)$	< 0.16
$\mathcal{B}(\bar{B}^0 \to D^0\omega)/\mathcal{B}(B^- \to D^0\rho^-)$	< 0.05
$\mathcal{B}(\bar{B}^0 \to D^{*0}\pi^0)/\mathcal{B}(B^- \to D^{*0}\pi^-)$	< 0.14
$\mathcal{B}(\bar{B}^0 \to D^{*0}\rho^0)/\mathcal{B}(B^- \to D^{*0}\rho^-)$	< 0.07
$\mathcal{B}(\bar{B}^0 \to D^{*0}\eta)/\mathcal{B}(B^- \to D^{*0}\pi^-)$	< 0.17
$\mathcal{B}(\bar{B}^0 \to D^{*0}\eta')/\mathcal{B}(B^- \to D^{*0}\pi^-)$	< 0.67
$\mathcal{B}(\bar{B}^0 \to D^{*0}\omega)/\mathcal{B}(B^- \to D^{*0}\rho^-)$	< 0.09

TABLE XV. Measurements of the $\bar{B}^0$ and B^- Masses [MeV].

Experiment	$M_{\bar{B}^0}$	M_{B^-}	$M_{\bar{B}^0} - M_{B^-}$
ARGUS	$5279.6 \pm 0.7 \pm 2.0$	$5280.5 \pm 1.0 \pm 2.0$	$-0.9 \pm 1.2 \pm 0.5$
CLEO 87	$5278.0 \pm 0.4 \pm 2.0$	$5278.3 \pm 0.4 \pm 2.0$	$-0.4 \pm 0.6 \pm 0.5$
CLEO 93	$5279.2 \pm 0.2 \pm 2.0$	$5278.8 \pm 0.2 \pm 2.0$	$0.41 \pm 0.25 \pm 0.19$
Average	$5278.9 \pm 0.2 \pm 2.0$	$5278.7 \pm 0.2 \pm 2.0$	0.2 ± 0.3

where $(\bar{q}_i q_j) = \bar{q}_i\gamma_\mu(1-\gamma_5)q_j$, G_F is the Fermi coupling constant, and V_{cb} is the CKM matrix element.

The spectator diagram is modified by hard gluon exchange between the initial and final quark lines. The effect of these exchanges can be taken into account by use of the renormalization group, with the result that an additional term is added to the Hamiltonian, which now contains two pieces, the original term multiplied by a coefficient $c_1(\mu)$, and an additional term multiplied by $c_2(\mu)$:

$$H_{eff} = \frac{G_F}{\sqrt{2}} V_{cb} \left\{ c_1(\mu) \left[(\bar{d}u) + (\bar{s}c) \right] (\bar{c}b) + c_2(\mu) \left[(\bar{c}u)(\bar{d}b) + (\bar{c}c)(\bar{s}b) \right] \right\} \tag{11}$$

The c_i are Wilson coefficients that can be calculated from QCD. However, the calculation is inherently uncertain because it is unclear at what mass scale, μ, these coefficients should be evaluated. The usual scale is taken to be $\mu \sim m_b^2$. Defining

$$c_\pm(\mu) = c_1(\mu) \pm c_2(\mu) \tag{12}$$

the leading-log approximation gives [57]

$$c_\pm(\mu) = \left(\frac{\alpha_s(M_W^2)}{\alpha_s(\mu)} \right)^{\frac{-6\gamma_\pm}{(33 - 2n_f)}} \tag{13}$$

where $\gamma_- = -2\gamma_+ = 2$, and n_f is the number of active flavors, which is usually taken to be five in this case.

TABLE XVI. B^- Branching fractions [%]

Mode	ARGUS	CLEO 1.5	CLEO II
$B^- \to D^0\pi^-$	$0.22 \pm 0.09 \pm 0.06 \pm 0.01$	$0.56 \pm 0.08 \pm 0.05 \pm 0.02$	$0.55 \pm 0.04 \pm 0.05 \pm 0.02$
$B^- \to D^0\rho^-$	$1.45 \pm 0.45 \pm 0.41 \pm 0.06$		$1.35 \pm 0.12 \pm 0.14 \pm 0.04$
$B^- \to D^0\pi^+\pi^-\pi^-$		$1.24 \pm 0.31 \pm 0.14 \pm 0.05$	
$B^- \to D^{*0}\pi^-$	$0.39 \pm 0.14 \pm 0.10 \pm 0.02$	$0.99 \pm 0.25 \pm 0.17 \pm 0.04$	$0.52 \pm 0.07 \pm 0.07 \pm 0.03$
$B^- \to D^{*0}\rho^-$	$0.96 \pm 0.58 \pm 0.36 \pm 0.04$		$1.68 \pm 0.21 \pm 0.27 \pm 0.07$
$B^- \to D_J^{(*)0}\pi^-$	$0.13 \pm 0.07 \pm 0.03 \pm 0.01$	$0.13 \pm 0.07 \pm 0.01 \pm 0.01$	
$B^- \to D^{*+}\pi^-\pi^-\pi^0$	$1.68 \pm 0.65 \pm 0.38 \pm 0.07$		
$B^- \to D_J^{(*)0}\rho^-$	$0.33 \pm 0.20 \pm 0.08 \pm 0.01$		
$B^- \to D^{*0}\pi^-\pi^-\pi^+$			$0.94 \pm 0.20 \pm 0.17 \pm 0.02$
$B^- \to D^{*0}a_1^-$			$1.88 \pm 0.40 \pm 0.34 \pm 0.04$
$B^- \to D^+\pi^-\pi^-$			< 0.14 (90% C.L.)
$B^- \to D^{*+}\pi^-\pi^-$	$0.24 \pm 0.13 \pm 0.05 \pm 0.01$	< 0.37 (90% C.L.)	$0.19 \pm 0.07 \pm 0.03 \pm 0.01$
$B^- \to D^{**0}(2420)\pi^-$	$0.30 \pm 0.08 \pm 0.06 \pm 0.01$		$0.11 \pm 0.05 \pm 0.02 \pm 0.01$
$B^- \to D^{**0}(2420)\rho^-$			< 0.14 (90% C.L.)
$B^- \to D^{**0}(2460)\pi^-$			< 0.13 (90% C.L.)
$B^- \to D^{**0}(2460)\rho^-$			< 0.47 (90% C.L.)
$B^- \to D^0D_s^-$	$1.65 \pm 0.82 \pm 0.42 \pm 0.07$	$1.66 \pm 0.70 \pm 0.71 \pm 0.07$	
$B^- \to D^0D_s^{*-}$	$1.10 \pm 0.82 \pm 0.30 \pm 0.04$		
$B^- \to D^{*0}D_s^-$	$0.77 \pm 0.53 \pm 0.18 \pm 0.03$		
$B^- \to D^{*0}D_s^{*-}$	$1.84 \pm 0.95 \pm 0.44 \pm 0.07$		
$B^- \to \psi K^-$	$0.08 \pm 0.04 \pm 0.01$	$0.09 \pm 0.02 \pm 0.02$	$0.11 \pm 0.01 \pm 0.01$
$B^- \to \psi' K^-$	$0.20 \pm 0.09 \pm 0.04$	< 0.05 (90% C.L.)	$0.06 \pm 0.02 \pm 0.01$
$B^- \to \psi K^{*-}$	$0.19 \pm 0.13 \pm 0.03$	$0.15 \pm 0.11 \pm 0.03$	$0.18 \pm 0.05 \pm 0.02$
$B^- \to \psi' K^{*-}$	< 0.53 (90% C.L.)	< 0.38 (90% C.L.)	< 0.30 (90% C.L.)
$B^- \to \psi K^-\pi^+\pi^-$	< 0.19 (90% C.L.)	$0.14 \pm 0.07 \pm 0.03$	
$B^- \to \psi' K^-\pi^+\pi^-$	$0.21 \pm 0.12 \pm 0.04$		
$B^- \to \chi_{c1}K^-$	$0.22 \pm 0.15 \pm 0.07$		$0.10 \pm 0.04 \pm 0.01$
$B^- \to \chi_{c1}K^{*-}$			< 0.21 (90% C.L.)

The additional term in the Hamiltonian in Eq. (11) corresponds to the "color suppressed" diagram. The quark pairings in this diagram are different from those in the spectator diagram, and lead to the decay modes discussed in section VI. From the observation of the $B \to \psi X_s$ decays, where X_s is a strange meson, the magnitude of the color-suppressed term can be deduced. In B^- decays, both spectator and color-suppressed diagrams are present and can interfere. By comparing the rates for B^- and $\bar{B}^0$ decays, both the size and the relative sign of the color suppressed term can be determined (see Sec. X B).

For comparisons between theoretical models and data we will use a standard set of values for the couplings, $V_{cb} = 0.041$ and $V_{ub}/V_{cb} = 0.075$, and for the B meson lifetime, $\tau_B = 1.44 \pm 0.04$ ps [73].

TABLE XVII. $\bar{B}^0$ Branching fractions in [%]

Mode	ARGUS	CLEO 1.5	CLEO II
$\bar{B}^0 \to D^+\pi^-$	$0.48 \pm 0.11 \pm 0.08 \pm 0.07$	$0.27 \pm 0.06 \pm 0.03 \pm 0.04$	$0.29 \pm 0.04 \pm 0.03 \pm 0.05$
$\bar{B}^0 \to D^+\rho^-$	$0.90 \pm 0.50 \pm 0.27 \pm 0.14$		$0.81 \pm 0.11 \pm 0.12 \pm 0.13$
$\bar{B}^0 \to D^+\pi^-\pi^-\pi^+$		$0.80 \pm 0.21 \pm 0.09 \pm 0.12$	
$\bar{B}^0 \to D^{*+}\pi^-$	$0.26 \pm 0.08 \pm 0.04 \pm 0.01$	$0.44 \pm 0.11 \pm 0.05 \pm 0.02$	$0.26 \pm 0.03 \pm 0.04 \pm 0.01$
$\bar{B}^0 \to D^{*+}\rho^-$	$0.65 \pm 0.28 \pm 0.26 \pm 0.03$	$2.11 \pm 0.89 \pm 1.23 \pm 0.08$	$0.74 \pm 0.10 \pm 0.14 \pm 0.02$
$\bar{B}^0 \to D^{*+}\pi^-\pi^-\pi^+$	$1.12 \pm 0.28 \pm 0.33 \pm 0.04$	$1.76 \pm 0.31 \pm 0.29 \pm 0.07$	$0.63 \pm 0.10 \pm 0.11 \pm 0.02$
$\bar{B}^0 \to D^{*+}a_1^-$			$1.26 \pm 0.20 \pm 0.22 \pm 0.03$
$\bar{B}^0 \to D^0\pi^+\pi^-$			< 0.16 (90% C.L.)
$\bar{B}^0 \to D^{**+}(2460)\pi^-$			< 0.22 (90% C.L.)
$\bar{B}^0 \to D^{**+}(2460)\rho^-$			< 0.49 (90% C.L.)
$\bar{B}^0 \to D^+D_s^-$	$1.09 \pm 0.83 \pm 0.44 \pm 0.16$	$0.58 \pm 0.33 \pm 0.24 \pm 0.09$	
$\bar{B}^0 \to D^+D_s^{*-}$	$1.73 \pm 1.09 \pm 0.67 \pm 0.26$		
$\bar{B}^0 \to D^{*+}D_s^-$	$0.80 \pm 0.57 \pm 0.22 \pm 0.03$	$1.17 \pm 0.66 \pm 0.52 \pm 0.05$	
$\bar{B}^0 \to D^{*+}D_s^{*-}$	$1.49 \pm 0.80 \pm 0.43 \pm 0.06$		
$\bar{B}^0 \to \psi K^0$	$0.09 \pm 0.07 \pm 0.02$	$0.07 \pm 0.04 \pm 0.02$	$0.08 \pm 0.02 \pm 0.01$
$\bar{B}^0 \to \psi' K^0$	< 0.31 (90% C.L.)	< 0.16 (90% C.L.)	< 0.08 (90% C.L.)
$\bar{B}^0 \to \psi \bar{K}^{*0}$	$0.13 \pm 0.06 \pm 0.02$	$0.13 \pm 0.06 \pm 0.03$	$0.17 \pm 0.03 \pm 0.02$
$\bar{B}^0 \to \psi' \bar{K}^{*0}$	< 0.25 (90% C.L.)	$0.15 \pm 0.09 \pm 0.03$	< 0.19 (90% C.L.)
$\bar{B}^0 \to \psi K^-\pi^+$		$0.12 \pm 0.05 \pm 0.03$	
$\bar{B}^0 \to \psi' K^-\pi^+$	< 0.11 (90% C.L.)		
$\bar{B}^0 \to \chi_{c1} K^0$			< 0.27 (90% C.L.)
$\bar{B}^0 \to \chi_{c1} \bar{K}^{*0}$			< 0.21 (90% C.L.)

B. Factorization

Factorization is the assumption that two body hadronic decays of B mesons can be expressed as the product of two independent hadronic currents, one describing the formation of a meson from the converted b quark and the light spectator quark, and the other describing the production of a meson by the hadronization of the virtual W^-. This description is expected to be valid for the external spectator decays where the large energy carried by the W^- causes the products of the W^- to be well separated from the spectator quark system [5], [74]. It has also been used to calculate color-suppressed and penguin diagrams, although it is not known whether factorization is a correct assumption for these diagrams.

There are number of tests of the factorization hypothesis that can be made by comparing rates and polarizations for semileptonic and hadronic B decays. These will be discussed in section IX. If factorization holds, then measurements of hadronic B decays can be compared to the theoretical models, and used to extract fundamental parameters of the Standard Model. For instance the CKM matrix element V_{ub} could be obtained from $\bar{B}^0 \to \pi^+\pi^-$ or $\bar{B}^0 \to D_s^-\pi^+$, and the decay constant f_{D_s} could be determined from $\bar{B}^0 \to D_s^- D^{*+}$.

TABLE XVIII. World average B^- branching fractions [%]

Mode	Branching Fraction
$B^- \to D^0\pi^-$	$0.49 \pm 0.05 \pm 0.02$
$B^- \to D^0\rho^-$	$1.36 \pm 0.18 \pm 0.05$
$B^- \to D^0\pi^+\pi^-\pi^-$	$1.24 \pm 0.34 \pm 0.05$
$B^- \to D^{*0}\pi^-$	$0.52 \pm 0.08 \pm 0.02$
$B^- \to D^{*0}\rho^-$	$1.54 \pm 0.31 \pm 0.06$
$B^- \to D_J^{(*)0}\pi^-$	$0.13 \pm 0.05 \pm 0.01$
$B^- \to D^{*+}\pi^-\pi^-\pi^0$	$1.68 \pm 0.76 \pm 0.07$
$B^- \to D_J^{(*)0}\rho^-$	$0.33 \pm 0.21 \pm 0.01$
$B^- \to D^{*0}\pi^-\pi^-\pi^+$	$0.94 \pm 0.26 \pm 0.04$
$B^- \to D^{*0}a_1^-$	$1.88 \pm 0.52 \pm 0.08$
$B^- \to D^+\pi^-\pi^-$	< 0.14 (90% C.L.)
$B^- \to D^{*+}\pi^-\pi^-$	$0.20 \pm 0.07 \pm 0.01$
$B^- \to D^{**0}(2420)\pi^-$	$0.16 \pm 0.05 \pm 0.01$
$B^- \to D^{**0}(2420)\rho^-$	< 0.14 (90% C.L.)
$B^- \to D^{**0}(2460)\pi^-$	< 0.13 (90% C.L.)
$B^- \to D^{**0}(2460)\rho^-$	< 0.47 (90% C.L.)
$B^- \to D^0 D_s^-$	$1.65 \pm 0.68 \pm 0.07$
$B^- \to D^0 D_s^{*-}$	$1.10 \pm 0.88 \pm 0.04$
$B^- \to D^{*0} D_s^-$	$0.77 \pm 0.56 \pm 0.03$
$B^- \to D^{*0} D_s^{*-}$	1.84 ± 1.05
$B^- \to \psi K^-$	0.10 ± 0.01
$B^- \to \psi' K^-$	0.07 ± 0.02
$B^- \to \psi K^{*-}$	0.17 ± 0.05
$B^- \to \psi' K^{*-}$	< 0.53 (90% C.L.)
$B^- \to \psi K^-\pi^+\pi^-$	0.14 ± 0.08
$B^- \to \psi' K^-\pi^+\pi^-$	0.21 ± 0.13
$B^- \to \chi_{c1} K^-$	0.10 ± 0.04
$B^- \to \chi_{c1} K^{*-}$	< 0.21 (90% C.L.)

C. Phenomenological Models of Hadronic B Decay

Several groups have developed models of hadronic B decays based on the factorization approach. To compute rates for all hadronic B decays the magnitude and sign of the color amplitude must also be known. It is difficult to calculate this amplitude from first principles in QCD. Instead a phenomenological approach was adopted by Bauer, Stech and Wirbel [75], in which two undetermined coefficients were assigned to the effective charged current, a_1, and the effective neutral current, a_2, parts of the B decay Hamiltonian. In reference [75] these coefficients were determined from a fit to a subset of the experimental data on charm decays. The values of a_1 and a_2 can be related to the QCD coefficients c_1 and c_2 by $a_1 = c_1 + \xi c_2$ and $a_2 = c_2 + \xi c_1$ where $\xi = 1/N_{\rm color}$. The values $a_1 = 1.26$ and $a_2 = -0.51$ that give the best fit to the experimental data on charm decay correspond to $1/N_{\rm color} \sim 0$

TABLE XIX. World average $\bar{B}^0$ branching fractions [%]

Mode	Branching Fraction
$\bar{B}^0 \to D^+\pi^-$	$0.30 \pm 0.04 \pm 0.04$
$\bar{B}^0 \to D^+\rho^-$	$0.82 \pm 0.16 \pm 0.12$
$\bar{B}^0 \to D^+\pi^-\pi^-\pi^+$	$0.80 \pm 0.23 \pm 0.12$
$\bar{B}^0 \to D^{*+}\pi^-$	$0.28 \pm 0.04 \pm 0.01$
$\bar{B}^0 \to D^{*+}\rho^-$	$0.74 \pm 0.16 \pm 0.03$
$\bar{B}^0 \to D^{*+}\pi^-\pi^-\pi^+$	$0.79 \pm 0.13 \pm 0.03$
$\bar{B}^0 \to D^{*+}a_1^-$	$1.26 \pm 0.30 \pm 0.05$
$\bar{B}^0 \to D^0\pi^+\pi^-$	< 0.16 (90% C.L.)
$\bar{B}^0 \to D^{**+}(2460)\pi^-$	< 0.22 (90% C.L.)
$\bar{B}^0 \to D^{**+}(2460)\rho^-$	< 0.49 (90% C.L.)
$\bar{B}^0 \to D^+D_s^-$	$0.66 \pm 0.38 \pm 0.10$
$\bar{B}^0 \to D^+D_s^{*-}$	$1.73 \pm 1.28 \pm 0.26$
$\bar{B}^0 \to D^{*+}D_s^-$	$0.93 \pm 0.50 \pm 0.04$
$\bar{B}^0 \to D^{*+}D_s^{*-}$	$1.49 \pm 0.91 \pm 0.06$
$\bar{B}^0 \to \psi K^0$	0.08 ± 0.02
$\bar{B}^0 \to \psi' K^0$	< 0.31 (90% C.L.)
$\bar{B}^0 \to \psi \bar{K}^{*0}$	0.15 ± 0.03
$\bar{B}^0 \to \psi' \bar{K}^{*0}$	0.15 ± 0.09
$\bar{B}^0 \to \psi K^-\pi^+$	0.12 ± 0.06
$\bar{B}^0 \to \psi' K^-\pi^+$	< 0.11 (90% C.L.)
$\bar{B}^0 \to \chi_{c1} K^0$	< 0.27 (90% C.L.)
$\bar{B}^0 \to \chi_{c1} \bar{K}^{*0}$	< 0.21 (90% C.L.)

[57]. However, there is no rigorous theoretical justification for this choice of $N_{\rm color}$ [76]. In section X B we will discuss the determination of the values of a_1 and a_2 from a fit to the B meson decay data.

D. Heavy Quark Effective Theory

It has recently been appreciated that there is a symmetry of QCD that is useful in understanding systems containing one heavy quark. This symmetry arises when the quark becomes sufficiently heavy to make its mass irrelevant to the nonperturbative dynamics of the light quarks. This allows the heavy quark degrees of freedom to be treated in isolation from the the light quark degrees of freedom. Heavy quark effective theory (HQET) has been developed by Isgur and Wise [77] who define a single universal form factor, $\xi(v.v')$, known as the Isgur-Wise function. In this function v and v' are the four velocities of the initial and final state heavy quarks. In the heavy quark limit all the form factors for hadronic matrix elements such as $B \to D^*$ and $B \to D$ can be related to this single function. The value of this function can then be determined from a measurement of the $D^* l\nu$ rate as a function of q^2 [77].

The evaluation of amplitudes for hadronic decays requires not only the assumption of factorization, but also the input of hadronic form factors and meson decay constants. As a result of the development of HQET it is now believed that many of the hadronic form factors for $b \to c$ transitions can be calculated quite well in an essentially model-independent way. This has been done by several groups [57], [78]. The comparison of these theoretical predictions with the experimental results can be used to test the range of validity of HQET, and the extent to which $1/M_Q$ corrections to the heavy quark symmetry are needed.

IX. TESTS OF THE FACTORIZATION HYPOTHESIS

A. Branching Ratio Tests

The large samples of reconstructed hadronic B decays have made possible the precise measurements of branching ratios discussed in section V. As an example of the use of these results to test the factorization hypothesis we will consider the specific case of $\bar{B}^0 \to D^{*+}\pi^-$. The amplitude for this reaction is

$$A = \frac{G_F}{\sqrt{2}} V_{cb} V_{ud}^* \langle \pi^- |(\bar{d}u)|0\rangle \langle D^{*+}|(\bar{c}b)|\bar{B}^0\rangle. \tag{14}$$

The V_{ud} CKM factor arises from the $W^- \to \bar{u}d$ vertex. The first hadron current that creates the π^- from the vacuum is related to the pion decay constant, f_π, by:

$$\langle \pi^-(p)|(\bar{d}u)|0\rangle = -i f_\pi p_\mu. \tag{15}$$

The other hadron current can be found from the semileptonic decay $\bar{B}^0 \to D^{*+}\ell^-\bar{\nu}_\ell$. Here the amplitude is the product of a lepton current and the hadron current that we seek to insert in Eq. (14). Factorization can be tested experimentally by verifying whether the relation

$$\frac{\Gamma\left(\bar{B}^0 \to D^{*+}\pi^-\right)}{\frac{d\Gamma}{dq^2}\left(\bar{B}^0 \to D^{*+}\ell^-\bar{\nu}_l\right)\Big|_{q^2=m_\pi^2}} = 6\pi^2 c_1^2 f_\pi^2 |V_{ud}|^2, \tag{16}$$

is satisfied. Here q^2 is the four momentum transfer from the B meson to the D^* meson. Since q^2 is also the mass of the lepton-neutrino system, by setting $q^2 = m_\pi^2 = 0.019\ GeV^2$ we are simply requiring that the lepton-neutrino system has the same kinematic properties as does the pion in the hadronic decay. V_{ud} and f_π have well measured values of 0.975 and 131.7 MeV respectively. For the coefficient c_1 we will use the value 1.12 ± 0.1 deduced from perturbative QCD [79]. The error in c_1 reflects the uncertainty in the mass scale at which the coefficient c_1 should be evaluated. In the original test of equation (16), Bortoletto and Stone [80] found that the equation was satisfied for c_1=1. In the following discussion we will denote the left hand side of Eq. (16) by R_{Exp} and the right hand side by R_{Theo}.

This type of factorization test can be extended to larger q^2 values by using other $\bar{B}^0 \to D^{*+}X^-$ decays, e.g. $X^- = \rho^-$ or a_1^-. For the ρ^- case Eq. (16) becomes:

$$R = \frac{\Gamma(\bar{B}^0 \to D^{*+}\rho^-)}{\frac{d\Gamma}{dq^2}(B \to D^* l\ \nu)|_{q^2=m_\rho^2}} = 6\pi^2 c_1^2 f_\rho^2 |V_{ud}|^2 \tag{17}$$

where the semileptonic decay is evaluated at $q^2 = m_\rho^2 = 0.60$ GeV^2. The decay constant on the right hand side of this equation can be determined from $e^+e^- \to \rho^0$ which gives $f_\rho = 215 \pm 4$ MeV. [1] For the factorization test with $\bar{B}^0 \to D^{*+}a_1^-$ we use $f_{a_1} = 205 \pm 16$ MeV [83] determined from τ decay. To derive numerical predictions for branching ratios, we must interpolate the observed differential q^2 distribution [84] for $B \to D^*\ell\,\nu$ to $q^2 = m_\pi^2$, m_ρ^2, and $m_{a_1}^2$, respectively. Until this distribution is measured more precisely we use theoretical models to perform this interpolation. The results from three models are given in Table XX. The differences between the models for $B \to D^*\ell\,\nu$ is small (See Fig. 23). Using the

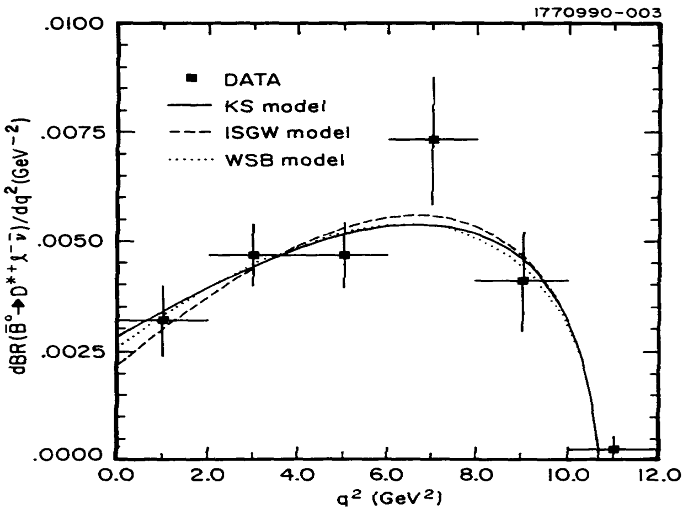

FIG. 23. The q^2 distribution for the decay $\bar{B}^0 \to D^{*+}\ell^-\bar{\nu}_\ell$. This is a weighted average from CLEO and ARGUS data. The curves are fits using various models of semileptonic decays (from Ref. [80]).

extrapolation of the q^2 spectrum [85] from the WSB model as the central value, we obtain from Eqs. (16) and (17) the results given in Table XXI. Some of the systematic uncertainties in R_{Exp} cancel if we form ratios of branching fractions, as does the QCD coefficient c_1 in R_{Theo}. Thus in the case of $D^{*+}\rho^-/D^{*+}\pi^-$, the expectation from factorization is given by $R_{Theo}(\rho)/R_{Theo}(\pi)$ times the ratio of the semileptonic branching ratios evaluated at the appropriate q^2 values. In Table XXII we show the comparison between the measured ratios and two theoretical predictions by Reader and Isgur [83], and the revised BSW model [57]. At the present level of precision, there is good agreement between the experimental results

[1] A second method uses the relation $\Gamma(\tau^- \to \nu\rho^-) = 0.804\frac{G_F^2}{16\pi}|V_{ud}^2|M_\tau^3 f_\rho^2$, where the ρ width has been taken into account [81]. This gives f$_\rho = 212.0 \pm 5.3$ MeV [82].

TABLE XX. Ingredients for Factorization Tests.

$\lvert c_1\rvert$	1.12 ± 0.1
f_π	131.74 ± 0.15 MeV
f_ρ	215 ± 4 MeV
f_{a_1}	205 ± 16 MeV
V_{ud}	0.975 ± 0.001
$\frac{d\mathcal{B}}{dq^2}(B \to D^* l\ \nu)\rvert_{q^2=m_\pi^2}(WSB)$	0.0023 GeV^{-2}
$\frac{d\mathcal{B}}{dq^2}(B \to D^* l\ \nu)\rvert_{q^2=m_\pi^2}(ISGW)$	0.0020 GeV^{-2}
$\frac{d\mathcal{B}}{dq^2}(B \to D^* l\ \nu)\rvert_{q^2=m_\pi^2}(KS)$	0.0024 GeV^{-2}
$\frac{d\mathcal{B}}{dq^2}(B \to D^* l\ \nu)\rvert_{q^2=m_\rho^2}(WSB)$	0.0025 GeV^{-2}
$\frac{d\mathcal{B}}{dq^2}(B \to D^* l\ \nu)\rvert_{q^2=m_\rho^2}(ISGW)$	0.0024 GeV^{-2}
$\frac{d\mathcal{B}}{dq^2}(B \to D^* l\ \nu)\rvert_{q^2=m_\rho^2}(KS)$	0.0027 GeV^{-2}
$\frac{d\mathcal{B}}{dq^2}(B \to D^* l\ \nu)\rvert_{q^2=m_{a_1}^2}(WSB)$	0.0032 GeV^{-2}
$\frac{d\mathcal{B}}{dq^2}(B \to D^* l\ \nu)\rvert_{q^2=m_{a_1}^2}(ISGW)$	0.0030 GeV^{-2}
$\frac{d\mathcal{B}}{dq^2}(B \to D^* l\ \nu)\rvert_{q^2=m_{a_1}^2}(KS)$	0.0033 GeV^{-2}

TABLE XXI. Comparison of R_{Exp} and R_{Theo}

	R_{Exp} (GeV^2)	R_{Theo} (GeV^2)
$\bar{B}^0 \to D^{*+}\pi^-$	1.22 ± 0.18	1.22 ± 0.17
$\bar{B}^0 \to D^{*+}\rho^-$	2.96 ± 0.65	3.26 ± 0.46
$\bar{B}^0 \to D^{*+}a_1^-$	3.9 ± 0.9	3.0 ± 0.50

TABLE XXII. Ratios of B decay widths.

	Exp.	Factorization	RI Model	BSW Model
$\mathcal{B}(\bar{B}^0 \to D^{*+}\rho^-)/\mathcal{B}(\bar{B}^0 \to D^{*+}\pi^-)$	2.64 ± 0.68	2.90 ± 0.26	$2.2 - 2.3$	2.8
$\mathcal{B}(\bar{B}^0 \to D^{*+}a_1^-)/\mathcal{B}(\bar{B}^0 \to D^{*+}\pi^-)$	4.5 ± 1.2	3.4 ± 0.27	$2.0 - 2.1$	3.4

and the expectation from factorization for the q^2 range $0 < q^2 < m_{a_1}^2$. Note that it is possible that factorization will be a poorer approximation for decays will smaller energy release or larger q^2. Factorization tests can be extended to higher q^2 using $B \to D^* D_s^{(*)}$ decays as will be discussed in section IX D .

B. Factorization and Angular Correlations

More subtle tests of the factorization hypothesis can be performed by examining the polarization in B meson decays into two vector mesons, as suggested by Körner and Goldstein [86]. Again, the underlying principle is to compare the hadronic decays to the appropriate semileptonic decays evaluated at a fixed value in q^2. For instance, the ratio of longitudinal to transverse polarization (Γ_L/Γ_T) in $\bar{B}^0 \to D^{*+}\rho^-$ should be equal to the corresponding ratio for $B \to D^*\ell\nu$ evaluated at $q^2 = {m_\rho}^2 = 0.6$ GeV^2.

$$\frac{\Gamma_L}{\Gamma_T}(\bar{B}^0 \to D^{*+}\rho^-) = \frac{\Gamma_L}{\Gamma_T}(B \to D^*\ell\nu)|_{q^2=m_\rho^2} \tag{18}$$

The advantage of this method is that it is not affected by QCD corrections [87].

For $B \to D^*\ell\nu$ decay, longitudinal polarization dominates at low q^2, whereas near $q^2 = q^2_{\rm max}$ transverse polarization dominates. There is a simple physical argument for the behaviour of the form factors near these two kinematic limits. Near $q^2 = q^2_{\rm max}$, the D^* is almost at rest and its small velocity is uncorrelated with the D^* spin, so all three D^* helicities are equally likely and we expect $\Gamma_T/\Gamma_L = 2$. At $q^2 = 0$, the D^* has the maximum possible momentum, while the lepton and neutrino are collinear and travel in the direction opposite to the D^*. The lepton and neutrino helicities are aligned to give $S_z = 0$, so near $q^2 = 0$ longitudinal polarization is dominant.

For $\bar{B}^0 \to D^{*+}\rho^-$, we expect 88% longitudinal polarization from the argument described above [88]. Similar results have been obtained by Neubert [89] and Kramer *et al.* [90] .

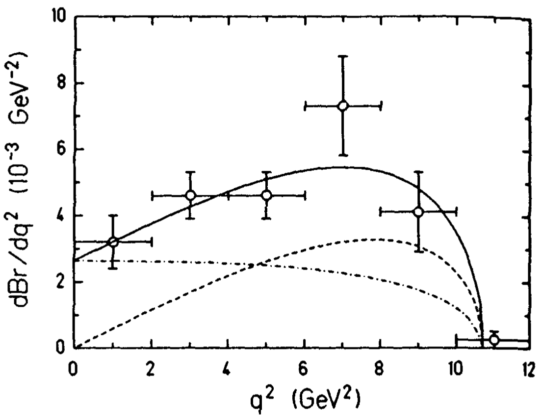

FIG. 24. The differential branching ratio for $\bar{B}^0 \to D^{*+}\ell\bar{\nu}_\ell$. The curves show the theoretical prediction for producing transversely (dashed) and longitudinally (dash-dotted) polarized D^* mesons, as well as the total decay rate (solid) (from Ref. [89]).

Fig. 24 shows the prediction of Neubert for transverse and longitudinal polarization in $B \to D^*\ell\nu$ decays. Using this figure we find Γ_L/Γ to be 85% at $q^2 = {m_\rho}^2 = 0.6$. The agreement between these predictions and the experimental result (Sec. V C)

$$\Gamma_L/\Gamma \;=\; 90 \pm 7 \pm 5\% \tag{19}$$

supports the factorization hypothesis in hadronic B meson decay for q^2 values up to m_ρ^2.

C. Tests of Spin Symmetry in HQET

In HQET the effect of the heavy quark magnetic moment does not enter to lowest order [91], and the assumption of factorization leads to the following predictions based on the spin symmetry of HQET:

$$\Gamma(\bar{B}^0 \to D^+\pi^-) = \Gamma(\bar{B}^0 \to D^{*+}\pi^-) \tag{20}$$

and

$$\Gamma(\bar{B}^0 \to D^+\rho^-) = \Gamma(\bar{B}^0 \to D^{*+}\rho^-). \tag{21}$$

After correcting for phase space and deviations from heavy quark symmetry it is predicted that $\mathcal{B}(\bar{B}^0 \to D^+\pi^-) = 1.03\ \mathcal{B}(\bar{B}^0 \to D^{*+}\pi^-)$ and $\mathcal{B}(\bar{B}^0 \to D^+\rho^-) = 0.89\ \mathcal{B}(\bar{B}^0 \to D^{*+}\rho^-)$. A separate calculation by Blok and Shifman using a QCD sum rule approach predicts that $\mathcal{B}(\bar{B}^0 \to D^+\pi^-) = 1.2\mathcal{B}(\bar{B}^0 \to D^{*+}\pi^-)$. This differs from the HQET prediction due to the presence of non-factorizable contributions [92].

From the experimental data we find

$$\frac{\mathcal{B}(\bar{B}^0 \to D^+\pi^-)}{\mathcal{B}(\bar{B}^0 \to D^{*+}\pi^-)} = 1.07 \pm 0.21 \pm 0.14 \tag{22}$$

and

$$\frac{\mathcal{B}(\bar{B}^0 \to D^+\rho^-)}{\mathcal{B}(\bar{B}^0 \to D^{*+}\rho^-)} = 1.11 \pm 0.32 \pm 0.16 \tag{23}$$

The second error bar is due to the uncertainty in the D branching fractions. The two ratios of branching fractions are consistent with the expectations from HQET spin symmetry and with the prediction from Blok and Shifman that includes nonfactorizable contributions. Similar tests will be possible using the modes $B \to D^{(*)}D_s^{(*)}$ once more precise measurements of the branching ratios are available.

Mannel *et al.* [91] observe that by using a combination of HQET, factorization, and data on $B \to D^*\ell\nu$, they can obtain model dependent predictions for $\mathcal{B}(\bar{B}^0 \to D^+\rho^-)/\mathcal{B}(\bar{B}^0 \to D^+\pi^-)$. Using three parameterizations of the universal Isgur-Wise form factor [93], they predict this ratio to be 3.05, 2.52, or 2.61. From the measurements of the branching ratios we obtain

$$\frac{\mathcal{B}(\bar{B}^0 \to D^+\rho^-)}{\mathcal{B}(\bar{B}^0 \to D^+\pi^-)} = 2.7 \pm 0.6 \tag{24}$$

The systematic errors from the D branching fractions cancel in this ratio. Again we find good agreement with the prediction from HQET combined with factorization.

D. Applications of Factorization

If factorization holds, hadronic B decays can be used to extract information about semileptonic decays. For example, we can determine the so far unmeasured rate $B \to$

$D^{**}(2420)\ell\nu$ from the branching ratio of $B \to D^{**}(2420)\pi$. By assuming that the rate for $B \to D^{**}(2420)\pi$ is related to $d\Gamma/dq^2(B \to D^{**}(2420)\ell\nu)$ evaluated at $q^2 = m_\pi^2$. Using the model of Colangelo *et al.* [78] to determine the shape of the form factors we obtain the ratio

$$\frac{\Gamma(B \to D^{**}(2420)\ell\nu)}{\Gamma(B \to D^{**}(2420)\pi)} = 3.2$$

Combining this result with the experimental value in Table XVIII we predict $\mathcal{B}(D^{**}(2420)l\nu) = 0.51 \pm 0.16\%$

A second application of factorization is the determination of f_{D_s} using the decays $B \to D^* D_s$. The rate for $\bar{B}^0 \to D^{*+} D_s$ is related to the differential rate for $\bar{B}^0 \to D^{*+}\ell^-\nu$ at $q^2 = m_{D_s}^2$ if factorization continues to be valid at larger values of q^2:

$$\frac{\Gamma\left(\bar{B}^0 \to D^{*+} D_s^-\right)}{\frac{d\Gamma}{dq^2}\left(\bar{B}^0 \to D^{*+}\ell^-\nu\right)\Big|_{q^2=m_{D_s}^2}} = 6\pi^2 \delta c_1^2 f_{D_s}^2 |V_{cs}|^2, \tag{25}$$

The factor $\delta = 0.37$ is required because the D^* in the $B \to D^* D_s$ final state is fully polarized, and should be compared with the rate of $B \to D^*\ell\nu$ at $q^2 = m_{D_s}^2$ in that polarization state only. Using the above result and the average branching ratio for $\mathcal{B}(B \to D^{*+} D_s^-) = 0.9 \pm 0.5\%$, we obtain

$$f_{D_s} = (288 \pm 64)\sqrt{3.7\%/B(D_s \to \phi\pi^+)}\ \mathrm{MeV}$$

This result can be compared to the value

$$f_{D_s} = (344 \pm 37 \pm 52)\sqrt{B(D_s \to \phi\pi^+)/3.7\%}\ \mathrm{MeV}$$

that has recently been obtained from a direct measurement of $D_s \to \mu\nu$ decays in continuum charm events [22]. Both these values of f_{D_s} are consistent with the theoretical predictions which are in the range $f_{D_s} = 200 - 290$ MeV [94], [95], [96]. If both the $D_s \to \phi\pi^+$ branching ratio and f_{D_s} are measured more precisely, then measurements of the branching ratios of $B \to D^* D_s$ decays can be used to test factorization in B decay at $q^2 = m_{D_s}^2$. In the near future, it will also be possible to test factorization in this q^2 range by measuring Γ_L/Γ in $B \to D^* D_s^*$ decays.

X. DETERMINATION OF THE COLOR SUPPRESSED AMPLITUDE

A. Color Suppression in B Decay

In the decays of charmed mesons the effect of color suppression is obscured by the effects of final state interactions (FSI), and soft gluon effects which enhance W exchange diagrams. Table XXIII gives ratios of several charmed meson decay modes with approximately equal phase space factors where the mode in the numerator is color suppressed while the mode in the denominator is an external spectator decay. With the exception of the decay $D^0 \to \bar{K}^0\rho^0$

TABLE XXIII. Measured Ratios of color suppressed to external spectator branching fractions.

Mode	Branching fraction [19]
$\mathcal{B}(D^0 \to \bar{K^0}\rho^0)/\mathcal{B}(D^0 \to K^-\rho^+)$	0.08 ± 0.04
$\mathcal{B}(D^0 \to \bar{K^0}\pi^0)/\mathcal{B}(D^0 \to K^-\pi^+)$	0.57 ± 0.13
$\mathcal{B}(D^0 \to \bar{K^{*0}}\pi^0)/\mathcal{B}(D^0 \to K^{*-}\pi^+)$	0.47 ± 0.23
$\mathcal{B}(D^0 \to \pi^0\pi^0)/\mathcal{B}(D^0 \to \pi^-\pi^+)$ [97]	0.77 ± 0.25
$\mathcal{B}(D_s^+ \to \bar{K^{*0}}K^+)/\mathcal{B}(D_s \to \phi\pi^+)$	0.95 ± 0.10
$\mathcal{B}(D_s^+ \to \bar{K^0}K^+)/\mathcal{B}(D_s \to \phi\pi^+)$	1.01 ± 0.16

it is clear that the color suppressed decays do not have significantly smaller branching ratios.

When the BSW model is used to fit the data on charm decays it gives values of $a_1 = 1.26$ and $a_2 = -0.51$. The BSW model assumes that the values of the coefficients can be extrapolated from $\mu = m_c^2$ to $\mu = m_b^2$ taking into account the evolution of the strong coupling constant α_s. This extrapolation gives the predictions $a_1 = 1.1$ and $a_2 = -0.24$ for B decays. The smaller magnitude of a_2 means that in contrast to the charm sector one expects to find a more consistent pattern of color suppression in B meson decays. Another approach uses the factorization hypothesis, HQET and model dependent form factors (RI model) [83]. In this approach, a_1 and a_2 are determined from QCD (with $1/N_{\rm color} = 1/3$), and color suppressed B decays are expected to occur at about 1/1000 the rate of unsuppressed decays. The observation of color suppressed B decays at a much greater level would indicate the breakdown of the factorization hypothesis. In Section VI C we obtained upper limits for color suppressed B decays with a D^0 or D^{*0} meson in the final state. In Table XXIV these results are compared to the predictions of the BSW and the RI models.

TABLE XXIV. Branching fractions of color suppressed B decays and comparisons with models.

Decay Mode	U. L. (%)	BSW (%)	$\mathcal{B}$ (BSW)	RI model(%)
$\bar{B^0} \to D^0\pi^0$	< 0.035	0.012	$0.20a_2^2(f_D/220\mathrm{MeV})^2$	$0.0013 - 0.0018$
$\bar{B^0} \to D^0\rho^0$	< 0.042	0.008	$0.14a_2^2(f_D/220\mathrm{MeV})^2$	0.00044
$\bar{B^0} \to D^0\eta$	< 0.075	0.006	$0.11a_2^2(f_D/220\mathrm{MeV})^2$	
$\bar{B^0} \to D^0\eta'$	< 0.080	0.002	$0.03a_2^2(f_D/220\mathrm{MeV})^2$	
$\bar{B^0} \to D^0\omega$	< 0.048	0.008	$0.14a_2^2(f_D/220\mathrm{MeV})^2$	
$\bar{B^0} \to D^{*0}\pi^0$	< 0.071	0.012	$0.21a_2^2(f_{D*}/220\mathrm{MeV})^2$	$0.0013 - 0.0018$
$\bar{B^0} \to D^{*0}\rho^0$	< 0.099	0.013	$0.22a_2^2(f_{D*}/220\mathrm{MeV})^2$	$0.0013 - 0.0018$
$\bar{B^0} \to D^{*0}\eta$	< 0.094	0.007	$0.12a_2^2(f_{D*}/220\mathrm{MeV})^2$	
$\bar{B^0} \to D^{*0}\eta'$	< 0.37	0.002	$0.03a_2^2(f_{D*}/220\mathrm{MeV})^2$	
$\bar{B^0} \to D^{*0}\omega$	< 0.15	0.013	$0.22a_2^2(f_{D*}/220\mathrm{MeV})^2$	

In contrast to charm decays, color suppression seems to be operative in hadronic decays of B mesons. The limits on the color suppressed modes with $D^{0(*)}$ and neutral mesons are still above the level expected by the two models, but we can already exclude a prediction by Terasaki [98] that $\mathcal{B}(\bar{B^0} \to D^0\pi^0) \approx 1.8\mathcal{B}(\bar{B^0} \to D^+\pi^-)$. To date, the only color suppressed B meson decay modes that have been observed are final states which contain charmonium mesons e.g. $B \to \psi K$ and $B \to \psi K^*$ [99].

B. Determination of $|a_1|$, $|a_2|$ and the Relative Sign of (a_2/a_1)

In the BSW model [57] , the branching fractions of the $\bar{B}^0$ normalization modes are proportional to a_1^2 while the branching fractions of the $B \to \psi$ decay modes depend only on a_2^2. A fit to the branching ratios for the modes $\bar{B}^0 \to D^+\pi^-$, $D^+\rho^-$, $D^{*+}\pi^-$ and $D^{*+}\rho^-$ using the model of Neubert *et al.* yields

$$|a_1| = 1.07 \pm 0.04 \pm 0.06 \tag{26}$$

and a fit to the modes with ψ mesons in the final state gives

$$|a_2| = 0.23 \pm 0.01 \pm 0.01 \tag{27}$$

The first error on $|a_1|$ and $|a_2|$ includes the uncertainties from the charm or charmonium branching ratios, the experimental systematics associated with detection efficiencies and background subtractions as well as the statistical errors from the branching ratios. The second error quoted is the uncertainty due to the B meson production fractions and lifetimes. We have assumed that the ratio of B^+B^- and $B^0\bar{B}^0$ production at the $\Upsilon(4S)$ is one [73], [100], and assigned an uncertainty of 10% to it.

TABLE XXV. Predicted branching fractions in terms of BSW parameters a_1, a_2

Mode	Neubert *et al.* [57]	Deandrea *et al.* [101]
$\bar{B}^0 \to D^+\pi^-$	$0.264a_1^2$	$0.276a_1^2$
$\bar{B}^0 \to D^+\rho^-$	$0.621a_1^2$	$0.713a_1^2$
$\bar{B}^0 \to D^{*+}\pi^-$	$0.254a_1^2$	$0.276a_1^2$
$\bar{B}^0 \to D^{*+}\rho^-$	$0.702a_1^2$	$0.943a_1^2$
$B^- \to D^0\pi^-$	$0.265[a_1 + 1.230a_2(f_D/220)]^2$	$0.276[a_1 + 1.155a_2(f_D/220)]^2$
$B^- \to D^0\rho^-$	$0.622[a_1 + 0.662a_2\ (f_D/220)]^2$	$0.713[a_1 + 0.458a_2(f_D/220)]^2$
$B^- \to D^{*0}\pi^-$	$0.255[a_1 + 1.292a_2\ (f_{D^*}/220)]^2$	$0.276[a_1 + 1.524a_2(f_{D^*}/220)]^2$
$B^- \to D^{*0}\rho^-$	$0.703[a_1^2 + 1.487a_1a_2\ (f_{D^*}/220)$	$0.943[a_1^2 + 1.31a_1a_2\ (f_{D^*}/220)$
	$+0.635a_2^2(f_{D^*}/220)^2]$	$+0.53a_2^2(f_{D^*}/220)^2]$
$B^- \to \psi K^-$	$1.819a_2^2$	$1.634a_2^2$
$B^- \to \psi K^{*-}$	$2.932a_2^2$	$2.393a_2^2$
$\bar{B}^0 \to \psi\bar{K}^0$	$1.817a_2^2$	$1.634a_2^2$
$\bar{B}^0 \to \psi\bar{K}^{*0}$	$2.927a_2^2$	$2.393a_2^2$

By comparing branching ratios of B^- and $\bar{B}^0$ decay modes it is possible to determine the the sign of a_2 relative to a_1. The BSW model, Ref. [57] predicts the following ratios:

$$R_1 = \frac{\mathcal{B}(B^- \to D^0\pi^-)}{\mathcal{B}(\bar{B}^0 \to D^+\pi^-)} = (1 + 1.23a_2/a_1)^2 \tag{28}$$

$$R_2 = \frac{\mathcal{B}(B^- \to D^0\rho^-)}{\mathcal{B}(\bar{B}^0 \to D^+\rho^-)} = (1 + 0.66a_2/a_1)^2 \tag{29}$$

TABLE XXVI. Ratios of normalization modes to determine the sign of a_2/a_1. The magnitude of a_2/a_1 is the value in the BSW model which agrees with our result for $B \to \psi$ modes.

Ratio	$a_2/a_1 = -0.22$	$a_2/a_1 = 0.22$	Experiment	RI model
R_1	0.53	1.61	1.63 ± 0.36	$1.20 - 1.28$
R_2	0.73	1.31	1.66 ± 0.46	$1.09 - 1.12$
R_3	0.51	1.65	1.86 ± 0.39	$1.19 - 1.27$
R_4	0.70	1.36	2.08 ± 0.61	$1.10 - 1.36$

$$R_3 = \frac{\mathcal{B}(B^- \to D^{*0}\pi^-)}{\mathcal{B}(\bar{B}^0 \to D^{*+}\pi^-)} = (1 + 1.29a_2/a_1)^2 \tag{30}$$

$$R_4 = \frac{\mathcal{B}(B^- \to D^{*0}\rho^-)}{\mathcal{B}(\bar{B}^0 \to D^{*+}\rho^-)} \approx (1 + 0.75a_2/a_1)^2 \tag{31}$$

Table XXVI shows a comparison between the experimental results and the two allowed solutions in the BSW model. In the experimental ratios the systematic errors due to detection efficiencies partly cancel. In the ratios R_3 and R_4 the D meson branching ratio uncertainties do not contribute to the systematic error.

A least squares fit to the ratios R_1 - R_3 gives $a_2/a_1 = 0.27 \pm 0.08 \pm 0.06$ where we have ignored uncertainties in the theoretical predictions. R_4 is not included in the fit since the model prediction in this case is not thought to be reliable [102]. The second error is due to the uncertainty in the B meson production fractions and lifetimes which enter into the determination of a_1/a_2 in the combination $(f_+\tau_+/f_0\tau_0)$. As this ratio increases, the value of a_2/a_1 decreases. The allowed range of $(f_+\tau_+/f_0\tau_0)$ excludes a negative value of a_2/a_1.

Other uncertainties in the magnitude [103] of f_D, f_{D^*} and in the hadronic form factors can change the magnitude of a_2/a_1 but not its sign. The numerical factors which multiply a_2/a_1 include the ratios of $B \to \pi (B \to \rho)$ to $B \to D$ $(B \to D^*)$ form factors, as well as the ratios of the meson decay constants. We assume values of 220 MeV for f_D and f_{D^*} [104]. To investigate the model dependence of the result we have recalculated $|a_1|$, $|a_2|$, and a_2/a_1 in the model of Deandrea *et al.* We find $|a_1| = 0.99 \pm 0.04 \pm 0.06$, $|a_2| = 0.25 \pm 0.01 \pm 0.01$, and $a_2/a_1 = 0.25 \pm 0.07 \pm 0.05$, consistent with the results discussed above. A different set of $B \to \pi$ form factors can be calculated using QCD sum rules. Using the form factors determined by Belyaev, Khodjamirian and Rückl [105] and by Ball [106], a_2/a_1 changes by 0.04. Kamal and Pham have also considered the effect of uncertainties in form factors, the effects of final state interactions, and annihilation terms. They conclude that these may change the magnitude of a_2/a_1 but not its sign [107].

The magnitude of a_2 determined from this fit is consistent with the value of a_2 determined from the fit to the $B \to \psi$ decay modes. The sign of a_2 disagrees with the theoretical extrapolation from the fit to charmed meson decays using the BSW model [108]. Table XXVII compares the corresponding charm decay ratios to the theoretical expectations for positive and negative values of a_2/a_1.

TABLE XXVII. Predicted (BSW) and measured ratios of widths of D^+ and D^0 modes in charm decay.

Mode	$a_2/a_1 = -0.40$	$a_2/a_1 = 0.40$	Ratio of widths (exp) [19]
$D^+ \to \bar{K}^0\pi^+/D^0 \to K^-\pi^+$	0.26	2.2	0.28 ± 0.05
$D^+ \to \bar{K}^0\rho^+/D^0 \to K^-\rho^+$	0.58	1.5	0.36 ± 0.10
$D^+ \to \bar{K}^{*0}\pi^+/D^0 \to K^{*-}\pi^+$	0.05	3.2	0.17 ± 0.07
$D^+ \to \bar{K}^{*0}\rho^+/D^0 \to K^{*-}\rho^+$	0.34	2.0	0.25 ± 0.12

XI. RARE HADRONIC DECAYS

A. Introduction

There are hadronic B meson decays that cannot be produced by the usual $b \to c$ transition. The results of the experimental search for these rare decay modes provides important information on the mechanisms of B meson decay and significant progress is being made with the collection of large samples of B mesons by the CLEO II experiment. As an indication of this we will discuss the first observation of radiative penguin decay as well as new experimental results on the decays $\bar{B}^0 \to \pi^+\pi^-$ and $\bar{B}^0 \to K^-\pi^+$ where a statistically significant signal has been observed in the sum of the two modes.

Decays of the kind $B \to D_s X_u$, where the X_u system hadronizes as pions, can occur via a $b \to u$ spectator diagram where the W forms a $c\bar{s}$ pair. Since other contributing diagrams are expected to be negligible these decays may provide a clean environment in which to measure V_{ub} in hadronic decays. Decays of the kind $\bar{B}^0 \to D_s^+ X_s^-$, where X_s is a strange meson, are also interesting since they are associated with a W exchange diagram.

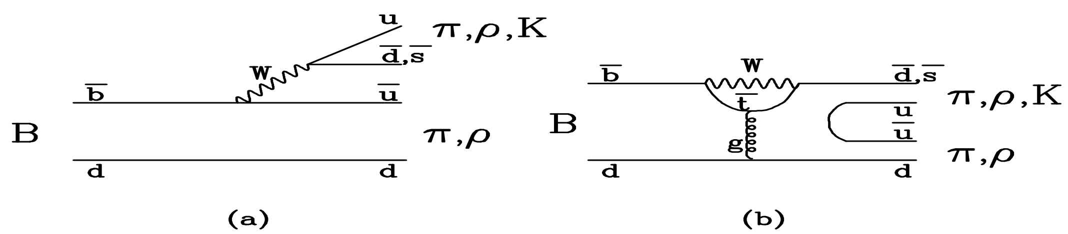

FIG. 25. Rare B meson decay diagrams: (a) $b \to u$ spectator and (b) gluonic penguin.

Charmless hadronic decays such as $\bar{B}^0 \to \pi^+\pi^-$, $B^- \to \pi^-\pi^0$, $\bar{B}^0 \to \pi^\pm\rho^\mp$ and $B^- \to \pi^0\rho^-$, are expected to be produced by the $b \to u$ spectator diagram (Fig. 25(a)), although there is a possible small contribution from a $b \to d$ penguin diagram (Fig. 25(b)). The decay $\bar{B}^0 \to \pi^+\pi^-$ has been discussed as a possible place to observe CP violation in the B meson system [109]. The final state is a CP eigenstate, and CP violation can arise from interference between the amplitude for the direct decay via the $b \to u$ spectator diagram, and the amplitude for the decay following $B^0\bar{B}^0$ mixing. In this decay the CP violating angle is different from the one accessible in $\bar{B}^0 \to \psi K_s$, so the measurement is complementary. There is a possible complication if the $b \to d$ penguin contribution to the amplitude is significant. This could be resolved if measurements are made on other rare hadronic decay modes to determine the role of the penguin amplitude in any observed CP violating effect [109].

Decays to charmless hadronic final states containing an s quark are expected to have a significant contribution from a $b \to s$ penguin diagram, although they can also occur through a Cabibbo suppressed $b \to u$ spectator diagram. The inclusive rates for the hadronic penguin diagrams $b \to sg$ and $b \to sq\bar{q}$ are estimated to be about 1% from the parton model, but predictions for the hadronization into exclusive final states are uncertain because the simple assumptions about factorization of the amplitude used for the spectator diagram may not be valid for loop diagrams.

B. Decays to D_s Mesons

These decays have recently been searched for by ARGUS [110] and CLEO II [111]. The upper limits are given in Table XXVIII along with theoretical predictions by Choudury*et al.* [112], and Deandrea *et al.* [101].

TABLE XXVIII. Theoretical predictions and experimental upper limits (90% C.L.) for B decays to D_s. All numbers quoted are branching fractions $\times 10^{-5}$

B Decay	Choudury	Deandrea	ARGUS	CLEO II
$D_s^+\pi^-$	1.9	8.1	<170.0	<27.0
$D_s^{*+}\pi^-$	2.7	6.1	<120.0	<44.0
$D_s^+\rho^-$	1.0	1.2	<220.0	<66.0
$D_s^{*+}\rho^-$	5.4	4.5	<250.0	<74.0
$D_s^+\pi^0$	1.8	3.9	<90.0	<20.0
$D_s^{*+}\pi^0$	1.3	3.0	<90.0	<32.0
$D_s^+\eta$		1.1		<46.0
$D_s^{*+}\eta$		0.8		<75.0
$D_s^+\rho^0$	0.5	0.6	<340.0	<37.0
$D_s^{*+}\rho^0$	2.8	2.4	<200.0	<48.0
$D_s^+\omega$		0.6	<340.0	<48.0
$D_s^{*+}\omega$		2.4	<190.0	<68.0
$D_s^+K^-$			<170.0	<23.0
$D_s^{*+}K^-$			<120.0	<17.0
$D_s^+K^{*-}$			<460.0	<97.0
$D_s^{*+}K^{*-}$			<580.0	<110.0

The experimental limits are still at least a factor of three above the theoretical predictions. If we compare the limits to the predictions of Deandrea *et al.* we note that the best constraint on $|V_{ub}/V_{cb}|$ will come from the CLEO II limit on $\bar{B}^0 \to D_s^+\pi^-$, but that this model dependent limit is still above the range $0.06 < |V_{ub}/V_{cb}| < 0.10$ allowed by the recent semileptonic data [6]. Combining several $D_s X_u$ modes the sensitivity to V_{ub} can be slightly improved. For example, using the BSW model CLEO obtains an upper limit of $|V_{ub}/V_{cb}| < 0.15$ (90% C.L.) [111].

C. Charmless Hadronic B Decay

Predictions of branching ratios for charmless hadronic decays were made by Bauer, Stech and Wirbel [75] using the $b \to u$ spectator diagram and the assumption of factorization. The possible contributions from penguin diagrams were neglected. These predictions have recently been updated by Deandrea *et al.* [101] using new estimates of the hadronic form factors. We compare their results to the experimental upper limits in Table XXIX. We have

TABLE XXIX. Theoretical predictions and experimental upper limits (90% C.L.) for charmless hadronic B decays. All numbers quoted are branching fractions $\times 10^{-5}$.

B Decay	Deandrea	ARGUS	CLEO 1.5	CLEO II
$\pi^+\pi^-$	1.8	<13.0	<7.7	<2.9
$\pi^\pm\rho^\mp$	5.2	<52.0		<29.0
$\rho^+\rho^-$	1.3			
$\pi^\pm a_1^\mp$		<90.0	<49.0	
$\pi^0\pi^0$	0.06			
$\pi^0\rho^0$	0.14	<40.0		
$\rho^0\rho^0$	0.05	<28.0	<29.0	
$\pi^-\pi^0$	1.4	<24.0		
$\pi^-\rho^0$	0.7	<15.0	<17.0	
$\pi^0\rho^-$	2.7	<55.0		
$\rho^-\rho^0$	0.7	<100.0		
$p\bar{p}\pi^-$		$(52 \pm 14 \pm 19)$	<14.0	

included in Table XXIX the reported observation of the decay $B^- \to p\bar{p}\pi^-$ by ARGUS [115], even though this has not been confirmed by later data from either ARGUS or CLEO [116].

There are two recent sets of theoretical predictions by Deshpande *et al.* [117] and Chau *et al.* [118] that take into account both penguin and spectator contributions and make predictions for a large number of charmless hadronic B decays. A selection of these predictions are shown in table XXX. Large contributions from the penguin amplitude are expected in decays such as $B \to K^{(*)}\phi$ and $B \to K^{(*)}\pi$. However, the decays $B \to K\rho$ are predicted to have very small penguin amplitudes due to cancellations in the contributions to the amplitude [117].

New upper limits have been presented for $\bar{B}^0 \to \pi^+\pi^-$ [3] and $\bar{B}^0 \to \pi^\pm\rho^\mp$ [123]. The CLEO II search for $\bar{B}^0 \to \pi^+\pi^-$ is discussed in detail in the next section. CLEO II also has a new limit on $\bar{B}^0 \to K^-\pi^+$ [3], and preliminary results on $\bar{B}^0 \to K^-\rho^+$ [123] as well as the

TABLE XXX. Theoretical predictions and experimental upper limits (90% C.L.) for $b \to s$ decays. All numbers quoted are branching fractions $\times 10^{-5}$

B Decay	Deshpande	Chau	ARGUS	CLEO 1.5	CLEO II
$K^-\pi^+$	1.1	1.7	<18.0	<7.7	<2.6
$K^-\rho^+$	0	0.2			<11.0
$K^0\pi^0$	0.5	0.6			
$K^0\rho^0$	0.01	0.04	<16.0	<50.0	
$K^{*-}\pi^+$	0.6	1.9	<62.0	<38.0	
$K^{*0}\pi^0$	0.3	0.5			
$K^-\pi^0$	0.6	0.8			
$K^-\rho^0$	0.01	0.06	<18.0	<8.0	
$K^0\pi^-$	1.1	1.2	<9.6	<10.0	
$K^0\rho^-$	0	0.03			
$K^{*0}\pi^-$	0.6	0.9	<17.0	<15.0	
$K^{*-}\pi^0$	0.3	0.9			
$K^0\phi$	1.1	0.9	<36.0	<42.0	<9.4
$K^{*0}\phi$	3.1	0.9	<32.0	<38.0	<19.0
$K^-\phi$	1.1	1.4	<18.0	<9.0	<1.7
$K^{*-}\phi$	3.1	0.8	<130.0		<12.0

$B \to K^{(*)}\phi$ modes [121]. The CLEO II limits on $\bar{B}^0 \to K^-\pi^+$ and $B^- \to K^-\phi$, which are expected to have a large penguin amplitude, are close to the theoretical predictions.

The experimental sensitivities to branching ratios have now reached the 10^{-5} range. Since the theoretical predictions for several B decay modes are in this range, it is possible that some signals will be observed soon. By measuring a sufficient number of charmless B decay modes (e.g. $\bar{B}^0 \to \pi^-\pi^+$, $B^- \to \pi^-\pi^0$, $\bar{B}^0 \to \pi^0\pi^0$) it may be possible to isolate the spectator and penguin contributions.

D. New Experimental Results on $\bar{B}^0 \to \pi^+\pi^-$ and $\bar{B}^0 \to K^-\pi^+$

The decay modes $\bar{B}^0 \to \pi^+\pi^-$, $\bar{B}^0 \to K^-\pi^+$, and $\bar{B}^0 \to K^+K^-$ [122], have been searched for by CLEO II using a data sample of 1.37 fb^{-1} taken on the $\Upsilon(4S)$ [3]. A sample of 0.64 fb^{-1} taken just below the resonance is used to study the continuum background. Since B mesons are produced nearly at rest on the $\Upsilon(4S)$, the final state has two nearly back-to-back tracks with momenta about 2.6 GeV/c. We distinguish candidates for B meson decays from continuum background using the difference, ΔE, between the total energy of the two tracks and the beam energy, and the beam-constrained mass, M_B. The r.m.s. resolutions on ΔE and M_B are 25 MeV and 2.5 MeV respectively.

Separation between $\pi^-\pi^+$, $K^-\pi^+$ and K^-K^+ events is provided by the ΔE variable, and by dE/dx information from the 51-layer main drift chamber. The ΔE shift between $K\pi$ and $\pi\pi$ events is 42 MeV if E_1 and E_2 are determined using the pion mass. This is $1.7\sigma_{\Delta E}$. The

dE/dx separation between kaons and pions at 2.6 GeV/c is found to be $(1.8 \pm 0.1)\sigma$ from a study of a sample of D^{*+}-tagged $D^0 \to K^-\pi^+$ decays. Thus, in the CLEO II experiment the total separation between $K\pi$ and $\pi\pi$ events is 2.5σ.

The background arises almost entirely from the continuum where the two-jet structure of the events can produce high momentum, back-to-back tracks. These events can be discriminated against by calculating the angle, θ_T, between the thrust axis of the candidate tracks, and the thrust axis of the rest of the event. The distribution of $\cos\theta_T$ is peaked at ± 1 for continuum events, and is nearly flat for $B\bar{B}$ events. A cut is made at $|\cos\theta_T| < 0.7$. Additional discrimination is provided by a Fisher discriminant [124], [125], $\mathcal{F} = \sum_{i=1}^{n} \alpha_i y_i$. The inputs y_i are the direction of the candidate thrust axis, the B meson flight direction, and nine variables measuring the energy flow of the rest of the event. The coefficients α_i are chosen to maximize the separation between $B\bar{B}$ signal events and continuum background events. The optimal cut on the Fischer discriminant is 84% efficient for signal and 40% efficient for background.

Two approaches are used to evaluate the amount of signal in the data sample. In the first approach a cut is made on $\mathcal{F}$ and events are classified as $\pi\pi$, $K\pi$ or KK according to the most probable hypothesis from the dE/dx information. The signal and background numbers are given in Table XXXI. The efficiency for the correct identification of a signal event in this analysis is 19%. The background is estimated using sidebands in the continuum and on-resonance data and scaling factors from Monte Carlo studies. There is no $B\bar{B}$ background in the signal region.

TABLE XXXI. Event yields, fitted branching fractions and 90% C.L. upper limits for $B^0 \to \pi^+\pi^-$, $B^0 \to K^+\pi^-$ and $B^0 \to K^+K^-$

Decay mode	Signal Events	Background	N_{fit}	B.R.$\times 10^{-5}$	U.L.$\times 10^{-5}$
$\pi^+\pi^-$	6	1.4±0.2	$7.2^{+4.3}_{-3.5}$	$1.3^{+0.8}_{-0.6} \pm 0.2$	< 2.9
$K^+\pi^-$	6	1.5±0.2	$6.4^{+3.9}_{-3.1}$	$1.1^{+0.7}_{-0.6} \pm 0.2$	< 2.6
K^+K^-	0	1.1±0.1	$0.0^{+0.8}_{-0.0}$	$0.0^{+0.2}_{-0.0}$	< 0.7
$\pi^+\pi^-$ or $K^+\pi^-$	12	2.9±0.3	$13.6^{+4.7}_{-3.9}$	$2.4^{+0.8}_{-0.7} \pm 0.2$	

To increase the efficiency of the search and to exploit the information contained in the distributions of the ΔE, M_B, $\mathcal{F}$ and dE/dx variables a second analysis is performed. The cuts described in the previous paragraph are removed, and an unbinned maximum-likelihood fit is made. In this fit the signal and background distributions are defined by probability density functions derived from Monte Carlo studies. The fit determines the relative contributions of $\pi^-\pi^+$, $K^-\pi^+$ and K^-K^+ to the signal and background. The best fit values for the signal yields $N_{\pi\pi}$, $N_{K\pi}$ and N_{KK}, are given in Table XXXI. Fig. 26 shows the $n\sigma$ contours in the plane $N_{\pi\pi}$ *vs.* $N_{K\pi}$, and Fig. 27 shows the projections of the likelihood fit onto the M_B and ΔE axes compared to the events observed. The efficiency for a signal event to be included in the likelihood analysis is 38%.

The best fit value shown in Fig. 26 is more than 4σ away from the point $N_{\pi\pi} = N_{K\pi} = 0$. After including the effect of systematic errors on the sum of $N_{\pi\pi}$ and $N_{K\pi}$ [124], it has been concluded that the significance of the sum is sufficient to claim the observation of a signal

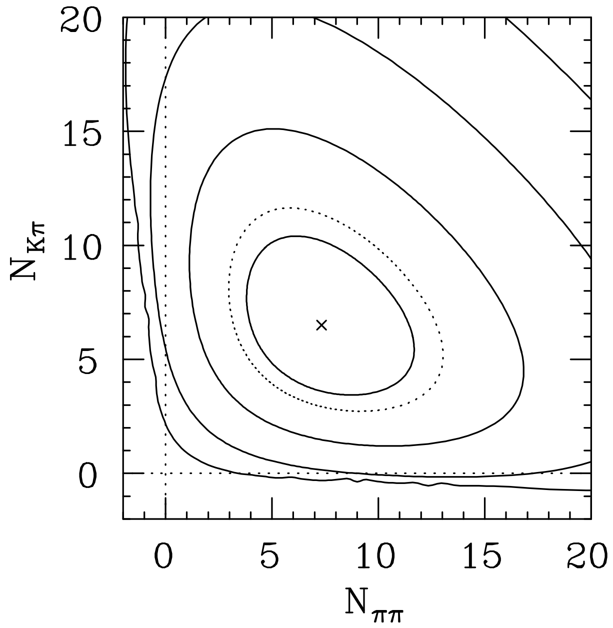

FIG. 26. Likelihood contours in the CLEO II analysis for the fit to $N_{\pi\pi}$ and $N_{K\pi}$. The best fit is indicated by the cross, the 1, 2, 3, and 4σ contours by solid lines, and the 1.28σ contour by the dotted line.

for charmless hadronic B decays. It should be emphasized that the present data do not have sufficient statistical precision to allow any conclusion to be reached about the relative importance of the two decays. While the CLEO II experiment does not measure signals for the individual decays $\bar{B}^0 \to \pi^+\pi^-$ and $\bar{B}^0 \to K^-\pi^+$, it does set stringent upper limits (Table XXXI).

Studies have been made of the amount of additional data that might be required to measure signals in the individual modes, and it is estimated that a sample of about 3 fb^{-1} is sufficient, assuming that the best fit continues to give the same yields for $N_{\pi\pi}$ and $N_{K\pi}$. Note that the separation between $\pi\pi$ and $K\pi$ provided by ΔE and dE/dx is adequate for this analysis, as can be seen from the nearly circular form of the contours in Fig. 26.

XII. ELECTROMAGNETIC PENGUIN DECAYS

A. Observation of $B \to K^*(892)\gamma$

The first observation of the electromagnetic decay $B \to K^*\gamma$ has been reported by CLEO II [4]. A data sample of 1.38 pb^{-1} taken on the $\Upsilon(4S)$ resonance was searched for both $\bar{B}^0 \to \bar{K}^{*0}\gamma$ and $B^- \to K^{*-}\gamma$, where the $\bar{K}^{*0}$ was detected in its $K^-\pi^+$ decay mode, and the K^{*-} in both the $K^-\pi^0$ and $K_s\pi^-$ decay modes. If a K^* candidate is within 75 MeV of the known K^* mass then it is combined with an isolated photon with an energy between 2.1 and 2.9 GeV. The photon candidate must not be matched to a charged track, and must have a shower shape consistent with an isolated photon. If the photon candidate forms a $\pi^0(\eta)$ meson when combined with any another photon with energy greater than 30(200) MeV it is rejected.

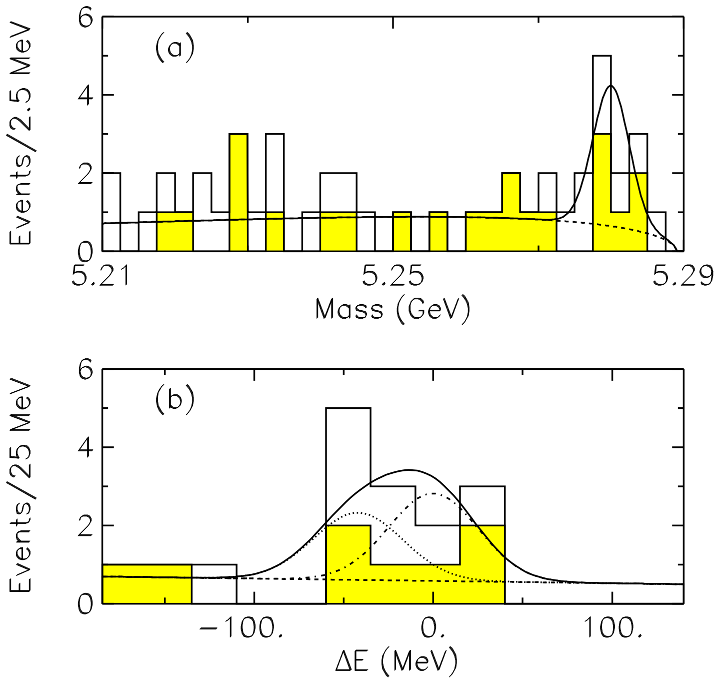

FIG. 27. CLEO II results on $B \to \pi^+\pi^-$ and $K^+\pi^-$. Comparison of on-resonance data (histogram) with projections of the likelihood fit (solid curve). (a) Projection onto M_B after cuts on ΔE and $\mathcal{F}$ (b) Projection onto ΔE after cuts on M_B and $\mathcal{F}$. The shaded portions of the histogram are $\pi\pi$ events, the unshaded are $K\pi$ events. The dotted and dot-dashed lines in (b) indicate the fit projections for $K\pi$ and $\pi\pi$ separately.

Candidates for B meson decays are identified using the variables $\Delta E = E_{K^*} + E_\gamma - E_{beam}$ and M_B. The r.m.s. resolutions on ΔE and M_B are 40 MeV and 2.8 MeV respectively.

TABLE XXXII. Summary of results for $B \to K^*\gamma$

	$\bar{B}^0 \to K^{*0}\gamma$	$B^- \to K^{*-}\gamma$	
	$\bar{K}^{*0} \to K^-\pi^+$	$K^{*-} \to K_s\pi^-$	$K^{*-} \to K^-\pi^0$
Signal Events	8	2	3
Continuum Background	1.1±0.2	0.05±0.03	0.8±0.3
$B\bar{B}$ Background	0.30±0.15	0.01±0.01	0.10±0.05
Detection Efficiency	(11.9±1.8)%	(2.0±0.3)%	(3.1±0.5)%
Branching Ratio	$(4.0\pm1.7\pm0.8)\times10^{-5}$	$(5.7\pm3.1\pm1.1)\times10^{-5}$	

There are two main sources of background from the continuum, $q\bar{q}$ jets and initial state radiation (ISR). These backgrounds are suppressed by applying cuts on the shape variables $R_2 < 0.5$, $|\cos\theta_T| < 0.7$, and $0.25 < s_\perp < 0.60$. The upper restriction on $s_\perp$ is useful for rejecting ISR background. By transforming the event into the frame where the photon is at rest, and defining new shape variables R_2' and $\cos\theta_T'$ in this frame, the ISR background can be further suppressed. There is a small amount of background to $B \to K^*\gamma$ from other $B\bar{B}$ events. The size of this background was determined from a high statistics Monte Carlo study. This study includes a feeddown from other $b \to s\gamma$ decays, which was estimated using the theoretical models for $b \to s\gamma$ discussed in the next section. The remaining background is mainly due to continuum e^+e^- annihilation. This contribution has been determined using ΔE, M_B sidebands in both the $\Upsilon(4S)$ and continuum data and scaling factors determined from Monte Carlo studies.

Supporting evidence that the events in the signal region are due to the decay $B \to K^*\gamma$ comes from a likelihood analysis similar to the one described in section XI D. In this analysis the distributions of the events in the variables M_B, ΔE, M_{K^*}, $\cos\Theta_{K^*}$ (the K^* helicity angle), $\cos\theta_B$, R_2, R_2', $s_\perp$, and $\cos\theta_T$ are compared to the distributions expected from Monte Carlo samples of signal and continuum background events [127]. This analysis gives results completely consistent with the signal and background yields given in Table XXXII.

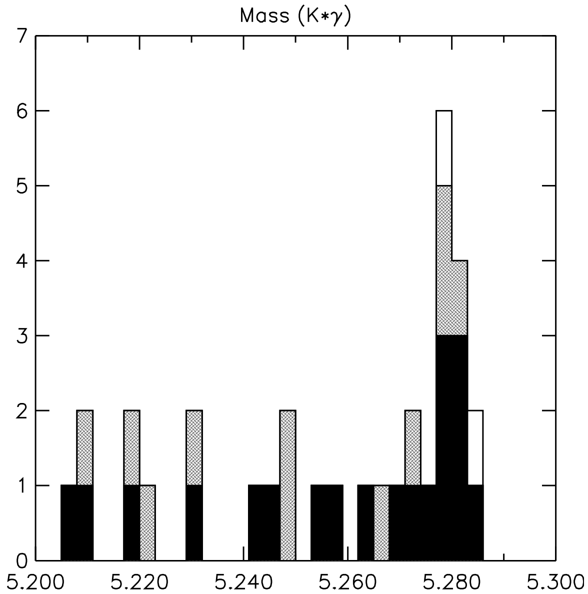

FIG. 28. The beam-constrained mass distribution from CLEO II for $B \to K^*\gamma$ candidates: $K^-\pi^+\gamma$ solid, $K^-\pi^0\gamma$ shaded, $K_s\pi^-\gamma$ unshaded

The eight $\bar{K}^{*0}\gamma$ and five $K^{*-}\gamma$ events in the signal region, $|\Delta E| < 90$ MeV and $5.274 < M_B < 5.286$ GeV, are a clear signal for the decay $B \to K^*\gamma$ (Fig. 28). The yields in the observed modes are consistent. Assuming that $\bar{B}^0 \to \bar{K}^{*0}\gamma$ and $B^- \to K^{*-}\gamma$ are equal, the average branching ratio is $(4.5 \pm 1.5 \pm 0.9) \times 10^{-5}$. This is in agreement with theoretical predictions from the electromagnetic penguin diagram [128].

B. Experimental Constraints on the $b \to s\gamma$ Inclusive Rate

At present, due to the uncertainties in the hadronization, only the inclusive $b \to s\gamma$ rate can be reliably compared with theoretical calculations. This rate can be measured from the endpoint of the inclusive photon spectrum in B decay. The signal for $b \to s\gamma$ is expected to peak in the region $2.2 < E_\gamma < 2.7$ GeV, with only 15% of the rate expected to be outside this range [128].

The experimental situation is shown in Fig. 29. In the CLEO II data there is an excess of 69 ± 43 events from B decays in the region $2.2 < E_\gamma < 2.7$ GeV. The contribution in the

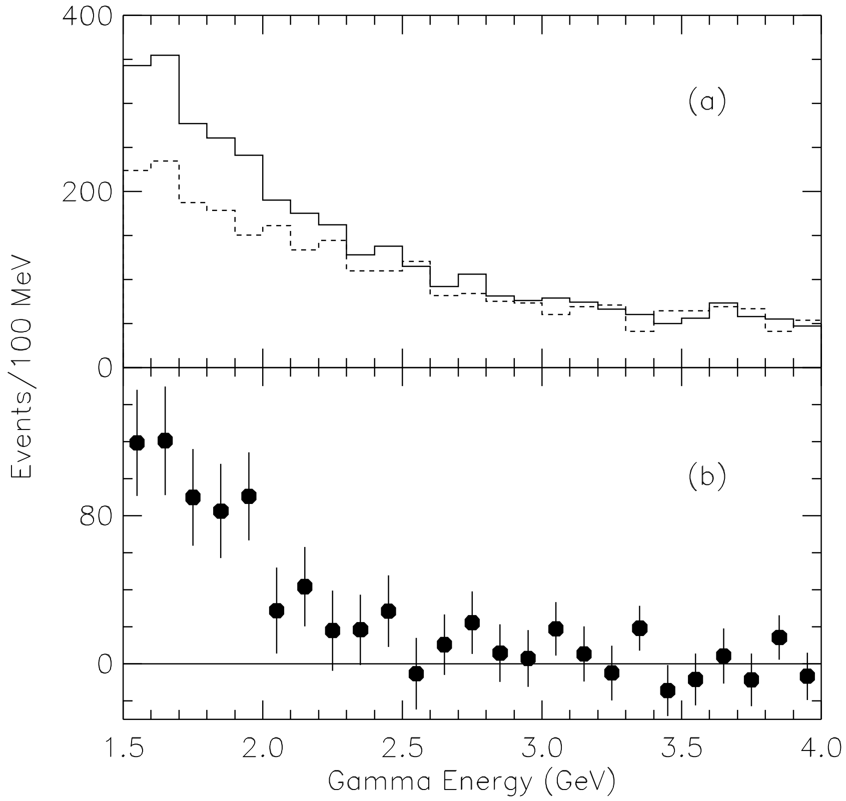

FIG. 29. Inclusive gamma spectrum from CLEO II for (a) On resonance (solid line) and scaled off resonance (dashed line) (b) excess of gammas from B decays

signal region due to photons coming from $b \to c$ decays is thought to be small compared to the expected signal from $b \to s\gamma$. A conservative upper limit is being quoted by not making a $b \to c$ subtraction, and by assuming that only 70% of the $b \to s\gamma$ rate is in the energy window [126].

An alternative approach to measuring the inclusive rate is to use the observed exclusive rate for $B \to K^*\gamma$. However, the fraction of the inclusive rate that hadronizes to a particular exclusive final state is not very well understood. Ali *et al.* [128] predict the mass distribution of the X_s system using an estimate of the Fermi momentum of the spectator quark ($p_F = 300$ MeV) [129] . By integrating this spectrum up to 1 GeV and assuming this region is dominated by the K^* resonance, the fraction of $K^*(892)\gamma$ is estimated to be $(13\pm3)\%$. Other authors have made predictions between 5% and 40% for the fraction of $K^*(892)\gamma$ [134]. A reasonable estimate that covers most of the theoretical predictions is $(13\pm6)\%$. Combining this number with the measured branching ratio for $B \to K^*\gamma$ a lower limit can be obtained for the inclusive rate. This approach would become more useful if additional exclusive channels with higher mass X_s systems were to be observed.

Using the inclusive measurement for the upper limit, and the observation of $B \to K^*\gamma$ for the lower limit, the present 95% C.L. limits on the inclusive rate are [126]:

$$0.8 \times 10^{-4} < \mathcal{B}(b \to s\gamma) < 5.4 \times 10^{-4} \tag{32}$$

It is anticipated that CLEO II will improve both of these limits, and will eventually observe a signal in the inclusive photon spectrum.

Searches have also been made for $b \to s\gamma$ processes at LEP. The L3 experiment has set an upper limit of 1.2×10^{-3} (90% C.L.) on the inclusive $b \to s\gamma$ rate [132]. The exclusive decays $\bar{B}^0 \to \bar{K}^{*0}\gamma$ and $B_s \to \phi\gamma$ have been searched for by the DELPHI experiment using the particle identification capabilities of the RICH detector. Upper limits of 3.6×10^{-4} and 19.0×10^{-4} are obtained for these two decays [133]. The results of the searches performed at the Z^0 are inferior to the results from CLEO II due to the smaller number of B mesons produced, and the large backgrounds from non $b\bar{b}$ processes. In the L3 analysis this large background is subtracted according to the predictions of the JETSET Monte Carlo. Another problem at LEP is that the photons have higher energies and are more difficult to distinguish from π^0 and η mesons.

C. Theoretical Implications of $b \to s\gamma$

There are many calculations of the inclusive rate for $b \to s\gamma$ [128], [130]. The rate has a logarithmic dependence on the top quark mass, m_t, and is proportional to the product of CKM matrix elements $|V_{ts}V_{tb}|^2$. Large leading order QCD corrections increase the rate by a factor of about 3.5. Using the limits $100 < m_t < 200$ GeV, and allowing the range of mass scales, μ, at which the QCD corrections are evaluated, to vary between $m_b/2$ and $2m_b$, Ali and Greub calculate the inclusive rate to be $(3.0 \pm 1.2) \times 10^{-4}$. This prediction is completely consistent with the experimental results discussed in the previous section. Ali and Greub have used the experimental bounds to determine the range of possible values for the ratio CKM matrix element $|V_{ts}/V_{cb}|$:

$$0.50 < |V_{ts}/V_{cb}| < 1.67$$

which is expected from unitarity to be close to 1.

The ratio $|V_{td}/V_{ts}|$ can be determined from a comparison of the decay rates for $B \to \rho\gamma$ (or $B \to \omega\gamma$) and $B \to K^*\gamma$. In this ratio many of the theoretical uncertainties are expected to cancel.

There has been recent interest in $b \to s\gamma$ as a probe of physics beyond the standard model [7,136]. There are possible additional contributions to the loop from a charged Higgs boson and from supersymmetric particles. Hewett [7] has considered two Higgs doublet models and shown that contributions comparable to the standard model are expected for a charged Higgs mass of order 100 GeV. In supersymmetric models there are also contributions from loops containing charginos, neutralinos and squarks that tend to cancel the charged Higgs and standard model contributions (in unbroken supersymmetry all contributions to the loop diagram cancel exactly) [135]. Several recent papers [136] investigate the parameter space allowed by $b \to s\gamma$ for particular models of the breaking of the supersymmetry. For most of the parameter space the charged Higgs contribution is the dominant one, and the present CLEO II upper limit on $b \to s\gamma$ constrains the charged Higgs mass to be greater than 200 GeV. This is more restrictive than constraints from direct searches at existing high energy colliders. An important consequence of this limit would be to forbid the decay $t \to bH^+$. The limit on the charged Higgs mass can be avoided in supersymmetric models if the stop mass is small since this leads to a large negative contribution from the chargino-stop loop. For this case the rate for $b \to s\gamma$ could even become smaller than the standard model prediction.

Other constraints on new physics have been derived from the bounds on $b \to s\gamma$. If there are anomalous $W - W - \gamma$ couplings, these can significantly modify the rate for $b \to s\gamma$. The CLEO measurements exclude certain regions of the parameter space of anomalous dipole and quadrupole couplings of the W boson that cannot be explored by direct studies of $W^+ - \gamma$ production at hadron colliders [137].

D. $b \to s\ell^+\ell^-$ Decays

The $b \to s\gamma$ diagram can be modified by replacing the real photon by a virtual photon or by a virtual Z^0 or other neutral boson that produces a lepton pair (see Fig. 30). This penguin diagram leads to both $B \to K\ell^+\ell^-$ and $B \to K^*\ell^+\ell^-$ decays, since the $B \to K$ transition is no longer forbidden by angular momentum conservation as it was for $b \to s\gamma$. Although the penguin amplitude for $b \to s\ell^+\ell^-$ is smaller than $b \to s\gamma$ the final states can be identified easily, and are particularly favorable for study at hadron colliders. As in the radiative penguin decay discussed previously, the process $b \to s\ell^+\ell^-$ is sensitive to high mass physics including charged Higgs bosons and non-standard neutral particles.

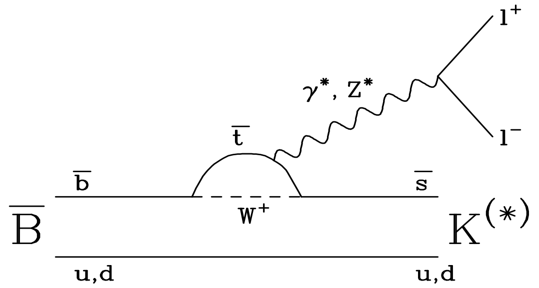

FIG. 30. Diagrams for the decays $B \to K^{(*)}\ell^+\ell^-$.

The penguin amplitude has been calculated by a number of authors [138], with results for the inclusive $b \to se^+e^-$ rate of $(1-2) \times 10^{-5}$ and for the $b \to s\mu^+\mu^-$ rate of $(4-8) \times 10^{-6}$. The exclusive channels $K^*\ell^+\ell^-$ and $K\ell^+\ell^-$ are expected to comprise $5-30\%$ of the inclusive rate. However, the theoretical description of $b \to s\ell^+\ell^-$ is more complicated than $b \to s\gamma$, since the final states $K^{(*)}\ell^+\ell^-$ can also be produced via "long distance" contributions from the hadronic decay $B \to K^{(*)}\Psi$ followed by $\Psi \to \ell^+\ell^-$ where Ψ stands for a real or virtual charmonium state [139]. Ali, Mannel and Morozumi [140] have performed a full analysis of $b \to s\ell^+\ell^-$ including both the penguin and the long distance contributions. Their predictions for the inclusive $b \to s\ell^+\ell^-$ rate are in the range $(2-6) \times 10^{-6}$ excluding the regions close to the ψ and ψ' mass where the long distance contributions dominate. There is interference between the penguin and long distance amplitudes over a wide range of dilepton masses. Ali *et al.* point out that the sign of the interference is controversial, and that information about the interference can be obtained both from the dilepton mass distribution, and from the forward-backward asymmetry of the lepton pair.

Experimental searches have been made by CLEO and ARGUS at the $\Upsilon(4S)$, and by UA1 in $p\bar{p}$ collisions. The CLEO and ARGUS analyses [141,142] make a simple veto on dilepton masses consistent with a real ψ or ψ', and see almost no background in their beam-constrained mass plots. The UA1 analysis [143] selects a range $3.9 < M(\ell^+\ell^-) < 4.4$ GeV which is believed to have small long distance contributions and no radiative tail from the Ψ. UA1 performs both an exclusive search for $\bar{B}^0 \to \bar{K}^{*0}\mu^+\mu^-$ and an inclusive search for $B \to X_s\mu^+\mu^-$. The upper limits from all the experimental measurements are summarized in Table XXXIII. These upper limits are all well above the theoretical predictions, but a detailed comparison of the various limits is complicated by the different dilepton mass ranges considered by the different analyses. The limits from UA1 suggest that $b \to s\ell^+\ell^-$ decays might eventually be observed at hadron colliders, as well as by $\Upsilon(4S)$ experiments that have collected large enough data samples to be sensitive to these decay modes.

TABLE XXXIII. Experimental upper limits (90% C.L.) for $b \to s\ell^+\ell^-$ decays. All numbers quoted are branching fractions $\times 10^{-5}$

B Decay	ARGUS	CLEO I	CLEO 1.5	UA1
$K^0e^+e^-$	<15.0	<56.0		
$K^-e^+e^-$	<9.0	<24.0	<5.7	
$K^0\mu^+\mu^-$	<26.0	<39.0		
$K^-\mu^+\mu^-$	<22.0	<36.0	<17.0	
$\bar{K}^{*0}e^+e^-$	<29.0		<6.9	
$K^{*-}e^+e^-$	<63.0			
$\bar{K}^{*0}\mu^+\mu^-$	<34.0		<16.0	<2.3
$K^{*-}\mu^+\mu^-$	<110.0			
$X_s\mu^+\mu^-$				<5.0

XIII. PURELY LEPTONIC B DECAY

A. B Decays to Two Leptons

The Standard Model allows B^0 and B_s mesons to decay to e^+e^- $\mu^+\mu^-$ or $\tau^+\tau^-$ via box diagrams or loop diagrams involving both W and Z propagators (see Fig. 31) [144]. The largest branching fraction is predicted to be 4×10^{-7} for $B_s \to \tau^+\tau^-$, and the smallest 2×10^{-15} for $B^0 \to e^+e^-$. The decays to the lighter leptons are suppressed by a helicity factor which is proportional to m_ℓ^2, and the B^0 decays are suppressed relative to the B_s decays by the factor $|V_{td}/V_{ts}|^2$. Decays to the final states $e^\pm\mu^\mp$, $e^\pm\tau^\mp$ and $\mu^\pm\tau^\mp$ are all forbidden in the Standard Model by lepton family number conservation.

A search for B^0 decays to two leptons has been made by CLEO II [145], and there are also searches for $B^0 \to \mu^+\mu^-$ by the UA1 and CDF collaborations at hadron colliders [143,146]. The 90% C.L. upper limits on the allowed processes are 5.9×10^{-6} for $B^0 \to e^+e^-$ (CLEO II), and 3.2×10^{-6} (CDF), 5.9×10^{-6} (CLEO II) and 8.3×10^{-6} (UA1) for $B^0 \to \mu^+\mu^-$. The hadron collider experiments can undoubtedly set similar limits on $B_s \to \mu^+\mu^-$, and presumably have not done so because the B_s mass was unknown until recently (see section VII B) .

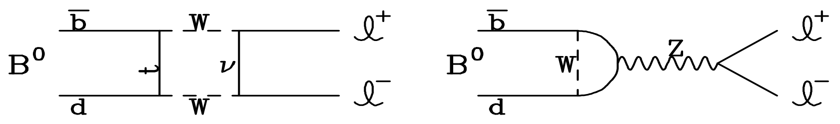

FIG. 31. Diagrams for the dilepton decays of B mesons.

CLEO II also sets limits on the lepton-flavor changing decays of 5.9×10^{-6} for $B^0 \to e^\pm\mu^\mp$, 7.9×10^{-4} for $B^0 \to e^\pm\tau^\mp$ and 1.2×10^{-3} for $B^0 \to \mu^\pm\tau^\mp$.

Several recent papers consider the relative sensitivity of various lepton-flavor changing decays to non-Standard Model couplings [147], [148] . Sher and Yuan argue that larger Yukawa couplings are expected for third generation quarks, and that these larger couplings not only enhance the sensitivity of the decays, but also make them less dependent on the detailed parameterization of the new couplings [147]. They make a comparison of B and K decays which suggests that $B_s \to \tau\mu$ has the best sensitivity, although it is unclear how to search for this channel experimentally. The more accessible channel $B_s \to \mu e$ could also have better sensitivity than the equivalent decay $K_L \to \mu e$, even though the upper limit on the latter is now in the 10^{-11} range. B^0 decays are less sensitive than B_s decays but are still of interest because they can be searched for in experiments at the $\Upsilon(4S)$.

B. The Decays $B \to \tau\nu$, $B \to \mu\nu$ and $B \to e\nu$.

The decay $B^+ \to \tau^+\nu$ proceeds through the annihilation of the constituent quarks in analogy to the $\pi^+ \to \mu^+\nu$ decay. The branching fraction is given by:

$$\mathcal{B}(B^+ \to \tau^+\nu) = \frac{G_F^2 m_B m_\tau^2}{8\pi}\left(1-\frac{m_\tau^2}{m_B^2}\right) f_B^2 |V_{ub}|^2 \tau_B$$

All the parameters in this equation are well known except the decay constant f_B and the CKM matrix element V_{ub}. Given a more accurate knowledge of V_{ub} from other measurements and the experimental observation of the decay $B^+ \to \tau^+\nu$, it would be possible to determine a value for f_B. The measurement of this decay constant is of fundamental importance for B physics since it enters into many other B decay measurements, including most notably $B\bar{B}$ mixing [149].

The present theoretical estimates of f_B from lattice QCD and QCD sum rules are in the range $f_B = (180 \pm 50)$ MeV [150]. Using this value of f_B and our standard values of V_{ub} and τ_B, we obtain a prediction of $\mathcal{B}(B^+ \to \tau^+\nu) = 4.0\times10^{-5}$. The decays $B^+ \to \mu^+\nu$ and $B^+ \to e^+\nu$ have smaller branching ratios of 1.4×10^{-7} and 3.3×10^{-12} respectively. The decays to the muon and electron are suppressed relative to the tau decay by a helicity factor proportional to m_ℓ^2.

CLEO II is investigating ways of observing these decay modes [151]. For $B^+ \to \tau^+\nu$ the method that has been tried is to start with a sample of 716 fully reconstructed B^- mesons, including many of the decay channels that have been discussed earlier in this review. The signature for the decay of the B^+ meson to $\tau^+\nu$, $\tau^+ \to \ell^+\nu\bar{\nu}$ or $\tau^+ \to \pi^+\nu$ is the presence of one and only one charged track and no neutral showers with energies greater than 200 MeV in addition to those tracks and showers that were used to reconstruct the B^- meson. No candidates are observed among the 716 reconstructed B^- events. The efficiency for finding a $B^+ \to \tau^+\nu$ event among these fully reconstructed B^- events, including the $\tau \to l\nu\bar{\nu}$ and $\tau \to \pi\nu$ branching fractions, is $(26.0 \pm 3.3)\%$. This leads to a 90% C.L. upper limit of $\mathcal{B}(B^+ \to \tau^+\nu) < 1.3\%$.

The technique that CLEO II is using for $B^+ \to \mu^+\nu$ is somewhat different. For this mode it is not necessary to fully reconstruct the other B meson. The B meson decays almost at rest into a μ^+ and a neutrino which are back-to-back and have energies of about 2.65 GeV. The muon is well identified and has little background. The neutrino is "detected" by calculating the missing momentum p_{miss} of the whole event. If all the decay products of the other B^- have been measured by the CLEO II detector p_{miss} will be a good estimator of the neutrino momentum. Then the analysis proceeds as if this were a fully reconstructed B decay, with the calculation of the energy difference, ΔE, and the beam-constrained mass, M_B. Since there is often a small amount of undetected energy from the decay of the other B, a cut is made at $-200 < \Delta E < +400$ MeV. This analysis is almost background free, and gives a 90% C.L. upper limit of $\mathcal{B}(B^+ \to \mu^+\nu) < 2.0 \times 10^{-5}$. A similar limit is obtained for $B^+ \to e^+\nu$.

The CLEO II limits of $B^+ \to \tau^+\nu$ and $B^+ \to \mu^+\nu$ are both two orders of magnitude above the theoretical predictions, giving rather uninteresting limits on f_B of 3.2 and 2.1 GeV for $|V_{ub}/V_{cb}| = 0.075$. However, it should be noted that the experimental searches are not yet background limited, so the upper limits on the branching ratios will improve linearly with future increases in statistics. Efforts are being made to improve the $B \to \tau\nu$ analysis either by relaxing the requirements for full reconstruction, or by adding more τ decay modes.

XIV. CONCLUSIONS

In the past two years significant progress in the area of hadronic B decay has been made. The data are now of sufficient quality to perform non-trivial tests of the factorization hypothesis including comparisons of rates for $D^{*+}X^-$ (where $X^- = \pi^-, \rho^-$, or a_1^-) with rates for $D^{*+}\ell^-\bar{\nu}$ at $q^2 = M_X^2$, as well as comparisons of the polarizations in $D^{*+}\rho^-$ with $D^{*+}\ell^-\bar{\nu}_\ell$. In all cases the factorization hypothesis is consistent with the data at the present level of experimental precision and for $q^2 < m_{a_1}^2$.

Improved measurements of branching ratios of two-body decays with a final state ψ meson have been reported from CLEO II and ARGUS. The decay $B \to \psi K^*$ is strongly polarized with $\Gamma_L/\Gamma = (84 \pm 6 \pm 8)$ %; therefore this mode will be useful for measuring CP violation.

There is no evidence for color suppressed decays to a charmed meson and light neutral hadron in the final state. The most stringent limit, $\mathcal{B}(\bar{B}^0 \to D^0\pi^0)/\mathcal{B}(\bar{B}^0 \to D^+\pi^-) < 0.07$ from CLEO II, is still above the level where these color suppressed B decays are expected in most models. The observation of $B \to \psi$ modes shows that color suppressed decays are present. Using results on exclusive $B \to \psi$ decays from CLEO 1.5, CLEO II and ARGUS, we find a value of the BSW parameter $|a_2| = 0.23 \pm 0.01 \pm 0.01$. We also report a new value for the BSW parameter $|a_1| = 1.07 \pm 0.04 \pm 0.06$. By comparing rates for B^- and $\bar{B}^0$ modes, it has been shown that the sign of a_2/a_1 is positive, in contrast to what is found in charm decays.

There has been dramatic progress in the study of rare decays. CLEO II has reported evidence for charmless hadronic B decay in the sum of $B \to K^+\pi^-$ and $B \to \pi^+\pi^-$ and has observed the first direct evidence for the radiative penguin decay $B \to K^*\gamma$ with a branching ratio of $(4.5 \pm 1.5 \pm 0.9) \times 10^{-5}$. CLEO II also sets limits on the inclusive process $0.8 \times 10^{-4} < \mathcal{B}(b \to s\gamma) < 5.4 \times 10^{-4}$. These results restrict the allowed range for V_{ts} and constrain physics beyond the Standard Model.

Large samples of reconstructed hadronic decays will be obtained in the next few years by the CLEO II collaboration as a result of further improvements in the luminosity of CESR, and in the performance of the CLEO II detector. This will permit accurate tests of the factorization hypothesis over the full q^2 range. The large tagged sample can be used to study inclusive properties of B^+ and B^0 decays and constrain f_B via $B^+ \to \tau^+\nu$. Measurements of additional decays to final states with charmonium mesons will be performed and other color suppressed decays will be observed.

A larger data sample should allow further results to be obtained on rare B decays including the observation of $B^0 \to \pi^+\pi^-$, $B^0 \to K^+\pi^-$ and a measurement of the inclusive process $b \to s\gamma$. The measurement of several rare hadronic decays would provide information on the relative importance of the penguin and spectator amplitudes. Additional electromagnetic penguin decays such as $B \to K^{**}\gamma$, $B \to K^*\ell^+\ell^-$ and $B \to \rho\gamma$ may be observed. These provide further constraints on Standard model parameters and extensions of the Standard Model.

A goal of the study of hadronic and rare B decays is to eventually measure CP asymmetries in B decays such as $B \to \psi K_s$ and $B \to \pi^+\pi^-$. In order to test the consistency of the Standard Model description of CP violation in these decays, the mechanisms of B decay must be well understood. This review shows that rapid progress is being made in understanding B decay.

ACKNOWLEDGMENTS

We thank H. Albrecht, A. Ali, C. Bebek, P. Colangelo, J. Hewett, N. Isgur, G. Kane, M. Neubert, V. Rieckert, J. Rodriguez, S. Menary and M. Zoeller for useful discussions. We thank our colleagues from the CLEO and ARGUS experiments for useful comments and for their contributions to the work discussed in this review. We thank the National Science Foundation, the Department of Energy, the University of Hawaii, Ohio State University and Syracuse University for their support.

REFERENCES

[1] Copies of the figures in this review are available on request from the authors.
[2] CLEO II Collaboration, M.S. Alam *et al.*, CLNS 94-1270, submitted to Phys. Rev. D.
[3] CLEO Collaboration, M. Battle *et al.*, Phys. Rev. Lett. **71**, 3922 (1993).
[4] CLEO Collaboration, R. Ammar *et al.*, Phys. Rev. Lett. **71**, 674 (1993).
[5] J. Bjorken, Nucl. Phys. B (Proc. Suppl) **11**, 325 (1989).
[6] CLEO Collaboration, J. Bartelt *et al.*, Phys. Rev. Lett. **71**, 511 (1993). S. Stone "Semileptonic B Decays", contribution to this book.
[7] J.L. Hewett, Phys. Rev. Lett. **70**, 1045 (1993).
[8] CLEO Collaboration, S. Behrends *et al.*, Phys. Rev. Lett. **50**, 881 (1983).
[9] CLEO Collaboration, M.S. Alam *et al.*, Phys. Rev. D **36**, 1289 (1987).
[10] CLEO Collaboration, D. Bortoletto *et al.*, Phys. Rev. D **45**, 21 (1992).
[11] The integrated luminosities quoted here are for the $\Upsilon(4S)$ data samples only.
[12] ARGUS Collaboration, H. Albrecht *et al.*, Phys. Lett. B **185**, 218 (1987).
[13] ARGUS Collaboration, H. Albrecht *et al.*, Phys. Lett. B **215**, 424 (1988).
[14] ARGUS Collaboration, H. Albrecht *et al.*, Z. Phys. C **48**, 543 (1990).
[15] G. Fox and S. Wolfram, Phys. Rev. Lett. 41, 1581 (1978).
[16] The definitions of thrust, sphericity and $s_\perp$ can be found in the contribution of M. Artuso in this volume.
[17] See contribution of V. Sharma to this volume.
[18] CLEO Collaboration, D.Akerib *et al.*, Phys. Rev. Lett. **71**, 3070 (1993).
[19] Particle Data Group, K. Hikasa *et al.*, Phys. Rev. D **45**, (1992).
[20] Mark III Collaboration, J. Adler *et al.*, Phys. Rev. Lett. **60**, 89 (1988).
[21] ARGUS Collaboration, H. Albrecht *et al.*, Z. Phys. C **54**, 1 (1992).
[22] CLEO Collaboration, D.Acosta *et al.*, Cornell preprint CLNS 93-1238.
[23] CLEO Collaboration, F. Butler *et al.*, Phys. Rev. Lett. **69**, 2041 (1992).
[24] Mark III Collaboration, D. Coffman *et al.*, Phys. Rev. Lett. 68, 282(1992).
[25] B. Gittelman and S. Stone, CLNS 87/81; M. Ito, PhD Thesis, Cornell University 1989.
[26] ARGUS Collaboration, Z. Phys. C **54**, 13 (1992).
[27] CDF Collaboration, F. Abe *et al.*, Phys. Rev. Lett. **69**, 3704 (1992).
[28] CLEO Collaboration, M. S. Alam *et al.*, Phys. Rev. Lett. **58**, 1814 (1987); CLEO Collaboration, G. Crawford *et al.*, Phys. Rev. D **45**, 572 (1992).
[29] ARGUS Collaboration, H. Albrecht *et al.*, DESY 93-052 1993; ARGUS Collaboration, H. Albrecht *et al.*, DESY 93-084 1993; ARGUS Collaboration, H. Albrecht *et al.*, Z. Phys. C **58**, 191 (1993); ARGUS Collaboration, H. Albrecht *et al.*, Z. Phys. C **58**, 199 (1993).
[30] ARGUS Collaboration, H. Albrecht *et al.*, Z. Phys. C **52**, 353 (1991); ARGUS Collaboration, H. Albrecht *et al.*, Z. Phys. C **54**, 1 (1992).
[31] CLEO Collaboration, D. Bortoletto *et al.*, Phys. Rev. D **45**, 21 (1992); CLEO Collaboration, D. Bortoletto *et al.*, Phys. Rev. Lett. **64**, 2117 (1990).
[32] M. Wirbel and Y.-L. Wu, Phys. Lett. B **288**, 430 (1989).
[33] H. Pietschmann and H. Rupertsberger, Z. Phys. C **27**, 93 (1993).
[34] ARGUS Collaboration, Phys. Lett. B **199**, 451 (1987).

[35] CLEO Collaboration, Y. Kubota *et al.*, CLEO CONF 93-26 submitted to the XVI Symposium on Lepton-Photon Interactions, Cornell, 1993.
[36] D. Coffman. Electromagnetic Radiative Corrections to the Process $\psi \to \ell^+\ell^-$. In preparation (1994).
[37] CLEO Collaboration, Y. Kubota *et al.*, ψ production in the $\Upsilon(4S)$ Energy Region, submitted to the 1991 Geneva Lepton-Photon conference. This paper also sets upper limits on ψ meson production from non $B\bar{B}$ decay of the $\Upsilon(4S)$ resonance.
[38] K. Honscheid, Proceedings of the Rencontres de Moriond 1992, Editions Frontieres.
[39] P. Krizan, Proceedings of the Rencontres de Moriond 1992, Editions Frontieres. H. Schroeder, Proceedings of the 25th International Conference on High Energy Physics, Singapore (1990).
[40] ARGUS Collaboration, H.Albrecht *et al.*, Phys. Lett. B **277**, 209 (1992)
[41] W.F.Palmer and B. Stech, Phys. Rev. D **48**, 4174 (1993).
[42] ARGUS Collaboration, H. Albrecht *et al.*, Z. Phys. C **42**, 519 (1989) and ARGUS Collaboration, H. Albrecht *et al.*, Phys. Lett. B **210**, 263 (1988).
[43] CLEO Collaboration, G. Crawford *et al.*, Phys. Rev. D **45**, 752 (1992).
[44] CLEO Collaboration, M. Procario *et al.*, Cornell preprint CLNS 93-1264.
[45] CLEO Collaboration, Y. Kubota *et al.*, Nucl. Inst. and Meth. A **320**, 66 (1992); the crystal performance is described in R. Morrison *et al.*, Phys. Rev. Lett. **67**, 1696 (1991).
[46] ARGUS used $D \to K_s$ modes.
[47] The resolution in beam constrained mass has a weak dependence on the decay channel. It varies between 2.6 MeV to 3.3 MeV.
[48] These are the fractions determined in the CLEO II analysis. The lowest fraction is for the mode $\bar{B}^0 \to D^{*+}\rho^-$ while the highest fraction is for the mode $B^- \to D^0\pi^-$.
[49] In the ARGUS experiment the beam constrained mass distributions were fitted to a slightly different background function with a kinematic threshold. The functional form of the background shape used was

$$f(x) = c_1 x \left(\sqrt{(1-(\frac{x}{E_{beam}})^2}\right) e^{c_2(1-(\frac{x}{E_{beam}})^2)}$$

CLEO 1.5 fitted the beam constrained mass distributions to the sum of a gaussian signal of width 2.5 MeV (r.m.s) and a background function of the form $w_1\ p + w_2\ p^2$ where $p = \sqrt{E_{beam}^2 - m^2}$ and the parameters w_1, w_2 are determined from the ΔE sidebands.
[50] Two models are considered: non-resonant $B \to D\pi^-\pi^0$ and $B \to D^{**}(2460)\pi^-$. Both give very similar $\pi^-\pi^0$ mass spectra and comparable limits on the non-rho contamination in the signal region.
[51] CLEO II considers two models: (1) The $\pi^-\pi^0$ system is produced non-resonantly following a phase space distribution or (2) the $D^{*+}\pi^-\pi^0$ is produced from the decay $D^{**}\pi^-$. Both give similar limits on the non-ρ fraction.
[52] P. Krieger, to appear in the Proceedings of the McGill Heavy Flavour Physics Conference (1993).
[53] CLEO Collaboration, S. Henderson *et al.*, Phys. Rev. D **45**, 2212 (1992).
[54] CLEO Collaboration, D. Bortoletto *et al.*, Phys. Rev. Lett. **64**, 2117 (1990).
[55] CLEO Collaboration, M. Daoudi *et al.*, Phys. Rev. D **45**, 3965 (1992).

[56] I. Dunietz *et al.*, Phys. Rev. D **43**, 2193 (1991).
[57] M. Neubert, V. Rieckert, Q. P. Xu and B. Stech in *Heavy Flavours*, edited by A. J. Buras and H. Lindner (World Scientific, Singapore, 1992).
[58] G. Kramer and W.F. Palmer, Phys. Lett. B **279**, 181 (1992).
[59] The requirement that the colors match gives a factor of 1/3 in the amplitude. Moreover, the W couples to the $d\bar{d}$ part of the π^0 wave function so there is an additional factor of $1/\sqrt{2}$ in the amplitude. This is also true for the ρ^0 and the ω mesons. The numerical factor is different for the case of the η/η' system.
[60] I.Dunietz and A.Snyder, Phys. Rev. D **43**, 1593 (1991). The D^0 meson, however, must decay to a CP eigenstate e.g. $B \to D^0\pi^0$, $D^0 \to K^-K^+$ could be used.
[61] These modes are also accessible via the W-exchange graph which is expected to be small in B decay.
[62] We use the PDG values for the η, η' and ω branching ratios.
[63] In the mode $\bar{B}^0 \to D^0\omega$, $\omega \to \pi^-\pi^+\pi^0$, Θ_N, the angle between the normal to the ω decay plane and the D^0 direction calculated in the D^0 rest frame, must satisfy $|\sin\Theta_N| > 0.6$.
[64] Ref. [19], p. III.38
[65] CLEO Collaboration, D. Bortoletto *et al.*, Phys. Rev. D **37**, 1719 (1988).
[66] C. P. Singh *et al.*, Phys. Rev. D **24**, 788 (1981); L.-H. Chan Phys. Rev. Lett. **51**, 253 (1983); K. P. Tiwari *et al.*, Phys. Rev. D **51**, 643 (1985); D. Y. Kim and S. N. Sinha, Ann. Phys. (N.Y.) **42**, 47 (1985).
[67] J. L. Goity and W. S. Hou, Phys. Lett. B **282**, 243 (1992); R. F. Lebed, Phys. Rev. D **47**, 1134 (1993).
[68] CDF Collaboration, F.Abe *et al.*, Phys. Rev. Lett. **71**, 1685 (1993)
[69] OPAL Collaboration, P.T. Acton *et al.*, Phys. Lett. B **295**, 357 (1992).
[70] ALEPH Collaboration, D. Buskulic, *et al.*, CERN-PPE-93-97, Jun 1993. Submitted to Phys.Lett.B.
[71] W. Kwong and J. Rosner, Phys. Rev. D **44**, 212 (1991).
[72] We make the approximation that V_{ud}, $V_{cs} \approx 0.975$
[73] Average B meson lifetime reported by M. Danilov, to appear in the proceedings of the 1993 European Physical Society Meeting, Marseille, (1993).
[74] M. J. Dugan and B. Grinstein, Phys. Lett. B **255**, 583 (1991); and references therein.
[75] M. Bauer, B. Stech, and M. Wirbel, Z. Phys. C **29**, 637 (1985); *ibid* **34**, 103 (1987); *ibid* **42**, 671 (1989).
[76] M.A. Shifman, Nucl. Phys. B. **388**, 346 (1992).
[77] N. Isgur and M. B. Wise, Phys. Lett. B **232**, 113 (1989); N. Isgur and M. B. Wise, Phys. Lett. B **237**, 527 (1990).
[78] P. Colangelo, G. Nardulli, N. Paver Phys. Lett. B **303**, 152 (1993); P. Colangelo, F. De Fazio, G. Nardulli, BARI-TH/92-131(1992).
[79] The error is due to the uncertainty in the scale at which to evaluate the Wilson coefficient.
[80] D. Bortoletto and S.Stone, Phys. Rev. Lett. **65**, 2951 (1990).
[81] X. Y. Pham, X. C. Vu, Phys. Rev. D **46**, 261 (1992).
[82] A value $f_\rho = 196$ MeV, often quoted in the literature, is derived from tau decays using the narrow width approximation i.e. by assuming the ρ resonance is a delta function.

[83] C. Reader and N. Isgur, Phys. Rev. D **47**, 1007 (1993). The authors emphasize that their results for color suppressed decay have large theoretical uncertainties and are order of magnitude estimates rather than predictions.
[84] Since the form factor for $B \to D^* \ell \nu$ is slowly varying, the width of the ρ^- meson does not significantly modify the result.
[85] The q^2 spectrum has been corrected for the new values of the CLEO II D^* and D branching ratios. [20], [18]
[86] J.Korner and G. Goldstein, Phys. Lett. B **89B**, 105 (1979).
[87] Peter Lepage (private communication). Also see V. Rieckert, Phys. Rev. D **47**, 3053 (1993).
[88] J.L. Rosner, Phys. Rev. D **42**, 3732 (1990).
[89] M. Neubert, Phys. Lett. B **264**, 455 (1991).
[90] G.Kramer, T.Mannel and W.F. Palmer, Z. Phys. C **55**, 497 (1992).
[91] T. Mannel *et al.*, Phys. Lett. B **259**, 359 (1991). Similar observations have been made by a large number of other authors.
[92] B. Blok and M. Shifman, Nucl. Phys. B **389**, 534 (1993).
[93] Three parameterizations of the Isgur-Wise function $\xi(vv^{'})$ are considered: (a) $\xi(vv^{'}) = 1 + 1/4a(v - v^{'})^2(v + v^{'})^2$ with $a = 0.54 \pm 0.01$, (b) $\xi(vv^{'}) = 1/[1 - (v - v^{'})^2/w_0^2]$ with $w_0 = 1.12 \pm 0.17$, due to Rosner [88] , and (c) $\xi(vv^{'}) = exp[b(v - v^{'})^2]$ with $b = 0.91 \pm 0.03$. All of these parameterizations are constrained by fitting to the average of the CLEO 1.5 and ARGUS data on $d\Gamma/dq^2(B \to D^* \ell \nu)$.
[94] C. Bernard *et al.*, "A Lattice Computation of the Decay Constants of B and D Mesons", BNL preprint 49068; C. Bernard *et al.*, Phys. Rev. D **38**, 3540 (1988); G. Martinelli "Heavy Flavour on the Lattice: Results and Prospects", to appear in the proceedings of the 5th International Symposium on Heavy Flavour Physics, Montreal, 1993; M. B. Gavela *et al.*, Phys. Lett. B **206**, 113 (1988); T. A. DeGrand and R. D. Loft, Phys. Rev. D **38**, 954 (1988).
[95] H. Krasemann, Phys. Lett. B **96**, 397 (1980); M. Suzuki, Phys. Lett. B **162**, 391 (1985); S. Godfrey and N. Isgur, Phys. Rev. D **32**, 189 (1985); S. N. Sinha, Phys. Lett. B **178**, 110 (1986); P. Cea *et al.*, Phys. Lett. B **206**, 691 (1988); S. Capstick and S. Godfrey, Phys. Rev. D **41**, 2856 (1988).
[96] C. Dominguez and N. Paver, Phys. Lett. B **197**, 423 (1987); S. Narison Phys. Lett. B **198**, 104 (1987); L. J. Reinders, Phys. Rev. D **38**, 947 (1988); M. A. Shifman, Usp. Fix. Nauk **151**, 193 (1987) [Sov. Phys. Usp. **30**, 91 (1987)].
[97] The $D^0 \to \pi^0\pi^0$ and $D^0 \to \pi^+\pi^-$ branching ratios are given in M. Selen *et al.*(CLEO collaboration), Phys. Rev. Lett. **71**, 1973 (1993).
[98] K. Terasaki, Phys. Rev. D **47**, 5177 (1993).
[99] The branching ratio for the modes $B \to \psi K$ and $B \to \psi K^*$ can be accommodated by the value $\xi \sim 0$ while $\xi \sim 1/3$ gives a branching ratio that is about a factor of 4 too low (see Ref. [76].
[100] CLEO Collaboration, D. Akerib *et al.*, CLEO CONF 93-17, CLEO paper submitted to EPS conference, Marseille 1993.
[101] A. Deandrea *et al.*, Phys. Lett. B **318**, 549 (1993). The predictions of the model by Deandrea *et al.* are rescaled for our values of $V_{cb} = 0.041$, $|V_{ub}/V_{cb}| = 0.075$, $\tau_B = 1.44$ ps and for $f_{D(D^*)} = 220$ MeV.

[102] Private communication, Volker Rieckert; The result of a fit including R_4 is not significantly different. We find in this case $a_2/a_1 = 0.282 \pm 0.07 \pm 0.06$.
[103] We considered variations of f_D between 120 MeV and 320 MeV. For $f_D = 320$ MeV we find $a_2/a_1 = 0.18$.
[104] J.L. Rosner, Proceedings of TASI-90, p.91-224, Boulder, Co. 1990.
[105] Belyaev, Khodjamirian, Rückl, CERN-TH 6880/93.
[106] P. Ball, Phys. Rev. D **48**, 3190 (1993); P. Ball, TUM-T31-39/93.
[107] A. N. Kamal and T. N. Pham, Ecole Polytechnique preprint A271.1193 .
[108] In the fits of Ref. [57] the CLEO 1.5 data favor a positive sign while the ARGUS data prefer a negative sign.
[109] M. Gronau, Phys. Rev. Lett. **63**, 1451 (1989); Y. Nir and H.R. Quinn, "Theory of CP Violation in B decays"; I. Dunietz, "CP Violation with Additional B Decays", contributions to this book.
[110] ARGUS Collaboration, H. Albrecht *et al.*, DESY Preprint, DESY 93-054 (1993).
[111] CLEO Collaboration, J. Alexander *et al.*, to appear in Physics Letters B.
[112] D. Choudury *et al.*, Phys. Rev. D **45**, 217 (1992). The predictions have been rescaled using $|V_{ub}/V_{cb}| = 0.075$
[113] ARGUS Collaboration, H. Albrecht *et al.*, Phys. Lett. B **241**, 278 (1990).
[114] CLEO Collaboration, D. Bortoletto *et al.*, Phys. Rev. Lett. **62**, 2436 (1989).
[115] ARGUS Collaboration, H. Albrecht *et al.*, Phys. Lett. B **209**, 119 (1988).
[116] CLEO Collaboration, C. Bebek *et al.*, Phys. Rev. Lett. **62**, 8 (1989); K. Schubert, Proceedings of the Symposium on Heavy Quark Physics, Cornell, ed. P.S. Drell and D. Rubin, AIP, NY (1989).
[117] N.G. Deshpande and J. Trampetic, Phys. Rev. D **41**, 895 (1990); N.G. Deshpande, "Theory of Penguins in B Decays", contribution to this book.
[118] L.L. Chau *et al.*, Phys. Rev. D **43**, 2176 (1991).
[119] ARGUS Collaboration, H. Albrecht *et al.*, Phys. Lett. B **254**, 288 (1991).
[120] CLEO Collaboration, P. Avery *et al.*, Phys. Lett. B **223**, 470 (1990).
[121] CLEO Collaboration, R. Ammar *et al.*, CLEO CONF 93-23 submitted to the XVI Symposium on Lepton-Photon Interactions, Cornell, 1993.
[122] The decay $\bar{B}^0 \to K^+K^-$ cannot be produced by a $b \to u$ spectator diagram or a $b \to s$ penguin transition. Thus it is expected to be small compared to $\bar{B}^0 \to \pi^+\pi^-$ and $\bar{B}^0 \to K^-\pi^+$.
[123] S. Playfer, Proceedings of the 1992 Division of Particles and Fields Conference, FERMILAB (1992).
[124] CLEO Collaboration, M. Battle *et al.*, Cornell Preprint, CLNS 93/1252 (1993).
[125] M.G. Kendall and A. Stuart, "The Advanced Theory of Statistics", Second Edition (Hafner, New York, 1968) Vol III.
[126] P. C. Kim, CLNS 93-1254, to appear in the proceedings of the Heavy Flavor Symposium 1993, McGill.
[127] CLEO Collaboration, R. Ammar *et al.*, Cornell Preprint CLNS 93/1212.
[128] A. Ali and C. Greub, Phys. Lett. B **259**, 182 (1991); A. Ali and C. Greub, Phys. Lett. B **287**, 191 (1992); A. Ali and C. Greub, Phys. Lett. B **293**, 226 (1992); A. Ali, T. Ohl and T. Mannel, Phys. Lett. B **298**, 195 (1993); A. Ali and C. Greub, DESY Preprint, DESY 93-065 (1993).

[129] CLEO collaboration, J. Bartelt *et al.*, CLEO CONF 93-19, submitted to Lepton Photon Conference Cornell (1993). The experimental result from the inclusive $b \to cl\nu$ analysis is $p_F = 282 \pm 75$ MeV.
[130] S. Bertolini, F. Borzumati and A. Masiero, Phys. Rev. Lett. **59**, 180 (1987); N.G. Deshpande *et al.*, Phys. Rev. Lett. **59**, 183 (1987); B. Grinstein, R. Springer and M.B. Wise, Phys. Lett. B **202**, 138 (1988); R. Grigjanis *et al.*, Phys. Lett. B **213**, 355 (1988).
[131] N.G. Deshpande *et al.*, Phys. Lett. B **214**, 467 (1988); P. Colangelo *et al.*, Z. Phys. C **45**, 575 (1990).
[132] L3 Collaboration, Phys. Lett. B **317**, 637 (1993).
[133] M. Battaglia (DELPHI Collaboration), Proceedings of the International Symposium on Heavy Flavour Physics, Montreal, 1993.
[134] T. Altomari, Phys. Rev. D **37**, 677 (1988); C.A. Dominguez *et al.*, Phys. Lett. B **214**, 459 (1988); N.G. Deshpande *et al.*, Z. Phys. C **40**, 369 (1988); T.M. Aliev *et al.*, Phys. Lett. B **237**, 569 (1990); P.J. O'Donnell and H. Tung, Phys. Rev. D **44**, 741 (1991).
[135] R. Barbieri and G. Giudice, CERN Preprint CERN-TH 6830/93.
[136] S. Bertolini *et al.*, Nucl. Phys. B. **353**, 591 (1991); V. Barger *et al.*, Phys. Rev. Lett. **70**, 1368 (1993); J. Lopez, D.V. Nanopoulos and G.T. Park, Phys. Rev. D **48**, 974 (1993); Y. Okada, Phys. Lett. B **315**, 119 (1993); R. Garisto and J.N. Ng, Phys. Lett. B **315**, 372 (1993); F. Borzumati, DESY Preprint, DESY 93-090(1993); S. Bertolini *et al.*, "Probing New Physics in FCNC B Decays and Oscillations", contribution to this book.
[137] S.P.Chia, Phys. Lett. B **240**, 465 (1990); K.A.Peterson, Phys. Lett. B **282**, 207 (1992); T.G.Rizzo, Phys. Lett. B **315**, 471 (1993); U.Baur, S.Errede, and J. Ohnemus, Florida State University preprint FSU-HEP-930322 (1993).
[138] B. Grinstein *et al.*, Nucl. Phys. B **319**, 271 (1989); W. Jaus and D. Wyler, Phys. Rev. D **41**, 3405 (1990).; P. J. O'Donnell and H. Tung, Phys. Rev. D **43**, 2067 (1991); P. J. O'Donnell, M. Sutherland and H. Tung, Phys. Rev. D **46**, 4091 (1992);
[139] P. Colangelo *et al.*, Z. Phys. C **45**, 575 (1990). The long distance contributions are expected to be small compared to the short distance contribution for $B \to K^*\gamma$.
[140] A. Ali, T, Mannel and T. Morozumi, Phys. Lett. B **273**, 505 (1991).
[141] CLEO Collaboration, P. Avery *et al.*, Phys. Lett. B **183**, 429 (1987); P. Avery *et al.*, Phys. Lett. B **223**, 470 (1989).
[142] ARGUS Collaboration, H. Albrecht *et al.*, Phys. Lett. B **262**, 148 (1991).
[143] UA1 Collaboration, C. Albajar *et al.*, Phys. Lett. B **262**, 163 (1991).
[144] A. Ali, C. Greub and T. Mannel, DESY preprint DESY 93-016
[145] R. Ammar *et al.*, Cornell preprint CLNS 93/1258.
[146] A. Morsch, Proceedings of the 4th San Miniato topical Seminar on the Standard Model and just beyond (1992) P.353 (World Scientific).
[147] M. Sher and Y. Yuan, Phys. Rev. D **44**, 1461 (1991).
[148] S.Davidson, D. Bailey, and B.A. Campbell, Center for Particle Astrophysics preprint CFPA-93-TH-29(1993).
[149] H. Schröder, "$B\bar{B}$ Mixing", contribution to this book.
[150] A. Sanda, Plenary talk at the Lepton-Photon Symposium, Cornell (1993).
[151] D. Cinabro, Proceedings of the 1992 Division of Particles and Fields Conference, Fermilab (1992), p.843.

APPENDIX

Tables XVI and XVII contain the B meson branching fraction as measured by the ARGUS, CLEO 1.5 and CLEO II experiments. In this appendix we list more technical information found in the ARGUS [12] - [14], [21], [40] and CLEO [10], [54], [37], [2] publications. This includes the number of signal events and the reconstruction efficiencies. Note that different experiments used different procedures to obtain branching ratios in modes where several D or ψ decay channels were used (see Sec. II C. The information provided here will be useful to estimate the signal yields for future B experiments and also to rescale the B meson branching ratios when more precise measurements of the charmed meson branching fraction become available.

TABLE XXXIV. Detailed B^- branching ratios. Experiment: ARGUS

B^- decay	Signal events	Branching ratio [%]
$B^- \to D^0\pi^-$	12 ± 5	$0.22 \pm 0.09 \pm 0.06 \pm 0.01$
$B^- \to D^0\rho^-$	19 ± 6	$1.45 \pm 0.45 \pm 0.41 \pm 0.06$
$B^- \to D^{*0}\pi^-$	9 ± 3	$0.39 \pm 0.14 \pm 0.10 \pm 0.02$
$B^- \to D^{*0}\rho^-$	7 ± 4	$0.96 \pm 0.58 \pm 0.36 \pm 0.04$
$B^- \to D_J^{(*)0}\pi^-$	6 ± 3	$0.13 \pm 0.07 \pm 0.03 \pm 0.01$
$B^- \to D^{*+}\pi^-\pi^-\pi^0$	26 ± 10	$1.68 \pm 0.65 \pm 0.38 \pm 0.07$
$B^- \to D_J^{(*)0}\rho^-$	5 ± 3	$0.33 \pm 0.20 \pm 0.08 \pm 0.01$
$B^- \to D^{*+}\pi^-\pi^-$	11 ± 6	$0.24 \pm 0.13 \pm 0.05 \pm 0.01$
$B^- \to D^0 D_s^-$	4.4 ± 2.2	$1.65 \pm 0.82 \pm 0.42 \pm 0.07$
$B^- \to D^0 D_s^{*-}$	2.3 ± 1.8	$1.10 \pm 0.82 \pm 0.30 \pm 0.04$
$B^- \to D^{*0} D_s^-$	2.0 ± 1.4	$0.77 \pm 0.53 \pm 0.18 \pm 0.03$
$B^- \to D^{*0} D_s^{*-}$	4.8 ± 2.5	$1.84 \pm 0.95 \pm 0.44 \pm 0.07$
$B^- \to \psi K^-$	6	$0.08 \pm 0.04 \pm 0.01$
$B^- \to \psi' K^-$	5	$0.20 \pm 0.09 \pm 0.04$
$B^- \to \psi K^{*-}$	2	$0.19 \pm 0.13 \pm 0.03$
$B^- \to \psi' K^{*-}$	< 3.9	< 0.53 at 90% C.L.
$B^- \to \psi K^-\pi^+\pi^-$	< 8	< 0.19 at 90% C.L.
$B^- \to \psi' K^-\pi^+\pi^-$	3	$0.21 \pm 0.12 \pm 0.04$
$B^- \to \chi_{c1} K^-$	4 ± 2.0	$0.22 \pm 0.15 \pm 0.07$

TABLE XXXV. Detailed $\bar{B}^0$ branching ratios. Experiment: ARGUS

$\bar{B}^0$ decay	Signal events	Branching ratio [%]
$\bar{B}^0 \to D^+\pi^-$	22 ± 5	$0.48 \pm 0.11 \pm 0.08 \pm 0.07$
$\bar{B}^0 \to D^+\rho^-$	9 ± 5	$0.90 \pm 0.50 \pm 0.27 \pm 0.14$
$\bar{B}^0 \to D^{*+}\pi^-$	12 ± 4	$0.26 \pm 0.08 \pm 0.04 \pm 0.01$
$\bar{B}^0 \to D^{*+}\rho^-$	19 ± 9	$0.65 \pm 0.28 \pm 0.26 \pm 0.03$
$\bar{B}^0 \to D^{*+}\pi^-\pi^-\pi^+$	26 ± 7	$1.12 \pm 0.28 \pm 0.33 \pm 0.04$
$\bar{B}^0 \to D^+D_s^-$	2.4 ± 1.8	$1.09 \pm 0.83 \pm 0.44 \pm 0.16$
$\bar{B}^0 \to D^+D_s^{*-}$	3.2 ± 2.0	$1.73 \pm 1.09 \pm 0.67 \pm 0.26$
$\bar{B}^0 \to D^{*+}D_s^-$	2.6 ± 1.8	$0.80 \pm 0.57 \pm 0.22 \pm 0.03$
$\bar{B}^0 \to D^{*+}D_s^{*-}$	3.9 ± 2.0	$1.49 \pm 0.80 \pm 0.43 \pm 0.06$
$\bar{B}^0 \to \psi K^0$	2	$0.09 \pm 0.07 \pm 0.02$
$\bar{B}^0 \to \psi' K^0$	< 2.3	< 0.31 at 90% C.L.
$\bar{B}^0 \to \psi \bar{K}^{*0}$	6	$0.13 \pm 0.06 \pm 0.02$
$\bar{B}^0 \to \psi' \bar{K}^{*0}$	< 3.9	< 0.25 at 90% C.L.
$\bar{B}^0 \to \psi' K^-\pi^+$	< 2.3	< 0.11 at 90% C.L.

TABLE XXXVI. Detailed B^- branching ratios. Experiment: CLEO 1.5

B^- decay	Signature	Signal	Eff.	BR [%]	Branching ratio [%]
$B^- \to D^0\pi^-$					$0.56 \pm 0.08 \pm 0.05 \pm 0.02$
	$D^0 \to K^-\pi^+$	19 ± 5	0.42	0.50 ± 0.12	
	$D^0 \to K^-\pi^+\pi^+\pi^-$	25 ± 6	0.27	0.49 ± 0.10	
	$D^0 \to \bar{K}^0\pi^+\pi^-$	10 ± 4	0.05	1.32 ± 0.55	
$B^- \to D^0\pi^+\pi^-\pi^-$					$1.24 \pm 0.31 \pm 0.14 \pm 0.05$
	$D^0 \to K^-\pi^+$	34 ± 8	0.32	1.24 ± 0.31	
$B^- \to D^{*0}\pi^-$					$0.99 \pm 0.25 \pm 0.17 \pm 0.04$
	$D^0 \to K^-\pi^+$	9 ± 3	0.13	0.97 ± 0.35	
	$D^0 \to K^-\pi^+\pi^+\pi^-$	12 ± 4	0.08	0.94 ± 0.35	
$B^- \to D_J^{(*)0}\pi^-$					$0.13 \pm 0.07 \pm 0.01 \pm 0.01$
	$D^0 \to K^-\pi^+$	2.2 ± 1.5	0.22	0.15 ± 0.10	
	$D^0 \to K^-\pi^+\pi^+\pi^-$	1.8 ± 1.5	0.13	0.11 ± 0.09	
$B^- \to D^{*+}\pi^-\pi^-$					< 0.37
	$D^0 \to K^-\pi^+$	< 8	0.22	< 0.54	
	$D^0 \to K^-\pi^+\pi^+\pi^-$	< 3.5	0.11	< 0.24	
$B^- \to D^0 D_s^-$					$1.66 \pm 0.70 \pm 0.71 \pm 0.07$
		5.0 ± 2.2	0.07	1.66 ± 0.70	
$B^- \to \psi K^-$					$0.09 \pm 0.02 \pm 0.02$
	$\psi \to \mu^+\mu^-, e^+e^-$	11 ± 3	0.41	0.09 ± 0.02	
$B^- \to \psi' K^-$					< 0.05
	$\psi' \to \mu^+\mu^-, e^+e^-$	< 2.3	0.53	< 0.10	
	$\psi' \to \psi\pi^+\pi^-$	< 2.3	0.23	< 0.11	
$B^- \to \psi K^{*-}$					$0.15 \pm 0.11 \pm 0.03$
	$\psi \to \mu^+\mu^-, e^+e^-$	2 ± 1	0.05	0.15 ± 0.11	
$B^- \to \psi' K^{*-}$					< 0.38
	$\psi' \to \mu^+\mu^-, e^+e^-$	< 2.3	0.08	< 0.70	
	$\psi' \to \psi\pi^+\pi^-$	< 2.3	0.03	< 0.82	
$B^- \to \psi K^-\pi^+\pi^-$					$0.14 \pm 0.07 \pm 0.03$
	$\psi \to \mu^+\mu^-, e^+e^-$	6 ± 3	0.14	0.14 ± 0.07	

TABLE XXXVII. Detailed $\bar{B}^0$ branching ratios. Experiment: CLEO 1.5

$\bar{B}^0$ decay	Signature	Signal	Eff.	BR [%]	Branching ratio [%]
$\bar{B}^0 \to D^+\pi^-$					$0.27 \pm 0.06 \pm 0.03 \pm 0.04$
	$D^+ \to K^-\pi^+\pi^+$	17 ± 4	0.33	0.23 ± 0.06	
	$D^+ \to \bar{K}^0\pi^+$	4 ± 2	0.09	0.56 ± 0.30	
$\bar{B}^0 \to D^+\pi^-\pi^-\pi^+$					$0.80 \pm 0.21 \pm 0.09 \pm 0.12$
	$D^+ \to K^-\pi^+\pi^+$	27 ± 9	0.22	0.40 ± 0.19	
	$D^+ \to \bar{K}^0\pi^+$	11 ± 4	0.06	2.70 ± 1.00	
$\bar{B}^0 \to D^{*+}\pi^-$					$0.44 \pm 0.11 \pm 0.05 \pm 0.02$
	$D^0 \to K^-\pi^+$	8 ± 3	0.34	0.36 ± 0.14	
	$D^0 \to K^-\pi^+\pi^+\pi^-$	9 ± 3	0.19	0.38 ± 0.12	
$\bar{B}^0 \to D^{*+}\rho^-$					$2.11 \pm 0.89 \pm 1.23 \pm 0.08$
	$D^0 \to K^-\pi^+$	2 ± 1	0.02	1.35 ± 0.90	
	$D^0 \to K^-\pi^+\pi^+\pi^-$	4 ± 2	0.02	1.90 ± 0.95	
$\bar{B}^0 \to D^{*+}\pi^-\pi^-\pi^+$					$1.76 \pm 0.31 \pm 0.29 \pm 0.07$
	$D^0 \to K^-\pi^+$	18 ± 4	0.15	0.17 ± 0.05	
	$D^0 \to K^-\pi^+\pi^+\pi^-$	18 ± 5	0.08	1.81 ± 0.57	
$\bar{B}^0 \to D^+D_s^-$					$0.58 \pm 0.33 \pm 0.24 \pm 0.09$
		3.0 ± 1.7	0.10	0.65 ± 0.31	
$\bar{B}^0 \to D^{*+}D_s^-$					$1.17 \pm 0.66 \pm 0.52 \pm 0.05$
		3.0 ± 1.7	0.05	1.17 ± 0.57	
$\bar{B}^0 \to \psi K^0$					$0.07 \pm 0.04 \pm 0.02$
	$\psi \to \mu^+\mu^-, e^+e^-$	3 ± 2	0.15	0.07 ± 0.04	
$\bar{B}^0 \to \psi' K^0$					< 0.16
	$\psi' \to \mu^+\mu^-, e^+e^-$	< 2.3	0.18	< 0.30	
	$\psi' \to \psi\pi^+\pi^-$	< 2.3	0.07	< 0.35	
$\bar{B}^0 \to \psi\bar{K}^{*0}$					$0.13 \pm 0.06 \pm 0.03$
	$\psi \to \mu^+\mu^-, e^+e^-$	7 ± 3	0.21	0.13 ± 0.06	
$\bar{B}^0 \to \psi'\bar{K}^{*0}$					$0.15 \pm 0.09 \pm 0.03$
	$\psi' \to \mu^+\mu^-, e^+e^-$	2 ± 1	0.25	0.19 ± 0.13	
	$\psi' \to \psi\pi^+\pi^-$	1 ± 1	0.10	0.11 ± 0.11	
$\bar{B}^0 \to \psi K^-\pi^+$					$0.12 \pm 0.05 \pm 0.03$
	$\psi \to \mu^+\mu^-, e^+e^-$	7 ± 3	0.19	0.12 ± 0.05	

TABLE XXXVIII. Detailed B^- branching ratios. Experiment: CLEO II

B^- decay	Signature	Signal	Eff.	BR [%]	Branching ratio [%]
$B^- \to D^0\pi^-$					$0.55 \pm 0.04 \pm 0.05 \pm 0.02$
	$D^0 \to K^-\pi^+$	76.3 ± 9.1	0.43	0.48 ± 0.06	
	$D^0 \to K^-\pi^+\pi^0$	134 ± 15	0.19	0.62 ± 0.07	
	$D^0 \to K^-\pi^+\pi^+\pi^-$	94 ± 11	0.22	0.57 ± 0.07	
$B^- \to D^0\rho^-$					$1.35 \pm 0.12 \pm 0.14 \pm 0.04$
	$D^0 \to K^-\pi^+$	80 ± 9	0.16	1.40 ± 0.18	
	$D^0 \to K^-\pi^+\pi^0$	42 ± 9	0.04	1.04 ± 0.23	
	$D^0 \to K^-\pi^+\pi^+\pi^-$	90.4 ± 12.1	0.08	1.53 ± 0.20	
$B^- \to D^{*0}\pi^-$					$0.52 \pm 0.07 \pm 0.07 \pm 0.03$
	$D^0 \to K^-\pi^+$	13.3 ± 3.8	0.16	0.36 ± 0.13	
	$D^0 \to K^-\pi^+\pi^0$	37.7 ± 6.9	0.08	0.63 ± 0.12	
	$D^0 \to K^-\pi^+\pi^+\pi^-$	20.0 ± 4.9	0.08	0.52 ± 0.13	
$B^- \to D^{*0}\rho^-$					$1.68 \pm 0.21 \pm 0.27 \pm 0.07$
	$D^0 \to K^-\pi^+$	25.7 ± 5.4	0.06	1.74 ± 0.37	
	$D^0 \to K^-\pi^+\pi^0$	43.8 ± 7.8	0.03	2.24 ± 0.40	
	$D^0 \to K^-\pi^+\pi^+\pi^-$	16.9 ± 4.6	0.03	1.19 ± 0.35	
$B^- \to D^{*0}\pi^-\pi^-\pi^+$					$0.94 \pm 0.20 \pm 0.17 \pm 0.02$
	$D^0 \to K^-\pi^+$	5.5 ± 2.9	0.05	0.51 ± 0.26	
	$D^0 \to K^-\pi^+\pi^0$	27.7 ± 7.2	0.02	1.74 ± 0.45	
	$D^0 \to K^-\pi^+\pi^+\pi^-$	15 ± 4	0.03	1.26 ± 0.37	
$B^- \to D^{*0}a_1^-$					$1.88 \pm 0.40 \pm 0.34 \pm 0.04$
	$D^0 \to K^-\pi^+$	5.5 ± 2.9	0.05	1.02 ± 0.52	
	$D^0 \to K^-\pi^+\pi^0$	27.7 ± 7.2	0.02	3.42 ± 0.90	
	$D^0 \to K^-\pi^+\pi^+\pi^-$	15.0 ± 4.5	0.03	2.52 ± 0.74	
$B^- \to D^+\pi^-\pi^-$					< 0.14
	$D^+ \to K^-\pi^+\pi^+$	< 10.3	0.11	< 0.14	
$B^- \to D^{*+}\pi^-\pi^-$		14.1 ± 5.4			$0.19 \pm 0.07 \pm 0.03 \pm 0.01$
$B^- \to D^{**0}(2420)\pi^-$					$0.11 \pm 0.05 \pm 0.02 \pm 0.01$
	$D^{**0} \to D^{*+}\pi^-$	8.5 ± 3.8		0.11 ± 0.05	
$B^- \to D^{**0}(2420)\rho^-$					< 0.14
	$D^{**0} \to D^{*+}\pi^-$	3.4 ± 2.1		< 0.14	
$B^- \to D^{**0}(2460)\pi^-$					< 0.13
	$D^{**0} \to D^{*+}\pi^-$	3.5 ± 2.3		< 0.28	
	$D^{**0} \to D^+\pi^-$	< 5.6	0.21	< 0.13	
$B^- \to D^{**0}(2460)\rho^-$					< 0.47
	$D^{**0} \to D^{*+}\pi^-$	3.2 ± 2.4		< 0.50	
	$D^{**0} \to D^+\pi^-$	< 6.1	0.08	< 0.47	

TABLE XXXIX. Detailed B^- branching ratios. Experiment: CLEO II

B^- decay	Signature	Signal	Eff.	BR [%]	Branching ratio [%]
$B^- \to \psi K^-$					$0.110 \pm 0.015 \pm 0.009$
	$\psi \to \mu^+\mu^-, e^+e^-$	58.7 ± 7.9	0.47	0.11 ± 0.01	
$B^- \to \psi' K^-$		7.0 ± 2.6			$0.061 \pm 0.023 \pm 0.009$
$B^- \to \psi K^{*-}$					$0.178 \pm 0.051 \pm 0.023$
	$K^{*-} \to K^- \pi^0$	6.0 ± 2.4	0.07	0.22 ± 0.09	
	$K^{*-} \to K_s \pi^-$	6.6 ± 2.7	0.17	0.13 ± 0.06	
$B^- \to \psi' K^{*-}$					< 0.30
	$K^{*-} \to K^- \pi^0$	1 ± 1		< 0.56	
	$K^{*-} \to K_s \pi^-$	1 ± 1		< 0.36	
$B^- \to \chi_{c1} K^-$					$0.097 \pm 0.040 \pm 0.009$
	$\chi_{c1} \to \gamma \psi$	6.0 ± 2.4	0.20	0.10 ± 0.04	
$B^- \to \chi_{c1} K^{*-}$					< 0.21
	$K^{*-} \to K^- \pi^0$	0	0.03	< 0.67	
	$K^{*-} \to K_s \pi^-$	0	0.11	< 0.30	

TABLE XL. Detailed $\bar{B}^0$ branching ratios. Experiment: CLEO II

$\bar{B}^0$ decay	Signature	Signal	Eff.	BR [%]	Branching ratio [%]
$\bar{B}^0 \to D^+\pi^-$					$0.29 \pm 0.04 \pm 0.03 \pm 0.05$
	$D^+ \to K^-\pi^+\pi^+$	80.6 ± 9.8	0.32	0.29 ± 0.04	
$\bar{B}^0 \to D^+\rho^-$					$0.81 \pm 0.11 \pm 0.12 \pm 0.13$
	$D^+ \to K^-\pi^+\pi^+$	78.9 ± 10.7	0.12	0.81 ± 0.11	
$\bar{B}^0 \to D^{*+}\pi^-$					$0.26 \pm 0.03 \pm 0.04 \pm 0.01$
	$D^0 \to K^-\pi^+$	19.4 ± 4.5	0.35	0.22 ± 0.05	
	$D^0 \to K^-\pi^+\pi^0$	31.9 ± 6.4	0.14	0.30 ± 0.06	
	$D^0 \to K^-\pi^+\pi^+\pi^-$	20.5 ± 5.2	0.15	0.27 ± 0.07	
$\bar{B}^0 \to D^{*+}\rho^-$					$0.74 \pm 0.10 \pm 0.14 \pm 0.02$
	$D^0 \to K^-\pi^+$	21.9 ± 5.2	0.12	0.71 ± 0.17	
	$D^0 \to K^-\pi^+\pi^0$	39.8 ± 7.2	0.05	1.08 ± 0.20	
	$D^0 \to K^-\pi^+\pi^+\pi^-$	14.6 ± 4.6	0.05	0.52 ± 0.17	
$\bar{B}^0 \to D^{*+}\pi^-\pi^-\pi^+$					$0.63 \pm 0.10 \pm 0.11 \pm 0.02$
	$D^0 \to K^-\pi^+$	13.5 ± 3.9	0.10	0.58 ± 0.17	
	$D^0 \to K^-\pi^+\pi^0$	21.7 ± 5.9	0.04	0.67 ± 0.18	
	$D^0 \to K^-\pi^+\pi^+\pi^-$	13.9 ± 4.4	0.04	0.65 ± 0.19	
$\bar{B}^0 \to D^{*+}a_1^-$					$1.26 \pm 0.20 \pm 0.22 \pm 0.03$
	$D^0 \to K^-\pi^+$	13.5 ± 3.9	0.10	1.16 ± 0.34	
	$D^0 \to K^-\pi^+\pi^0$	21.7 ± 5.9	0.04	1.34 ± 0.36	
	$D^0 \to K^-\pi^+\pi^+\pi^-$	13.9 ± 2.4	0.04	1.30 ± 0.38	
$\bar{B}^0 \to D^0\pi^+\pi^-$					< 0.16
	$D^0 \to K^-\pi^+$	< 10.1	0.19	< 0.16	
$\bar{B}^0 \to D^{**+}(2460)\pi^-$					< 0.22
	$D^{**+} \to D^0\pi^+$	< 5.6	0.26	< 0.22	
$\bar{B}^0 \to D^{**+}(2460)\rho^-$					< 0.49
	$D^{**+} \to D^0\pi^+$	< 5.1	0.11	< 0.49	
$\bar{B}^0 \to \psi K^0$					$0.075 \pm 0.024 \pm 0.008$
	$\psi \to \mu^+\mu^-, e^+e^-$	10.0 ± 3.2	0.34	0.08 ± 0.02	
$\bar{B}^0 \to \psi' K^0$		0			< 0.08
$\bar{B}^0 \to \psi \bar{K}^{*0}$					$0.169 \pm 0.031 \pm 0.018$
	$\psi \to \mu^+\mu^-, e^+e^-$	29.0 ± 5.4	0.23	0.17 ± 0.03	
$\bar{B}^0 \to \psi' \bar{K}^{*0}$		4.2 ± 2.3			< 0.19
$\bar{B}^0 \to \chi_{c1} K^0$					< 0.27
	$\chi_{c1} \to \gamma\psi$	1 ± 1	0.14	< 0.27	
$\bar{B}^0 \to \chi_{c1} \bar{K}^{*0}$					< 0.21
	$\chi_{c1} \to \gamma\psi$	1.2 ± 1.5	0.13	< 0.21	